DESIGNING BIOMIMETICALLY INSPIRED MATERIALS FOR POTENTIAL ORTHOPEDIC TISSUE ENGINEERING APPLICATIONS

Jason Christopher Dyke

A dissertation submitted to the faculty at the University of North Carolina at Chapel Hill in partial fulfillment of the degree of Doctor of Philosophy in the Department of Chemistry

Chapel Hill
2014

Approved by:

Wei You

Ching-Chang Ko

James Cahoon

Valerie Ashby

Scott Warren

©2014
Jason Christopher Dyke
ALL RIGHTS RESERVED

ABSTRACT

Jason Christopher Dyke: Designing Biomimetically Inspired Materials for Potential Orthopedic Tissue Engineering Applications
(Under the direction of Wei You)

Described herein is the progress made towards modifying and improving established Hydroxyapatite-Gelatin (HAp-Gel) bioceramics. Initial attempts to improve this composite were aimed at incorporating a biomimetic polymer into the HAp-Gel matrix in order to improve long-range interactions in the system. This was done in order to address shortcomings of HAp-Gelatin composites (e.g. low toughness) without sacrificing its favorable properties. Novel degradable copolymers were used, inspired by lactide and trimethylene carbonate monomers. These copolymers demonstrated tunable properties (e.g. molecular weight, glass transition temperature) and were shown to improve fiber bridging in a composite, without sacrificing biocompatibility. Unfortunately, these composites were plagued by poor interfacial adhesion.

To address this, a catecholamine based polymer, polydopamine (PD), was incorporated into this HAp-Gel ceramic matrix. This macromolecule has demonstrated excellent adhesion to numerous substrates. This PD containing composite was shown to have a strong dependence of mechanical properties on processing temperature. Specifically, it was shown that at low temperatures, PD is able to polymerize unimpeded, while the sol-gel component is hindered. The sequential PD/sol-gel polymerizations leads to a unique interpenetrated polymer network with excellent mechanical properties and good biocompatibility.

Finally, studies about catecholamine adhesives were expanded in order to study the structure-property relationship which leads to their remarkable polymerizations and adhesive properties. It was found that

unbound catecholamines (e.g. catechol with propylamine) behave similarly to bound catecholamines such as dopamine. This result has profound implications on the design and implementation of catecholamine based adhesives, and further tests are underway to determine their ability to replace dopamine in bioceramic composites.

ACKNOWLEDGEMENTS

First and foremost I would like to thank my advisor Wei You for his knowledge and patience with me throughout the last five years. Synthetic organic chemistry has not always been the easiest job for me, but throughout my time at UNC Wei's patience has helped me become a better chemist and scientist. More importantly, Wei has been an incredible mentor and friend to me during my time at UNC Chapel Hill, and he is a major reason I will remember my time in North Carolina so fondly. I would also like to thank Dr. Ching-Chang Ko for his guidance and help while we established a new collaboration between the You and Ko labs. Dr. Ko's advice and input were invaluable for getting our collaboration off the ground and his support helped me branch into the exciting field of biomaterials science.

Starting this collaboration was fun, and exciting, but also sometimes very difficult. Despite the hardships, everyday it was a privilege to be able to come to work in the You lab. I want to thank the members of the You Group, past and present, who helped build an amazing environment in which to work. Without the support of my friends at the group, my time at UNC would have been much more challenging and much less rewarding. I would like to specifically thank Dr. Huaxing Zhou, Dr. Rycel Uy, Dr. Andrew Stuart, and Kelly Knight for their guidance, support, and assistance in my early years at UNC. They helped me to find my feet in a synthetic lab and in a new state, where I initially felt very out of place. I would also like to thank our current members, Sam Anderson, Travis Lajoie, Adam Alman, Josh Yablonski, Rob Bruce, Wentao Li, Elizabeth Kenan, Qianqian Zhang, David Dirkes, Seunghun Eom, Maggie Radack and Allison Kelly for many great lunch conversations and reprieves from lab. I also want to thank Huamin Hu for her invaluable help with experiments, and her eagerness to carry this project forward. I will miss all of you, and I will never forget the wonderful times I had with each of you during my time at UNC. I sincerely hope that our paths will cross again soon and I can't wait to see where we all end up in the next phase of our lives!

I would like to acknowledge Professors James Cahoon, Valerie Ashby, and Scott Warren for serving as members on my defense committee and thank them for taking the time to help me in my transition away from my graduate studies. My gratitude is also with John Whitley, Wonhee Jeong, and Dominica Wong for their invaluable help with experimental design.

I would also like to thank my undergraduate advisor, Dr. Lyudmila Bronstein. Her guidance through my undergraduate work was vital to me, and helped me take an interest in research and materials science in particular. Her kindness and knowledge helped lead me to a path towards UNC, for which I am eternally grateful to her.

Last but certainly not least, I would like to thank my friends and family. They have always been there to support me through the entirety of my academic career. Without their love and support I surely would not have made it to where I am today. To my parents: Thank you for always supporting my dreams and ambitions and helping to foster a sense of curiosity and wonder in me. To my grandparents: thank you for showing me what a good attitude and hard work can accomplish, and for always reminding me to count my blessings. To my sister: Thank you for always being there to listen and give me advice (and cover for me when I didn't take that advice.) Your support was instrumental in me surviving the graduate school experience. You all have provided me with a wonderful blueprint on how to live my life, and I hope I can continue to make you proud.

To my family,

Daniel, Sally, Jessica, and Apollo

TABLE OF CONTENTS

LIST OF TABLES

LIST OF FIGURES

CHAPTER 1: INTRODUCTION TO CURRENT BONE-REPAIR MATERIALS AND DESIGN STRATEGIES

Bone injuries are caused by numerous factors such as disease, aging, or trauma. When left untreated, this damage can lead to chronic pain and loss of function, both of which will greatly lower a person's quality of life and even expedite death It has been reported that every year, over 1.5 million American's suffer a fracture caused by bone disease, and in 1995 the total expenditure for osteoporosis related treatments exceeded $13 billion in the United States.[1] Despite the prevalence of these injuries and the need to adequately replace the function of this damaged tissue, current treatment options remain limited due to the complexity of natural osseous tissue.

Human bone is comprised of several different tissues, and in general, they share two common features. First, these tissues contain an inorganic component composed primarily of $Ca_{10}(PO_4)_6(OH)_2$, commonly referred to as hydroxyapatite (HAp). Second, they contain an organic component, composed predominately of the protein collagen. This structural protein is present in various connective tissues found in mammals, and indeed makes up a substantial portion of proteins found in mammalian extracellular matrix (ECM).[2] In bone, the HAp mineral phase is embedded within a dense collagen organic phase, and these collagen macromolecules make the normally brittle inorganic apatites more flexible. This embedded structure helps to improve elasticity and toughness in natural bone. The toughening of bone is accomplished by more than simply adding collagen to mix though; in fact the HAp phase nucleates directly from, and ultimately encapsulates these collagen fibers. Following this encapsulation, the inorganic

and organic components are highly organized on several levels to form a complex hierarchical structure, illustrated in **Figure 1.1**.[3] These HAp-coated collagen fibers are wound together to create larger mineralized collagen fibrils, which can be formed into lamellar sheets, which ultimately wrap together to form the final bone tissue. The intricate, highly organized structuring of human bone helps it to achieve the remarkable mechanical properties (i.e. low weight with high compressive strength) that are crucial for skeletal function.

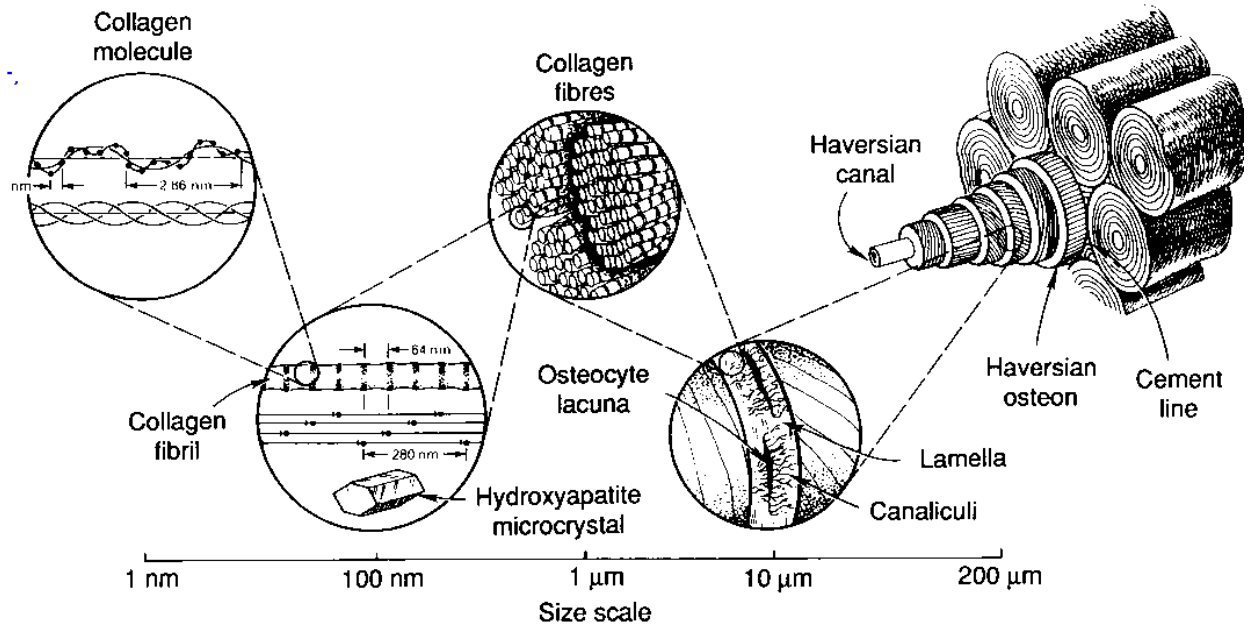

Figure 1.1 *Hierarchical structure of bone, starting with collagen nucleating HAp, and being formed into several layers to maximize mechanical strength while minimizing weight.*

Besides this hierarchical structure, the complexity of human bone also stems from the intricate mechanical and chemical bonding between HAp and collagen. Because of the complex bonding and organization observed in natural osseous tissue, damage is difficult to satisfactorily repair. As such, the prevalence of bone injuries has forced significant research to be focused on developing materials suitable for potential therapeutic orthopedic applications. Despite the

considerable advances which have been made to address these concerns, all current treatment strategies and materials have significant drawbacks. For this reason, replicating the properties of bone with natural or synthetic biomaterials remains an elusive goal.

1.1 Limitations of Natural Bone Treatment Options

Because of its unique structural organization and properties, natural bone presents the best match for replacing lost or damaged tissue. Although using bone is the ideal replacement, current methods utilizing natural tissue can have serious drawbacks.

Replacing bone from natural sources,, called grafting, involves taking healthy tissue from a donor for implantation into the afflicted individual. Currently, several methods of graft treatments are available; allografting involves harvesting tissue from a genetically different donor of the same species, while xenografts involve taking donor tissue from animal sources. Both of these methods present unique challenges. For example, these foreign tissue grafts can be rejected at the implant site, due to the same immunologic factors observed with other transplants. This rejection by the host's immune system can cause additional damage at the implant site.[4] Furthermore, these grafts present a greater risk for infection than other replacement strategies, further complicating the potential therapeutic benefit.[5] For these reasons, it is generally believed that autografts are a superior source of natural bone tissue.

Autografts present an alternative to the foreign grafts mentioned above. This process involves harvesting bone tissue elsewhere on the patient's body and transplanting it to the defect site. The source of this graft bone is usually the patient's hip, specifically the iliac crest, or the rib cage. Autografting is favored as it removes the possibility for host rejection of the tissue and lowers the overall risk of infection.[5] Autografts are not the panacea for bone repair, however, as this method also presents many potential drawbacks. An obvious concern with autografts is the

limited tissue supply, simply due to the lack of suitable donor sites on a patient. Autografts also present the risk of donor site morbidity, a complication which arises when tissue surrounding the newly excised begins to necrose, creating another bone injury while attempting to treat the first.[6] Though complications are not incredibly common using autografts, patients who require a substantial amount of tissue to be excised, or patients who are already immunocompromised experience greater risks of complications.[7] In addition to this, many patients report chronic pain from the implant site, lowering the thereapeutic value of this approach.[8] These possible complications ultimately make the autograft option impossible for some patients, and sub-optimal for many more. The potential limitations and negative consequences grafting treatment options highlight the need for improvements through alternative synthetic treatments.

1.2 Permanent Synthetic Bone Replacement Materials

Although finding synthetic biomaterials to replace natural bone is an ideal solution to address the problems associated with tissue grafts, the complexity of natural bone makes replicating its properties with synthetic materials incredibly difficult. Despite this, three main types of synthetic materials have been established for use as therapeutic orthopedic materials; ceramics, metals, and plastics.[9] Of these, the most successful materials for bone replacements have been ceramics and metals due to their high mechanical strength and resistance to corrosion. Plastics are less ideal to function as load bearing bone replacement materials because, in general, their mechanical properties are not sufficient for this purpose. Furthermore, they show low resistance to bulk erosion resistance,[10] making them even less suitable for the mechanical stresses associated with normal skeletal function. However, the freedom of design and tunable properties associated with plastics have allowed for numerous uses in other, non-loadbearing functions in orthopedic applications, such as sutures, bone screws, tacks, and plates,[11,12] as well

as in blends with other, stronger materials. [13-15]

Most early attempts in designing bone replacement alternatives were focused around finding materials which would permanently assume the function of the injured tissue.[16] The majority of these early implants were designed to be nonporous and inert. Through this strategy, it was hoped that the implanted material would not negatively interfere with the function of the body, nor would they be altered by implantation. By using inert materials, it was also believed that these materials would resist degradation through wear and corrosion, helping extend the lifetime of these materials to make permanent implantations feasible. Nonporous materials also seemed favorable as they provided a complete barrier at the interface of the implant and the hard tissue, minimizing potential adverse interaction with the surrounding tissue. Several types of permanent, bioinert material implants were attempted, including silica and aluminum-oxide ceramics, as well as metals such as steel and titanium alloys. After implantation, these implants were usually observed to be sequestered by a fibrous tissue of variable thickness, allowing them to serve their purpose while not interfering with the body. [17]

In practice, these permanent implants have their own problems. For example, modulus mismatch between very hard metal or ceramic implants and the somewhat softer bone can lead to microdamage near the implant-bone interface.[18] This damage can manifest itself in numerous ways. One concern is that friction at the interface can eventually lead to erosion of the implant. Even if the implant is completely inert, friction can cause the implant to release wear-particles through repeated mechanical loading associated with normal use. These wear particles can cause numerous adverse conditions, such as inflammation around the implant,[19] or even toxic injury to the patient.[20] Furthermore, damage near the implant can result in loosening of the implant itself.[21,22] This loosening could eventually lead to mechanical failure of the implant,[23] causing

additional injury and necessitating further surgery in order to repair the damage caused by the implant. Since these materials are designed to be permanent implants, it is often difficult to repair or replace them, leading to further complications and hindering the therapeutic value of this approach.

Modulus mismatch between implant and bone can lead to other undesired effects on the function of the implant through a process known as stress shielding. This occurs when a high modulus implant shields the surrounding bones from feeling mechanical loading associated with normal skeletal function.[24] The lack of mechanical load reaching the surrounding tissue causes the native tissue to lose strength, as the body deems it a waste of resources to continue to maintain the osseus tissue surrounding the implant. This process leads to drastically weakened tissue, which is then more susceptible to future injury. Therefore, when stress on a tissue is being shielded by an implant, the risk of the surrounding tissue failing is just as important as the risk of the implant itself failing.

Complications associated with stress shielding arise due to the way bone is maintained in the body. Through a process known as bone remodeling, osteoclast cells are constantly removing mature bone tissue through a process known as bone resorption. This tissue is replaced by other cells known as osteoblasts, which lay down new cellular matrix and are eventually mineralized within this matrix through a process known as ossification. This remodeling behavior, illustrated in **Figure 1.2,** has been shown to follow a process called Wolff's law, which states that a healthy individual's body will continuously remodel its own osseus tissue in response to changes in mechanical loading. This means that the bone of a healthy individual will become stronger in response to increased load on that particular bone. In this instance, remodeling occurs primarily to fix microdamage and fractures present through repeated, heavy mechanical loading.[25]

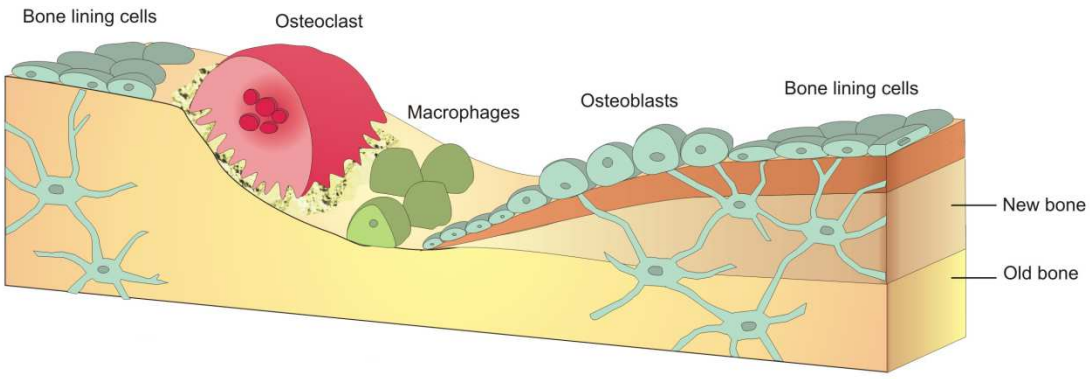

Figure 1.2 *Resorption of osseous tissue by osteoblasts and macrophages, and the subsequent deposition of new tissue by ossification through osteoblast activity.*

Reinforcing these bones lowers the risk of future injury associated with heavy use, and this repair strategy allows the body to focus on the bones most affected (i.e. the most damaged) and reinforce them accordingly. Conversely, if the tissue stops feeling the effect of skeletal loading (i.e. it is being stress shielded) the remodeling behavior will result in the body resorbing the tissue.[26] This happens because it is metabolically costly to maintain bone, and if the body recognizes there is no need to reinforce and maintain a portion of osseous tissue, it will degrade this tissue in order utilize the nutrients in a more useful way elsewhere.

As there were many drawbacks to using totally inert, nonporous implants, alternative treatment strategies and materials were also investigated. It was found that porous inert bioceramics such as pure hydroxyapatite, and ceramic-coated metals (e.g. HAp-coated titanium) can allow for a small amount of osseous tissue ingrowth.[27] This infiltration is called “biological fixation” as this ingrowth mechanically attaches the implant to natural bone. This ingrowth is accomplished via migration of cells into the pores of the implanted material allowing the cells to begin filling in these pores with newly synthesized proteins commonly found in the extracellular

matrix (ECM.)[28] This newly laid ECM effectively attaches the new osseous tissue to the permanent implant, creating a strong mechanical bond between the two. At the same time, provided the pores are suitably designed, a channel is created between the newly formed ECM and the surrounding healthy tissue. This allows for nutrients to move into the new cells, and waste to be removed, effectively expanding healthy tissue into, and around, the permanent implant. This approach was observed to eliminate many negative consequences of other nonporous permanent implants, such as implant loosening and encapsulation.[29] Despite the improvements these biologically fixed implants demonstrated over nonporous implants, major concerns such as modulus mismatch, and longevity remained important concerns, necessitating investigation of better materials.

1.3 Temporary Bone Replacement Options and Scaffolds

There are other classes of ceramics, however, which are considered bioactive, allowing favorable interactions with biological tissue to take place at the implant surface. These materials are capable of achieving "bioactive fixation" whereby a material such as a bioglass can form a favorable interface with the tissue surrounding the implant.[30] Bioactive fixation involves creating mechanical bonds like those seen with biological fixation, but in addition, strong chemical bonding is achieved through the implant material's inherent ability to react with the body. Since these materials are somewhat similar to bone, and not inert towards the body, the newly forming ECM can effectively incorporate a small amount of these ceramic materials directly into itself.[31] This gives better adhesion than the biologically "fixed" implants mentioned above, simply by virtue of chemically bonding the implant material, to a limited degree, into the ECM of the cells which interpenetrate the scaffold after material implantation.

Advances in biomaterials science have identified another class of ceramic materials with

excellent potential for therapeutic applications: resorbable bioceramics.[31,32] These materials are similar to the bioactive ceramics mentioned above, but they differ in several important ways. Primarily, these materials are not permanent, and are capable of degrading over a specified period of time. This allows the slow interpenetration of osseous tissue, which leads the "bioactive fixation" to happen continuously at the materials surface. Small portions of the material are incorporated into the newly forming ECM before degrading away, and as the material degrades it is slowly replaced by natural tissue. **Table 1.1** gives examples of each of the classes of biomaterials discussed above, and gives a summary of their interactions with the body.

Figure 1.3 summarizes different classes of biomaterials, and gives examples of each type, also briefly discussing how the body interacts with each of these different classes. As can be seen in **Figure 1.3**, implants with low relative bioactivity (e.g. Al_2O_3 or Si_3N_4) exhibit effectively no interfacial bone after long implantation times, indicating they are largely

Table 1.1: Classes of Biomaterials and General Properties

Material Type	Examples	Advantages	Disadvantages
Dense, nonporous, nearly inert ceramics and/or metal alloys.	Al_2O_3, Titanium or Steel alloys Si_3N_4	Strong mechanical properties, relative ease of manufacture	Stress shielding, fibrous encapsulation, possible release of wear-particles
Porous, inert implants, allowing ingrowth of small amount of natural tissue	Hydroxyapatite and HAp-coated metals	"Biological Fixation" mechanical bonding, strong mechanical properties	Longevity of implants, corrosion of material at interface, stress shielding
Dense, nonporous, surface reactive materials allowing chemical bonding with natural bone	45S5 Bioglass KGS Cervital 55S4 Bioglass	Bioactive fixation, good mechanical properties, excellent bone-implant interface, mechanical and chemical bonding	Longevity of implant and often difficult fabrication
Nonporous or porous, resorbable ceramics designed to be remodeled naturally	Tricalcium phosphate, HAp-Gelatin, Plaster of Paris	Utilizes natural healing pathways to remove implant and replace with healthy tissue	Coordinating degradation and healing times, complex fabrication

partitioned from the rest of the body. Implants that are largely inert but porous (e.g. pure HAp) show increasing percentages of interfacial bone, though the inert nature of these materials require long periods of time for substantial in-growth to be observed. Materials considered bioactive (e.g. various bioglasses) show very rapid increases in the interfacial bone content, demonstrating their ability to react favorably with newly forming surrounding osseous tissue. The materials which are considered to be resorbable have the highest relative reactivity, and present the opportunity for allowing constantly expanding interfacial bone as their interface is continuously degrading to be replaced by natural tissue.

In recent years, these resorbable, bioactive materials have become fundamental in medical use for their ability to replace various types of natural tissue. Their unique properties allow them to be used to create a degradable, functional substitute for human tissues. This is accomplished by processing these materials into scaffolds, which are designed to function as a 3-D template which acts as a blueprint to direct different types of cells into the implant.[32] For these applications, it is vital to ensure that the scaffold will be strong enough to withstand forces generated through skeletal function. This strength must be sufficiently high to allow for highly porous materials to be used, allowing the ingrowth of native cells.[33]

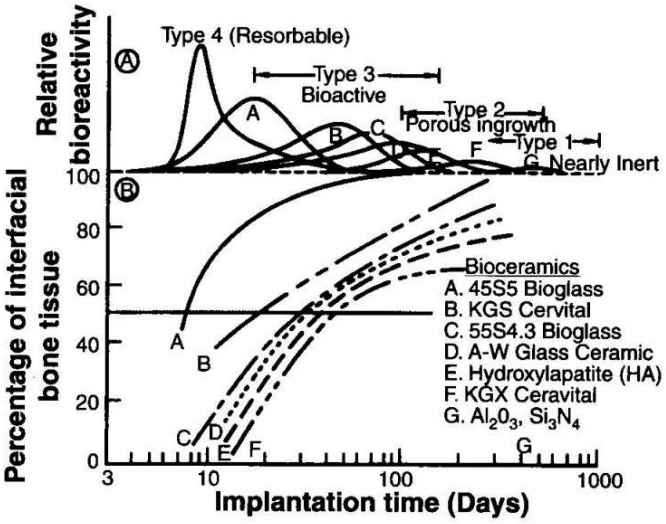

Figure 1.3 *Interfacial bone content and relative reactivity of several established commercial biomaterials. Bioactive materials (A-D) show the largest ingrowth of bone (excluding resorbable materials.) Porous materials show good interfacial bone content after sufficiently long implantation time (E-F) Inert materials (G) show minimal interaction with surrounding tissue*

Different materials are used for their mechanical and biochemical properties to replace various tissues.[12] Many polymers are capable of functioning for soft tissue repairs, while various bioceramics have shown promise in replacing bone. Materials suitable for scaffolding bone are called *osteoconductive*, for their ability to promote the growth of healthy osseous tissue. Since these scaffolds are designed to degrade over time, they allow the cells to continuously create healthy tissue at the implant tissue interface. As the scaffold degrades, either enzymatically or hydrolytically, the interface continuously expands as well. This ensures that new, healthy ECM is constantly being laid by ingrown cells as the material degrades. To expedite this healing process, these scaffolds can also be doped with a combination of stem cells, or partially differentiated cells and growth factors to help facilitate more efficient healing.[34] This approach allows for the body to heal itself more gradually, while the scaffold serves as a temporary matrix providing structural support and protection for the wound site along with cells vital to the healing process.

An important consideration for designing scaffolds is the coordinating the implant's degradation time with the rate of healing, ensuring a gradual transfer of physiological load from the scaffold to new tissues. Degradation time can be influenced by a number of factors, such as material composition, processing method, and pore size.[35] As the scaffold degrades, the interpenetrated cells continue to remodel the matrix. This remodeling will begin to slowly transfer load-bearing function away from the scaffold and onto the newly laid ECM.. This allows in-grown cells to *gradually* feel forces associated with their normal function. As mentioned before, the body will continuously reinforce bone matrix according to Wolff's law ,[36] so as these cells gradually feel increased mechanical loading, they will respond in kind by constantly reinforcing their own matrix to accommodate this increased load. As the scaffold slowly

degrades, it allows the ECM to gradually experience greater mechanical loading. The progressive loading from the implant to healing tissues causes many cycles of this remodeling to occur slowly as the scaffold degrades.[37,38] This loss of mechanical strength and subsequent transfer of load to the newly formed, natural tissue in an idealized scaffold is illustrated in **Figure 1.4.**[35] This ensures the delicate new tissue is not required to support full physiological load until it has become sufficiently strong, preventing further injury from occurring while the body is still healing.[38] This behavior creates a completely natural tissue to replace a damaged one, effectively avoiding many of the negative aspects of allografts and permanent implants.

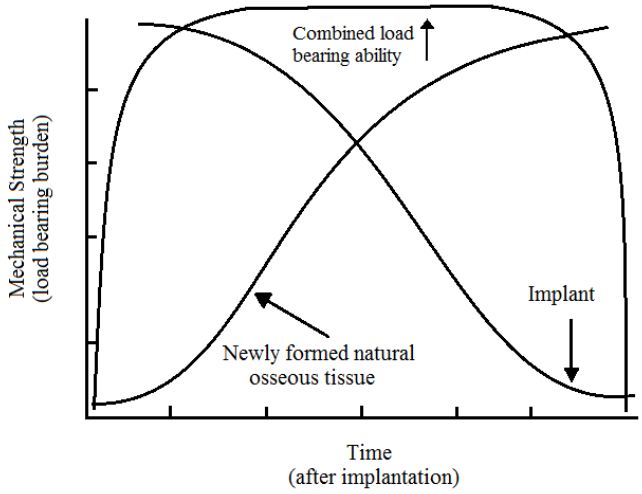

Figure 1.4 *shows an idealized representation of the loss of mechanical strength of implanted materials associated with the degradation of that material in vivo. The loss of strength is compensated by the remodeling of this material into natural osseous tissue, allowing a gradual transfer of load onto new tissue, and ensuring a sufficient strength to be maintained through the combined load bearing ability of both the implant and natural tissue.*

In light of required robust physical properties, and specific surface chemistries necessary for successful orthopedic scaffolds, several materials have been identified to possess qualities that show great potential. Materials such as hydroxyapatite,[39,40] tricalcium phosphate (TCP),[13,39]and Calcium Phosphate Cement (CPC)[41] have received significant attention for use in orthopedic applications due to their superb biocompatibility, high strength, and good osteoconductivity.[42] However, despite these favorable properties, these materials are not ideal for all bone scaffolding applications. Indeed, the high strength of these materials is hindered by their brittle nature and slow degradation time, necessitating research into new biomaterials. [29,39]

1.4 Hydroxyapatite-Gelatin Composite Materials

In response to the need for new bone replacement materials, Ko *et al*. created a novel bioceramic by blending hydroxyapatite with gelatin, forming a composite referred to as HAp-Gel.[43]. Rather than utilizing collagen (specifically type-1 collagen) as the organic phase of this composite, as is seen in bone, HAp-Gel uses the hydrolyzed form of collagen known as gelatin. This replacement had profound implications on the composite. On one hand, gelatin is a cheaper alternative than collagen, making this an attractive material to study in terms of making biomaterials accessible to a wider range of patients. Additionally its properties show lower batch to batch variation than collagen. Because of the hydrolysis of collagen to gelatin, purification and processing have less impact on the final structure. Alternatively, this material loses much of toughening associated with collagen, as the hierarchical structure of bone is not maintained during HAp-Gel processing. However, a substantial mechanical binding is present. It was observed that as the carboxylate groups of gelatin are responsible for HAp nucleation and growth, maintaining some degree of robust mechanical properties required for these implants.[43]

In principle, HAp-Gel did successfully mimic the composition of natural bone, and was also able to demonstrate promise for *in vivo* and *in vitro* resorption. This material demonstrated shorter degradation times than pure HAp materials, making it more useful as a potential temporary scaffold material.[43] However, challenges remain in developing useful scaffolds from these composites as they demonstrate poor processability when wet, and insufficient toughness when porous. Initial attempts to increase toughness were made by adding a cross-linker, glutaraldehyde (GA), and this route ultimately did yield to materials with better mechanical properties. HAp-Gel/GA materials were not suitable for scaffolding materials, however, as negative consequences were observed from unreacted GA, as well as the inability to form

sufficiently strong materials when porous.[44,45] Unfortunately, greater strength in these composites was shown to be related to increasing GA content, however, increasing GA content was also shown to decrease cell viability. The need for these materials to maintain sufficient mechanical properties when porous is an important consideration for potential scaffolding materials. Without this porous architecture, cells are unable to interpenetrate and ultimately remodel the scaffold, making these materials useless for tissue engineering applications. Though good initial results were obtained, demonstrating the promise of HAp-Gel based materials, the negative results also highlighted the need to investigate new cross-linking chemistries.

Problems with HAp-Gel/GA samples were ultimately improved by incorporation of a different cross-linking agent (*N*, *N'*-bis [(3-trimethoxysilyl)propyl]ethylene diamine, commonly referred to as (enTMOS).[46] This cross-linker utilizes a common sol-gel process, the condensation polymerization of trialkoxysilanes, which yields a bioactive glass, which is demonstrated in **Figure 1.5**.

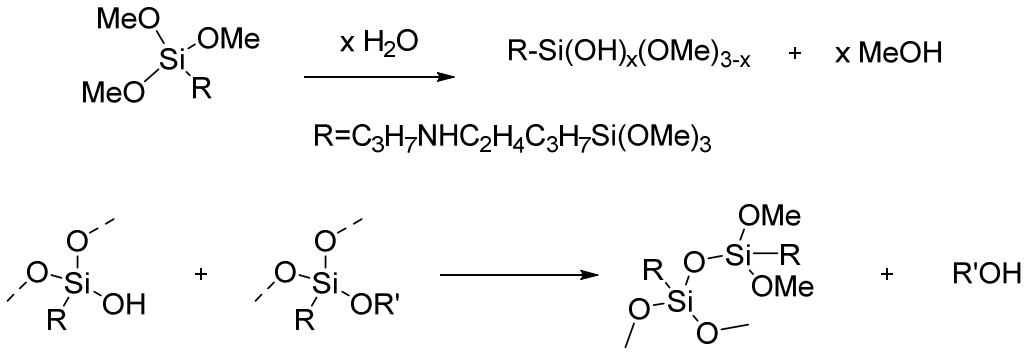

Figure 1.5 *Hydrolysis condensation reaction leading to cross-linked sol-gel materials*.

This sol-gel approach to cross-linking HAp-Gel yields a material referred to as hydroxyapatite-gelatin modified silane (HAp-Gemosil). It was shown that enTMOS was able to strongly bind HAp-Gel further helping to strengthen this composite. This binding came from the

ability of enTMOS Si-O bonds to interact with PO_4^{3-} present in HAp-Gel. Furthermore, the amines on enTMOS were observed to hydrogen bond with carboxylate groups on gelatin, further strengthening this interaction. HAp-Gemosil also had numerous other advantages over previous HAp-Gel based materials, including faster setting time, better processability when wet, better stability after setting, and the ability to fill arbitrary shapes. This last property is especially important when trying to reconstruct bony defects, such as those caused by cancer or other non-traumatic bone injuries. Furthermore, it demonstrated excellent compressive strength, and also the ability to form a porous material through the use of salt-leaching techniques. Salt-leaching was shown to effectively yield HAp-Gemosil materials with tunable pore size, though pore size was shown to be inversely proportional to mechanical strength. This material proved to be an excellent substrate for the spreading and proliferation of MC3T3-E1 preosteoblasts. These cells were shown to migrate into and spread out over the material, suggesting a favorable substrate for cellular interaction. Furthermore, alkaline phosphatase activity assays also showed that these materials also did not hinder metabolic activity or differentiation of plated preosteoblasts.[45,46] These results are shown in **Figure 1.6.**

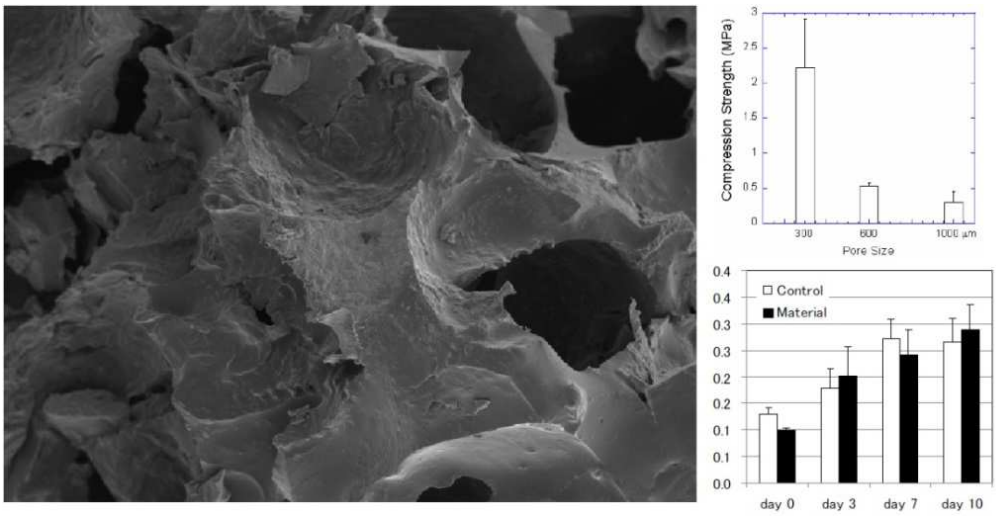

Figure 1.6 *(Left) SEM image of porous HAp-Gemosil Material, (Upper right) Strength related to pore size and (Lower right) ALP activity on porous HA-Gemosil*

This material also demonstrated signs of osteoconductivity. Alizarin red stains were used to demonstrate mineralization patterns *in vitro*, as shown in **Figure 1.7.** In these studies, it can clearly be seen that cells plated on HAp-Gemosil samples were observed to create mineralization patterns that are similar to those observed in trabecular bone. The pattern observed for the control sample saw a relatively homogeneous dispersion of spots with no clear connectivity between the spots. The patterned formation on the Gemosil plates is reminiscent of a 2-D construct of osseous tissue, and it was observed that osteoblasts were found to spread over the interconnected mineralized pattern, with no cells observed between the network. This is in contrast to the control group which showed cells covering over the entire surface. This implies as the HAp-Gemosil component degrades, it could be remodeled by osteoblasts into an interconnected network similar to natural bone. The combination of these properties, plus the relative ease of processing and low cost of HAp-Gemosil materials made this an excellent potential scaffold material for further studies.

Though HAp-Gemosil materials demonstrated significant potential as scaffold materials, they weren't without flaws. While this material had excellent compressive strength, the flexural strength was too low for consideration in clinical applications.[45,46] The high strength but low toughness of this material was not well suited for *in vivo* applications due to concerns about the possibility of brittle implant failure, and modulus mismatch. The problems of low toughness were also exacerbated when these composites were porous, making this material unlikely to be useful for current clinical applications. Furthermore, though the siloxane matrix is bioactive and allows the ingrowth of new bone tissue, it is still a permanent component of this composite, leading to questions about its interaction in the body on a time scale relevant for permanent implants. Ideally, all components of this composite would be degradable,

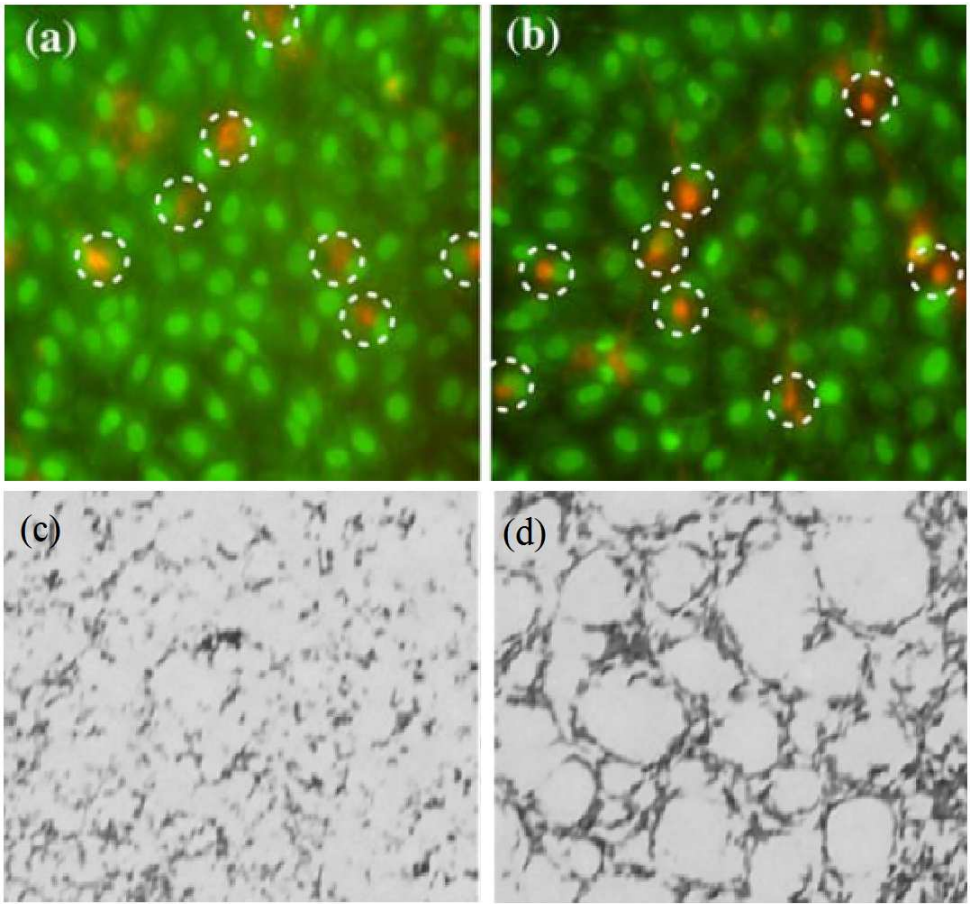

Figure 1.7 *Viability assays(a-b) and mineralization studies(c-d) of osteoblast plated on control and HAp-Gemosil. Control samples showed good cell viability (a) but no clear remodeling behavior (c) contrasting with Gemosil showing similar viability (b) and also signs of preliminary remodelling (d)*

in this way; negative side effects of potentially toxic byproducts and long term stability of the implant are both avoided.

Initial results with various HAp-Gel based systems have demonstrated that the hydroxyapatite-gelatin is an excellent starting point for designing and investigating orthopedic tissue scaffolds. Numerous considerations must be taken into account when planning for and designing new materials based on previous results in order to ensure that favorable properties are not diminished when addressing the shortcomings of previous materials. One way to do this is through biomimetic design, whereby examples in nature are used to guide the design of new

materials. Based on this rationale, it can be seen that the one thing all of these previous composites lacked was a suitable mimic for the collagen found in natural bone. This is an important component of the composite as a substantial amount of bone's toughness comes from collagen being mineralized within the HAp matrix as it grows.[3] So it naturally follows that it is possible to incorporate polymers into these HAp-Gel composites to mimic the role of collagen that is not preserved when gelatin is substituted for collagen. In the above examples, all of the cross-linkers (e.g. enTMOS, GA) used were utilized in order to maximize short range interactions in the composite, allowing for improved mechanical strength. By mimicking collagen with a synthetic polymer, these composites can benefit from additional long range interaction. This allows distant portions of the composite to connect physically and chemically, which is vital for improving flexural strength and toughening a composite by helping to delocalize stress throughout a larger area of the material and prevent damage.

As mentioned previously, polymers on their own are not well suited for orthopedic scaffolding applications due to their low mechanical strength. However, extensive work has been done blending polymers with various inorganic materials,[14,39] and this approach has been shown to improve the performance of these biocomposites by altering their degradation profiles and softening these high modulus materials.[10,11] Synthetic polyesters such as poly(lactic acid) (PLLA),[9,47,48] poly(glycolic acid) (PLGA)[49], poly(ε-caprolactone) (PCL)[13,40] and poly(trimethylene carbonate) (PTMC)[50-53] have been investigated in blends for a variety of medical applications. Each of these polymers has unique mechanical and degradative properties allowing them to be utilized in a wide range of biomaterials. Though homopolymers have good properties for *in vivo* applications, they are often limited by their diversity in function. The utilization of copolymers presents significant synthetic freedom in design,[49] allowing properties

to be isolated and optimized in order to maximize toughness of a composite.[49,51] This optimization can come from choice of monomers, type of architecture (i.e. diblock, triblock, random, alternating) molecular weight, and final material processing (e.g. braided fibers, sintered bulk material etc.) Therefore, copolymers present a useful way to tune the properties of biocomposites such as crystallinity, glass transition temperature (T_g), modulus, degradation behavior and mechanical strength, all of which can be specifically optimized for use in preparing scaffolds. [51,54]

In light of these design parameters and the success of previous HAp-Gemosil composites, it was decided to construct a degradable bioceramic/polymer composite. It was hypothesized that cross-linking a polymer inspired by enTMOS with the HAp-Gemosil composite would allow for better long-range order, leading to better load bearing and processability of the material when compared to non-polymeric enTMOS blended composites. This biomimetic approach would allow for improved interfacial adhesion over other polymer blends based on physical cross-linking only. Additionally better long-range order could be obtained when compared to composites that are only cross-linked by small molecules. Cross-linking a biocompatible polymer into hydroxyapatite-gelatin nanocomposites will better mimic the short and long range interactions seen in natural bone and optimize toughness while retaining bioactivity of the bioceramics.[15]

REFERENCES

(1) Ray, N. F.; Chan, J. K.; Thamer, M.; Melton, L. J. *Journal of Bone and Mineral Research* **1997**, *12*, 24-35.

(2) Field, R. A.; Riley, M. L.; Mello, F. C.; Corbridge, J. H.; Kotula, A. W. *J. Anim Sci.* **1974**, *39*, 493-499.

(3) Lakes, R. S. *Nature* **1993**, *361*, 4.

(4) Friedlaender GE, G. V. *AAOS Workshop* **1991**, 6-8.

(5) Guha SC, P. M. *British Journal of Plastic Surgery* **1983**, *36*, 305-6.

(6) Coventry MB, T. E. *Journal of Bone and Joint Surgery* **1972**, *54*, 83-101.

(7) Banwart, J. C.; Asher, M. A.; Hassanein, R. S. *Spine* **1995**, *20*, 1055-1060.

(8) Keller EE, T. W. *Journal of Oral and Maxillofacial Surgery* **1987**, *45*, 11-14.

(9) Roether, J. A.; Boccaccini, A. R.; Hench, L. L.; Maquet, V.; Gautier, S.; Jérôme, R. *Biomaterials* **2002**, *23*, 3871-3878.

(10) Middleton, J. C.; Tipton, A. J. *Biomaterials* **2000**, *21*, 2335-2346.

(11) Puppi, D.; Chiellini, F.; Piras, A. M.; Chiellini, E. *Progress in Polymer Science* **2010**, *35*, 403-440.

(12) Shoichet, M. S. *Macromolecules* **2009**, *43*, 581-591.

(13) Zhou, Y.; Hutmacher, D. W.; Varawan, S.-L.; Lim, T. M. *Polymer International* **2007**, *56*, 333-342.

(14) Deng, X.; Hao, J.; Wang, C. *Biomaterials* **2001**, *22*, 2867-2873.

(15) Durucan, C.; Brown, P. W. *Advanced Engineering Materials* **2001**, *3*, 227-231.

(16) Wiles, P. *British Journal of Surgery* **1953**, *45*, 488.

(17) Hulbert, S. F. Y., F.A; Matthews, R.S. *Journal of Biomedical Materials Research* **1970**, *4*, 433-456.

(18) Akeson, W. H.; Woo, S. L. Y.; Rutherford, L.; Coutts, R. D.; Gonsalves, M.; Amiel, D. *Acta Orthopaedica* **1976**, *47*, 241-249.

(19) Limin Wang, M. S. D. *Tissue Engineering* **2007**, *13*, 16.

(20) Bergsma, J. E.; de Bruijn, W. C.; Rozema, F. R.; Bos, R. R. M.; Boering, G. *Biomaterials* **1995**, *16*, 25-31.

(21) Bodén, H.; Adolphson, P.; Öberg, M. *Archives of Orthopaedic and Trauma Surgery* **2004**, *124*, 382-392.

(22) Venesmaa, P. K.; Kröger, H. P. J.; Miettinen, H. J. A.; Jurvelin, J. S.; Suomalainen, O. T.; Alhava, E. M. *Journal of Bone and Mineral Research* **2001**, *16*, 2126-2131.

(23) Teoh, S. H. *International Journal of Fatigue* **2000**, *22*, 825-837.

(24) H.W.J. Huiskes, B. v. R. *Clin. Orthop.* **1992**, *274*, 10.

(25) Frost, H. *The Angle Orthodontist* **1994**, *64*, 175-188.

(26) H.W.J. Huiskes, H. W., B. van Rietbergen, *Clin. Orthop.* **1992**, *274*, 10.

(27) Eckhardt, A. A., H *Arch Orthop Trauma Surg* **2003**, *123*, 28-35.

(28) Bobyn, J. D. W., G.C *Clinical Orthopaedics and Related Research®* **1980**, *150*, 263-270.

(29) Radin SR, D. P. *J Biomed Mater Res.* **1994**, *28*, 1303-9.

(30) Bauer, T. W. S., S *Clinical Orthopaedics and Related Research®* **2002**, *395*, 11-22.

(31) Hench, L. L. *Journal of the American Ceramic Society* **1991**, *74*, 1487-1510.

(32) Rezwan, K.; Chen, Q. Z.; Blaker, J. J.; Boccaccini, A. R. *Biomaterials* **2006**, *27*, 3413-3431.

(33) Imam Khasim, H. R.; Henning, S.; Michler, G. H.; Brand, J. *Macromolecular Symposia* **2010**, *294*, 144-152.

(34) Langer, R. V., J.P. *Science* **1993**, *260*, 920-926.

(35) Raghunath, J.; Rollo, J.; Sales, K. M.; Butler, P. E.; Seifalian, A. M. *Biotechnol Appl Biochem* **2007**, *46*, 73-84.

(36) Brand, R. *Clinical Orthopaedics and Related Research®* **2010**, *468*, 1047-1049.

(37) Bougherara, H.; Klika, V.; Maršík, F.; Mařík, I. A.; Yahia, L. H. *Journal of Biomedical Materials Research Part A* **2010**, *95A*, 9-24.

(38) B. van Rietbergen, H. W. J. H., H. Weinans, D.R. Sumner, T.M. Turner, J.O. Galante *J. Biomech* **1993**, *26*, 13.

(39) Bucholz, R. C. A. H. R. *Orthop Clin North Am* **1987**, *18*, 323-34.

(40) Shokrollahi, P.; Mirzadeh, H.; Scherman, O. A.; Huck, W. T. S. *Journal of Biomedical Materials Research Part A* **2010**, *95A*, 209-221.

(41) Tas, A. *J. Mater. Sci: Mater Med* **2008**, *19*, 2231-2239.

(42) Ishihara K, A. H., Nakabayashi N, Morita S, Furaya K *J Biomed Mater Res.* **1992**, *26*, 937-45.

(43) Chang, M. C.; Ko, C.-C.; Douglas, W. H. *Biomaterials* **2003**, *24*, 2853-2862.

(44) Ko CC, O. M., Fallgatter AM, Hu W-S. *J. Material Research* **2006**, *21*, 8.

(45) Chiu, C.-K. F., Joao; Luo, TJ M.; Ko, Ching-Chang *J Mater Sci: Mater Med* **2012**, *23*, 2115-2126.

(46) Luo, T.-J.; Ko, C.-C.; Chiu, C.-K.; Llyod, J.; Huh, U. *Journal of Sol-Gel Science and Technology* **2010**, *53*, 459-465.

(47) Oh, J. K. *Soft Matter* **2011**, *7*, 5096-5108.

(48) Declercq, H.; Cornelissen, M.; Gorskiy, T.; Schacht, E. *Journal of Materials Science: Materials in Medicine* **2006**, *17*, 113-122.

(49) Jiang, T.; Nukavarapu, S. P.; Deng, M.; Jabbarzadeh, E.; Kofron, M. D.; Doty, S. B.; Abdel-Fattah, W. I.; Laurencin, C. T. *Acta Biomaterialia* **2010**, *6*, 3457-3470.

(50) Bat, E.; van Kooten, T. G.; Feijen, J.; Grijpma, D. W. *Macromolecular Bioscience* **2011**, *11*, 952-961.

(51) Bat, E.; Plantinga, J. e. A.; Harmsen, M. C.; van Luyn, M. J. A.; Zhang, Z.; Grijpma, D. W.; Feijen, J. *Biomacromolecules* **2008**, *9*, 3208-3215.

(52) Andronova, N.; Albertsson, A.-C. *Biomacromolecules* **2006**, *7*, 1489-1495.

(53) Dargaville, B. L.; Vaquette, C.; Peng, H.; Rasoul, F.; Chau, Y. Q.; Cooper-White, J. J.; Campbell, J. H.; Whittaker, A. K. *Biomacromolecules* **2011**, *12*, 3856-3869.

(54) Jiang, X.; Vogel, E. B.; Smith, M. R.; Baker, G. L. *Macromolecules* **2008**, *41*, 1937-1944.

CHAPTER 2: PERFORMANCE OF BIOCERAMIC COMPOSITES CONTAINING POLY(*L*-LACTIDE-*CO*-PROPARGYL CARBONATE)-*G*-AZIDO SILANE

2.1. Introduction to Polymer Bioceramic composites

Natural bone is a lightweight mineral composite consisting of inorganic apatite, mainly hydroxyapatite (HAp), within a dense matrix of organic collagens. The long fibrous collagen makes the normally brittle HAp more resilient, helping to improve flexural strength in natural bone.[1] The hierarchy HAp-collagen structure, however, cannot be reproduced easily using engineering principles. Sequentially, autografts (tissues from the host) have become the gold standard for replacement of damaged tissues.

Due to the drawbacks (e.g., donor site morbidity, shortage of resources) of autografts, the need for alternate alloplastic materials is clear. Orthopedic biomaterials, in particular, have been heavily studied, and comprehensively reviewed by Puppi[2] and Shoichet[3] in greater detail. In particular, significant progress has been achieved in engineering materials capable of degrading *in vivo*, either by hydrolytic or enzymatic activity to promote formation of natural osseous tissue, through growth of tissue into the composite material.[4]

This *biodegradable* approach allows for the body to heal itself more gradually, with the scaffold serving as a *temporary* matrix until sufficiently strong osseous tissue can assume a physiological load.[5,6]

Adapted with permission from the *Journal of Materials Chemistry* **2012,** *22,* 22888, by Jason Dyke, Kelly Knight, Huaxing Zhou, Chi-Kai Chiu, Ching-Chang Ko, and Wei You

In response to the needs, several classes of biocompatible and biodegradable polymers have been established for numerous medical applications. Polyesters such as poly(lactic acid) (PLLA)[7-9], poly(glycolic acid) (PLGA)[10], poly(ε-caprolactone) (PCL)[11,12] and poly(trimethylene carbonate) (PTMC)[13-15] have been investigated as native or as in blends[16,17] for a variety of medical applications. Each of these polymers has unique mechanical and degradative properties allowing them to be utilized in a wide range of biomaterials.[2,3,18-21] Though homopolymers have good properties for *in vivo* applications, they are often limited by their diversity in function. Therefore, copolymers present a useful way to obtain tunable properties such as molecular weight, crystallinity, glass transition temperature (T_g), modulus, degradation behavior and tensile strength, all of which can be specifically optimized for use in preparing scaffolds.[10,13] Furthermore, the structure of many of these monomers can be synthetically altered to tailor their properties. These monomers can be combined in nearly endless ways to form functional materials with application specific properties. Because of this, it is important for synthetic chemists to formulate new monomers and design new monomers and polymers in an attempt to improve the utility of materials engineered for specific applications.

Recently, Ko and co-workers created a composite of Hydroxyapatite-Gelatin (HAp-Gel)[22] that mimicked the natural composition and properties of bone[23] and was able to demonstrate promise for *in vivo* and *in vitro* biocompatibility.[24] However, challenges remained in developing useful grafts from these composites because they demonstrated poor processability and insufficient strength when porous. These problems were ultimately improved by incorporation of an additional cross-linking agent, (*N*, *N'*-bis [(3-trimethoxysilyl)propyl]ethylene diamine (enTMOS).[25] This small molecule is capable of undergoing hydrolysis-condensation of alkoxy-silanes to produce a silsesquioxane matrix within the hydroxyapatite-gelatin modified

siloxane (HAp-Gemosil) composite. This helps give additional structural support to the composite and can help impart the network strength of the silane matrix into the composite, leading to enhanced mechanical properties and molding ability. While this matrix did improve the compressive strength and processability of the composite, the short chain siloxane based matrix was brittle and still susceptible to tensile failure. It was clear that a more robust composite was needed in order to further advance this system for potential scaffolding applications. One possible solution is to design and incorporate a biocompatible and cross-linkable polymer of sufficient chain length into the composite.

First, we chose a copolymer of PLLA and PTMC to blend into Hap-Gemosil composites. PLLA has demonstrated previous success in use with hydroxyapatite ceramic composites,[16,26,27] and PLLA's biocompatibility has long been established. However, at physiologic temperature, PLLA is brittle and can contribute to low composite strength.[28] Therefore, an amorphous TMC derivative, Propargyl Carbonate (PC), was synthesized and utilized as the co-monomer. This monomer can act to soften PLLA and toughen brittle composites[29], as demonstrated in previous studies where P(LLA-*co*-TMC) copolymers showed a decrease in T_g with increasing TMC incorporation.[30-32] The combination of both properties from PLLA and PPC (a derivatized PTMC) polymer could help P(LLA-*co*-PC) copolymers to exhibit good flexural strength and elongation, ideal for creating a more robust ceramic composite. In addition, both PLLA and PTMC polymers have unique degradative properties, allowing the degradation behavior of future composites of this formulation to be controlled. Finally, from the synthetic perspective, both of these monomers are ideal candidates for ring-opening polymerizations (ROP), whereby byproducts are avoided and polymers of high MW can be readily obtained.[31-33] Since both monomers share a common method of polymerization, copolymer composition is more easily

controlled. More importantly, cyclic carbonates can be easily derived[34] and the modifications present on PC would allow the incorporation of a pendant silane graft monomers onto the polymer backbone (*vide infra*), while also imparting similar properties to PTMC.

Second, we designed the chosen copolymer to cross-link within the HAp-Gemosil composite because this would lead to improved tensile strength via better long range interaction when compared with physically blending polymer into the composites. Specifically, this approach – designing polymers with cross-linkable grafts – would provide two advantages: (a) increase interfacial adhesion over polymer blends, and (b) enhance long range interactions when compared with composites that are only cross-linked by small molecules (e.g., enTMOS). Consequently, the composite would more effectively mimic the short and long range chemical interactions seen within bone, thereby improving tensile strength of the composite.[35] This should in turn help to resist tensile loading by distributing forces more evenly through the composite, rather than at the point of application.[36] Since HAp-Gemosil composites were originally cross-linked using an amino-silane (enTMOS), it would be ideal to design the copolymer to bear a similar cross-linkable silane group.

However, the sensitivity of the graft monomer's silane groups precluded their direct incorporation prior to polymerization. Therefore, we employed the CuAAC Chemistry ('Click" reactions) to impart the silane functionality to the polymer via post-polymerization functionalization by quantitatively coupling the graft monomer azide to the main chain alkyne of the polymer backbone.[37,38] Thus the PC monomer was synthesized to bear a pendant acetylene group, while the azide functionality was linked with the silane (e.g., 5-azido-*N*-(3-(trimethoxysilyl) propyl) pentanamide). After the copolymerization of LLA and PC, the terminal alkyne group of the copolymer would easily react with the azido-silane (AS) graft monomer via

CuAAC chemistry. This post-polymerization functionalization approach allows the grafting of the silane functionality to occur *after* polymerization, ensuring the fidelity of the silane groups is maintained. P(LLA-*co*-PC)(AS) can then be blended with HAp-Gel and cross-linked in the presence of enTMOS to produce a fully cross-linked composite through hydrolysis–condensation of trialkoxysilyl groups present on both the copolymer and enTMOS. Such programmed composite would improve adhesion through coordination of grafted amide and triazole groups to free carboxylate groups on gelatin and also through silane cross-linking to HAp.

Based on this rationale, we have synthesized and characterized a series of P(LLA-*co*-PC) polymers via Ring-Opening Polymerization (ROP) and functionalized the polymers with pendant silanes. Composites formed by incorporating these polymers with HAp-Gemosil were easily molded and set quickly. To determine the impact of blending P(LLA-*co*-PC)(AS) with HAp-Gemosil, transwell plates were filled with this new composite material and preosteoblasts MC3T3-E1 were cultured in the bottom of these plates for 21 days. It was observed that throughout this period, the growth curves of cells in the presence of either HAp-Gemosil or HAp-Gemosil/P(LLA-*co*-PC)(AS) composites were very similar, suggesting that the synthesized polymer can help improve mechanical properties without negatively impacting the biocompatibility. In addition, both materials showed similar cellular growth curves to those of the control samples, suggesting these materials provide a suitable substrate for cellular attachment and proliferation. Furthermore, biaxial bending tests were undertaken to determine the impact that incorporating P(LLA-*co*-PC)(AS) into a ceramic composite has on flexural strength. It was also observed that this polymer helped increase fiber bridging within the composite, leading to higher flexural strength than that of non-polymeric HAp-Gel composites. These results suggest that the design of this copolymer, and the use of graft monomers as cross-

linking agents possess merit for future study in expanding their applications for bioceramic composites.

2.2 Monomer and Cross-Linker Synthesis

The hydrolysable cyclic TMC inspired carbonate monomer, propargyl carbonate (PC), was synthesized in good yield over four steps from established methods[39] as shown in **Figure 2.1**.

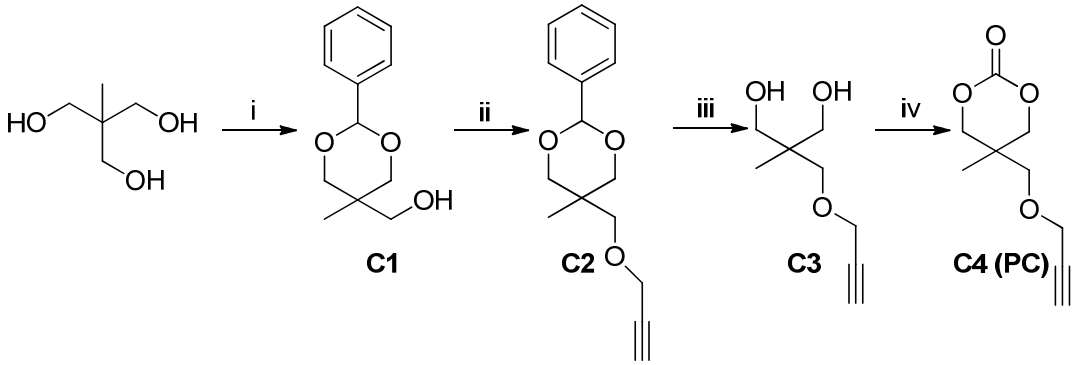

Figure 2.1 *Synthesis of PC monomer from 1,1,1-Tris(hydroxyl methyl)ethane (THME)*

Due to the sensitive nature of both the azide and silane groups on the graft monomer molecule, azido-silane (AS), it is important to utilize a synthesis that would allow for highly pure products in nearly quantitative yields over all steps under mild conditions. The chosen route is highlighted in **Figure 2.2**. To accomplish this, 5-Bromovaleryl chloride was first reacted with 3-aminopropyl trimethoxy silane to yield 5-bromo-*N*-(3-(trimethoxysilyl)propyl)pentanamide (**G1** in **Figure 2.2**). An S_N2 reaction with sodium azide was then performed to yield 5-azido-*N*-(3-(trimethoxysilyl)propyl)pentanamide (AS, **G2** in **Figure 2.2**). Both steps offered products in nearly quantitative yield with no need for purification as confirmed by NMR.

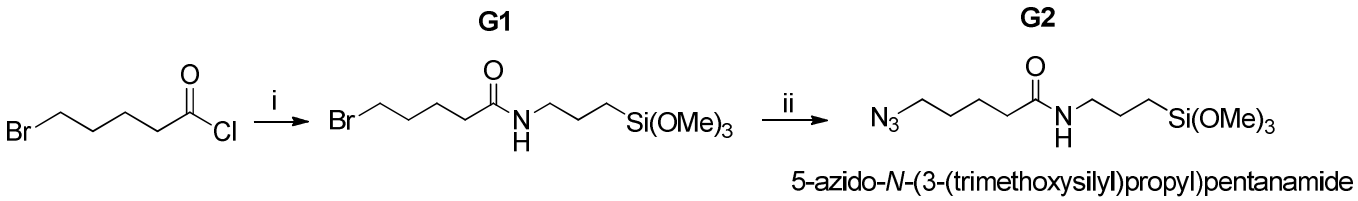

Figure 2.2 *Synthesis of enTMOS inspired, azido-silane graft monomer (AS)*

2.3 Synthesis and Characterization of Copolymers from $Sn(Oct)_2$ Catalyzed ROP

TMC homopolymer and PLLA have different physical properties,[18,19] therefore the percent incorporation of the PC unit (a TMC derivative) in the copolymer would impact important polymer properties such as molecular weight and T_g.[28,30-32,34] More importantly, these properties would determine whether or not the newly designed copolymers are suitable for specific applications.[17] Therefore, understanding the polymerization behavior and related properties of the copolymers precedes the development of composites. To accomplish this, we systematically varied the mol% PC in the load (0 – 100%) to investigate its effect on the polymerization and properties of the copolymer. This information would assist in future composite planning by helping elucidate the underlying chemistry that dictates polymer properties, since these polymer properties will determine how polymers interact within a ceramic composite. The copolymerization was carried out at 120 ºC in toluene and for 20 hours using a $Sn(Oct)_2$ catalyst and 4-*tert*-butylbenzyl alcohol as the initiator **(Figure 2.3**). $Sn(Oct)_2$ was chosen because its versatility in ROP catalysis and ability to run at high temperature. 4-*tert*-butylbenzyl alcohol initiator was employed since its steric bulk can help inhibit intramolecular chain trans-esterification during polymerization.

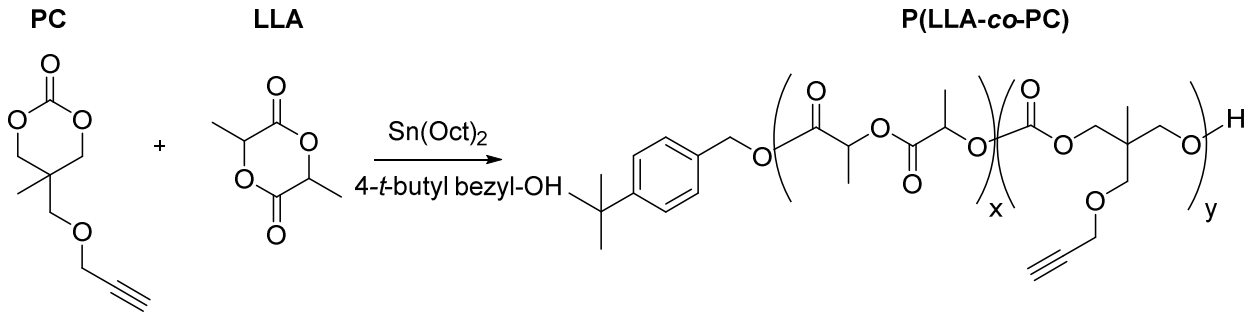

Figure 2.3 *Ring-opening copolymerization of L-Lactide (LLA) and the TMC derivative monomer, Propargyl Carbonate (PC)*

^{1}H NMR was used to determine the ratio of incorporated carbonate to lactide in the polymer by comparing integrations of carbonate methyl (δ = 0.995 ppm) peaks and lactide methine (δ = 5.18 ppm) peaks, while GPC traces were taken from a THF solution of polymer to determine the molecular weight. The number averaged molecular weight (M_n) and %PC incorporation are plotted against the mol% PC loading in **Figure 2.4A** and **2.4B** respectively. The most notable feature from **Figure 2.4A** is that the M_n decreases with the increased loading of the PC monomer, similarly observed by Gu et al. in a recent study.[31] Interestingly, the mol% incorporation of PC in the copolymer, shown in Figure 1B, is consistently lower than the mol% PC loading. Both of these observations can be attributed to the faster rate of polymerization of LLA compared with that of PC as previously reported for similar TMC-LLA copolymers.[30] Previous reports of lactide-carbonate copolymerizations showed that reaction times of >48 hours are needed to obtain high molecular weight copolymers that incorporated a high molar fraction of carbonate monomers.[31]

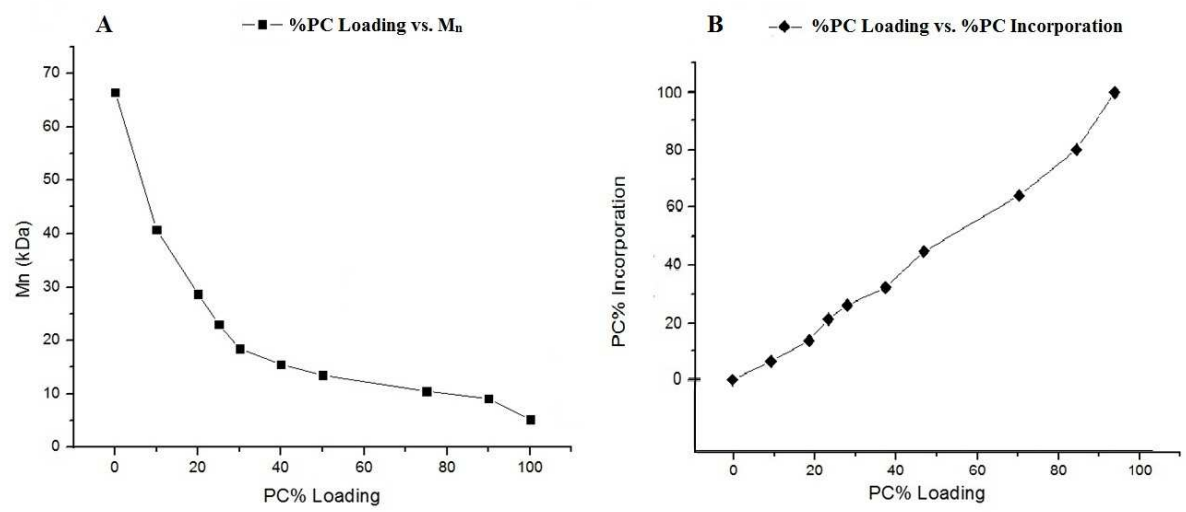

Figure 2.4. *Copolymerization behavior of LLA-PC Ring Opening Polymerizations (A) Polymer molecular weight (M_n) as a function of increasing %PC load. (B) %PC present in the polymer chain as a function of mol fraction loaded before polymerization.*

However, at these elevated temperatures and reaction times, PLLA segments could thermally degrade more readily than polycarbonate segments.[30] In our cases, LLA is consumed faster than PC, resulting in a portion of PC monomers not being incorporated into the copolymer chain in the chosen reaction time (20 h). Instead, these unconsumed PC monomers form low molecular weight (MW) chains (2 – 4 kDa) consisting primarily of poly-propargyl carbonate, or remain as unreacted PC monomer. Due to the low MW and rubbery nature of PC, both remain soluble in methanol and are washed away during precipitation.

Detailed NMR analyses of all polymers elucidate further structural information of these polymers and the random nature of the copolymerization. To identify the chemical origin of each shift in the copolymers, a transition from PLLA homopolymer to PPC homopolymer with a P(LLA-*co*-PC)44.6% copolymer is shown in **Figure 2.5A**. The most interesting and diagnostic feature comes from the lactide protons (**Figure 2.5B**). In low mol %PC samples, a single peak is observed for the methine protons at δ = 5.18 ppm(proton **a** in Figure 2B). As the mol %PC

increases, this methine signal begins to split, with a second peak appearing at δ = 5.02 ppm (proton **b** in **Figure 2.5B**). This secondary methine peak arises as a result of inductive effects on those methine peaks that neighbor a carbonate unit. These protons would feel a weaker de-shielding effect due to the lower electron withdrawing nature of the carbonate when compared with the ester in LLA, and thus will be shifted slightly upfield. This effect is observed only in LLA methine protons that are adjacent to a carbonate in the copolymer. During the copolymerization, if a propagating polymer chain end belongs to a lactide monomer and this "lactide" chain end opens up another lactide monomer, then all methine peaks are equivalent and no alternate shift is observed. When the propagating "lactide" chain end attacks a carbonate

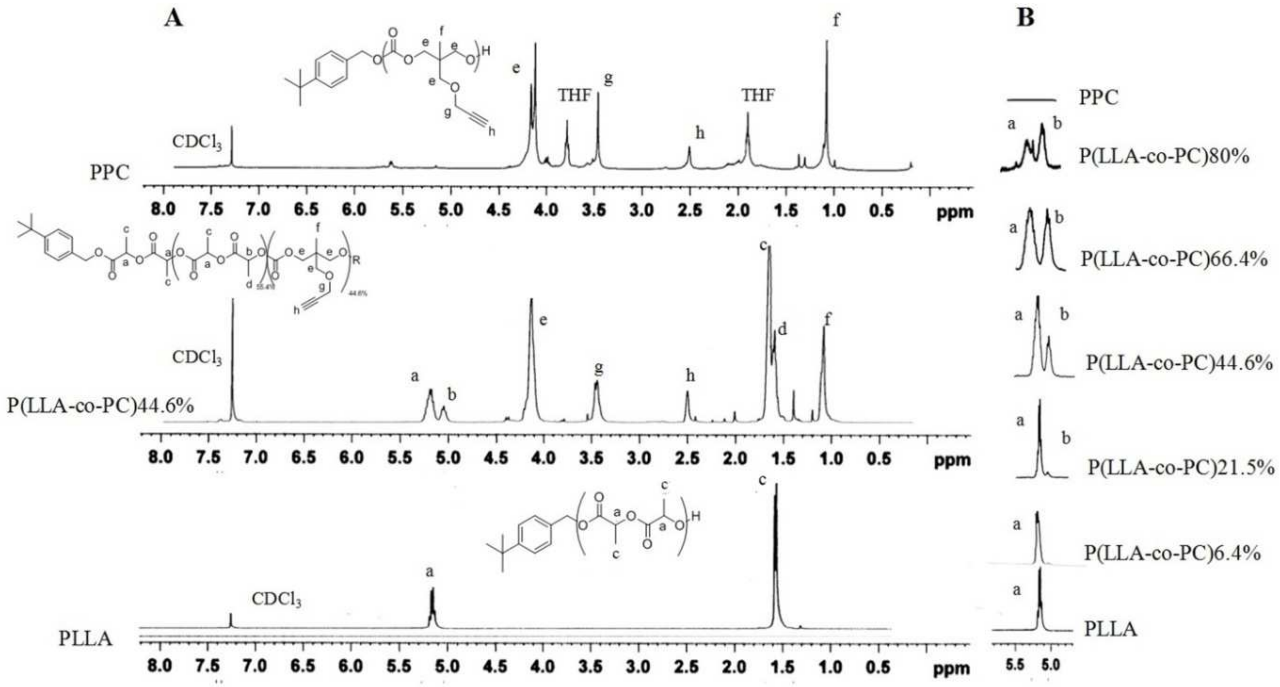

Figure 2.5(A) *NMR spectra for PLLA and PPC homopolymers, as well as a 44.6% PC Containing P(LLA-co-PC) copolymer, illustrating the rise of a secondary methane peak, indicating a statistically random polymerization.* **2.5(B)** *Shows this secondary methane peak growing as the %PC in the copolymer increase.*

however, the additional oxygen on newly incorporated carbonate carbonyl helps slightly shield the α-methine proton that is next to the carbonate and leads to the appearance of a second peak upfield of the first (Figure 2A). This splitting effect is highlighted in Figure 2B. The relative ratio of these methine protons at different chemical shifts (5.18 ppm vs. 5.02 ppm) gradually decreases as the mol % PC increases in the copolymer, indicating the statistically "random" nature of the copolymerization. A summary of polymer composition is given below in **Table 2.1**.

An important implication of employing the copolymer of LLA and PC is to lower the T_g of the copolymer. PLLA is below its T_g at the physiological temperature and the incorporation of PC into its backbone can help reduce crystallinity and lower the T_g of the resultant copolymer.

Table 2.1. Summarized polymerization data for P(LLA-*co*-PC) copolymers.

PC Loading (%PC)[a]	%PC Incorporation[b]	M_n (kDa)[c]	M_w (kDa)
0	0	66.7	93.7
10	6.4	53.0	57.8
20	13.5	28.7	46.6
25	21.05	23.0	35.8
30	25.9	18.6	33.5
40	32.1	15.5	23.3
50	44.6	13.5	22.6
75	64.1	10.5	12.4
90	80	9.1	11.3
100	100	5.2	9.4

[a] Copoymers of LLA and PC, denote by the % loading of PC during polymerization
[b] Incorporation measured by H^1 NMR
[c] Measured by GPC with THF eluent

This provides a route for altering the crystallinity and helping to make the copolymer less brittle. This will allow for improved mechanical properties to be observed under physiological conditions and in turn, helping to raise flexural strength of future composites *in vivo*.[31,40] To demonstrate the impact on the T_g of the copolymer by the introduction of PC into PLLA, DSC traces of three polymers with different mol% incorporation of PC were obtained and compared (**Figure 2.6**).

It is clearly observed that the T_g decreases with the increased PC content. Specifically, the T_g drops from 57.9 ºC for PLLA, to 53.7 ºC for P(LLA-co-PC)(AS)6.4%, and finally to 52.8 ºC for P(LLA-co-PC)(AS)21%. The amorphous nature of the PC monomer helps to influence T_g by altering chain rigidity and hindering the chain's ability to pack effectively.

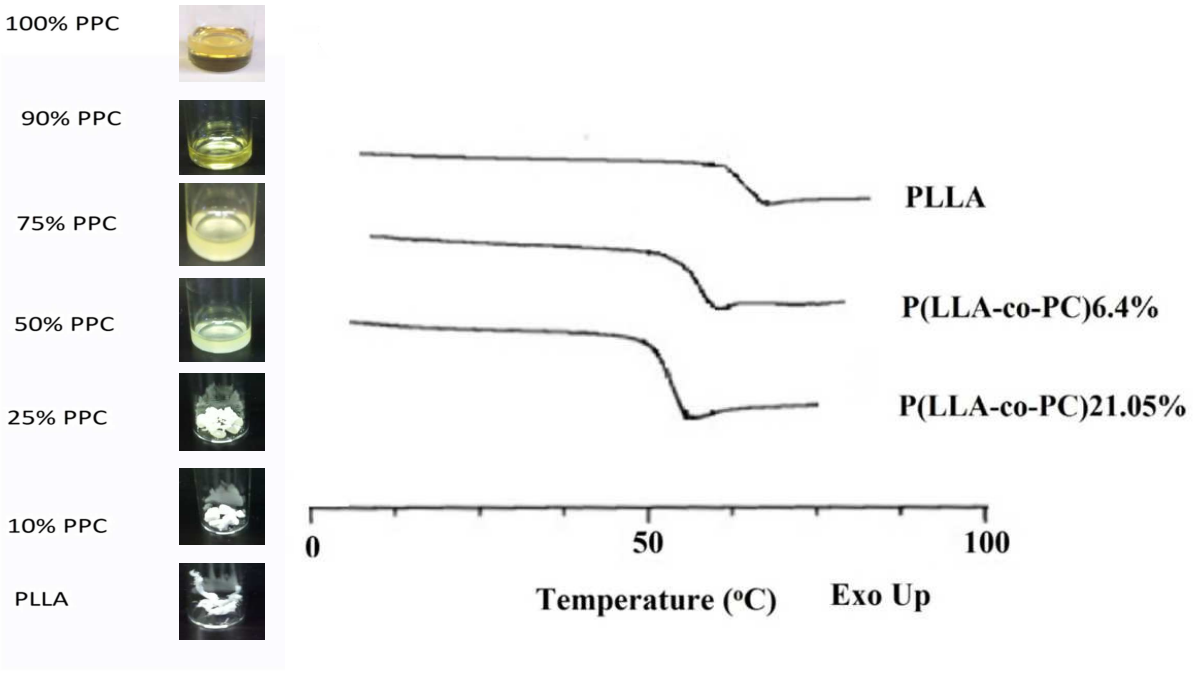

Figure 2.6 *DSC Traces and physical appearance of polymers. Left: Images of several polymers to demonstrate changes in physical appearance caused by changes in polymer chain length and distribution. Right: DSC traces for three of these polymers are given to demonstrate the tunability of T_g as a function of increased %PC content on the polymer backbone.*

Since both the HAp and enTMOS portions of the composite are very brittle, addition of a rubbery copolymer can help improve polymer tensile strength by increasing flexibility and elongation at break within the composite.[14]

PLLA and high PLLA content polymers appear as white fibrous solids at room temperature (0 – 10% PC incorporation) due to the high LLA content. As the mol% PC increases in the polymer, MW decreases and polymers becomes slightly more yellow in appearance, less fibrous and softer. Above 50 mol% PC incorporation, the polymers appear as viscous yellow/orange liquids. These polymers are largely amorphous due to the high PC content in the backbone, which serves to add steric bulk, reduce symmetry, and lower rigidity when compared with LLA segments. The short chain length of these polymers also obstructs effective packing and crystallization of adjacent chains. Examples of the physical appearance of several polymers are also given in Figure 3 for reference.

2.4 Post-Polymerization CuAAC Click Functionalization and Amalgamation

After determining that PC can successfully copolymerize with LLA to give polymers with controlled composition and properties, it was important to functionalize the pendant acetylene of PC to help understand how this functionalized polymer can be processed into HAp-Gemosil composites. CuAAC (a "Click" reaction) allows nearly quantitative coupling of terminal azides to alkynes via Cu(I) catalysis, with few byproducts and little purification needed.[41] This approach was attempted for several PC functionalized copolymers and coupling was observed to be successful.[10,42] This reaction is highlighted in **Figure 2.7**

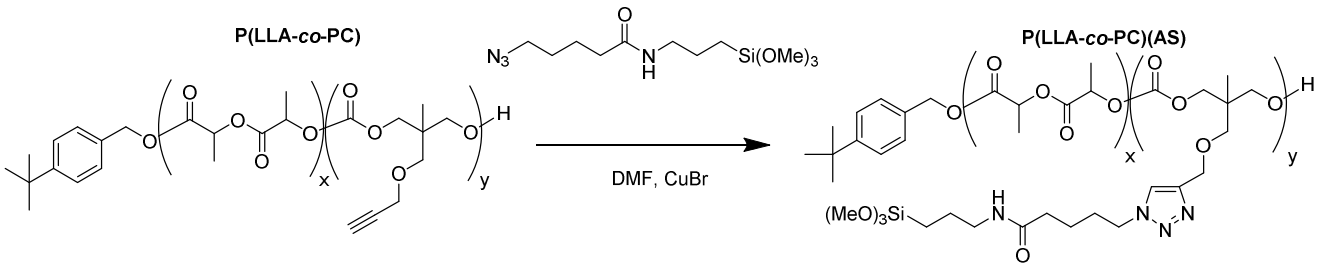

Figure 2.7 *Post-polymerization functionalization of P(LLA-co-PC) with AS via CuAAC "Click" reaction*

However, after the CuAAC reaction, the recovery of polymer after attempted removal of residual copper catalyst proved difficult without initiating minor cross-linking of the grafted AS backbone groups. This cross-linking and subsequent loss of solubility confirmed the coupling reactions were successful. Fortunately, complete gelation was not observed for polymers with low mol %PC (<45%), due to the low density of AS on the backbone. However, the AS functionalized polymers showed poor solubility in PBS buffer and as-formed composites (i.e., copolymer mixed with HAp-Gel) showed poor properties after setting. To remedy this, 10% acetone in PBS buffer was used to facilitate dissolving P(LLA-*co*-PC)(AS) and subsequent blending the polymer with HAp-Gel to create a more homogenous composite. More importantly, using this two-solvent processing, the partially soluble white powder formed after CuAAC can now be further reacted through these un-crosslinked, free alkoxysilyl groups with another silane containing cross-linking reagent, enTMOS, for better setting. The use of enTMOS allows rapid condensation of trialkoxy silanes, to rapidly form a strong cross-linked composite. In our investigation, this functionalized polymer powder is finely ground with HAp-Gel and blended with enTMOS, allowing enTMOS to bond to free siloxane groups of P(LLA-*co*-PC)(AS). This reaction incorporates the newly prepared copolymer into the composite siloxane matrix through

enTMOS. This multiple crosslinking via enTMOS creates a fully linked gel which can be easily formed and allows for chemical linking of polymer to HAp-Gel to enTMOS, increasing long range adhesion and strength. This composite formation and subsequent sol-gel condensation between enTMOS and AS is highlighted in **Figure 2.8.**

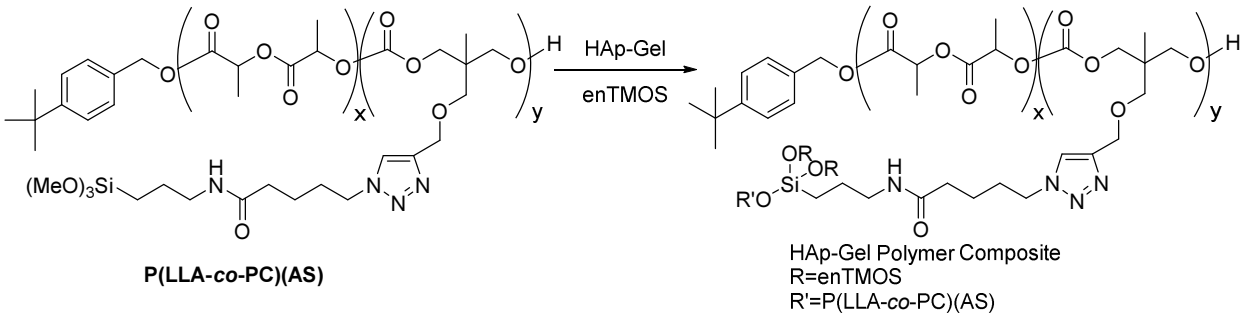

Figure 2.8 *Illustration of amalgamation with HAp-Gel and condensation reactions with enTMOS leading to fully set composite*

After successfully forming these new composites with our designed copolymers incorporated, it was important to see how these newly formed P(LLA-*co*-PC)(AS) composites compared to other previously tested materials. To this end, we carried out the cellular and mechanical studies to determine the effect that polymer blending has on composites when compared with previously studied HAp-Gemosil samples. **Figure 2.9** presents the results of the 21 day MTS assay, It can be seen from these data that, when compared with the control sample, both previous HAp-Gemosil and new HAp-Gemosil/P(LLA-*co*-PC)(AS) composites showed similar biocompatibility over a 21 day period. Furthermore, the resultant growth curves of MC3T3-E1 cells were similar for all three groups. Cells grew up to 7 days and, then, leveled out. This indicates proliferation of cells until reaching they are able to saturate the material. At this point, the number of cells stays relatively constant, demonstrating no substantial leaching of

toxic materials out of the composite over the 21 day time interval. There were no differences in absorbance between the materials and the control, showing no difference in cell viability among the tested substrates.

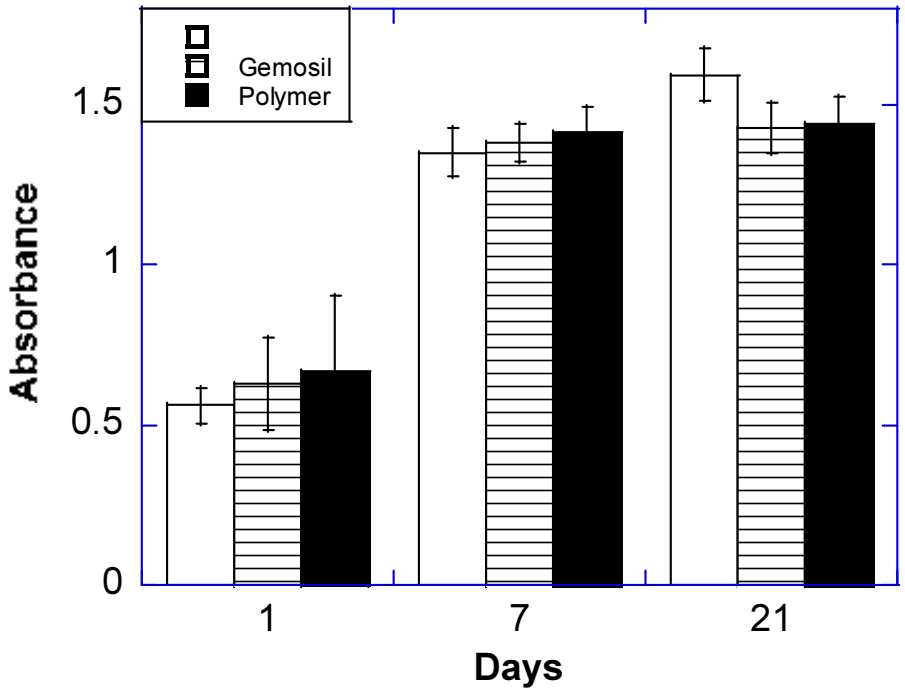

Figure 2.9 *MTS Assay of Control compared to HAp-Gel and HAp-Gel- P(LLA-co-PC)AS 13.5% Composites showing cell viability. Cells were plated in 96 well plates and viability was measured by formazan absorbance at Days 1, 7, and 21*

These data suggest that the incorporation of P(LLA-*co*-PC)(AS) had little to no negative effect on the biocompatibility of HAp-Gemosil composites, and that both materials behaved quite similarly to the control samples with no plated material.

As previously mentioned, HAp-Gemosil composites lacked sufficient flexural strength for use in orthopedic applications. The incorporation of a cross-linkable polymer was expected to help improve long range interaction within the composite. As presented in **Figure 2.10**, the higher flexure strength of HAp-Gemosil/P(LLA-*co*-PC)(AS) composites than that of the original HAp-Gemosil indicates an effect of fiber bridging coming from the blended long chain copolymers. In fact, the polymer containing composites demonstrated an increase in flexural

strength of nearly 40% compared to HAp-Gemosil composites. On average, flexural strength of HAp-Gemosil

(41± 9 MPa) increased for HAp-Gemosil/P(LLA-*co*-PC)(AS) (58± 14 MPa).

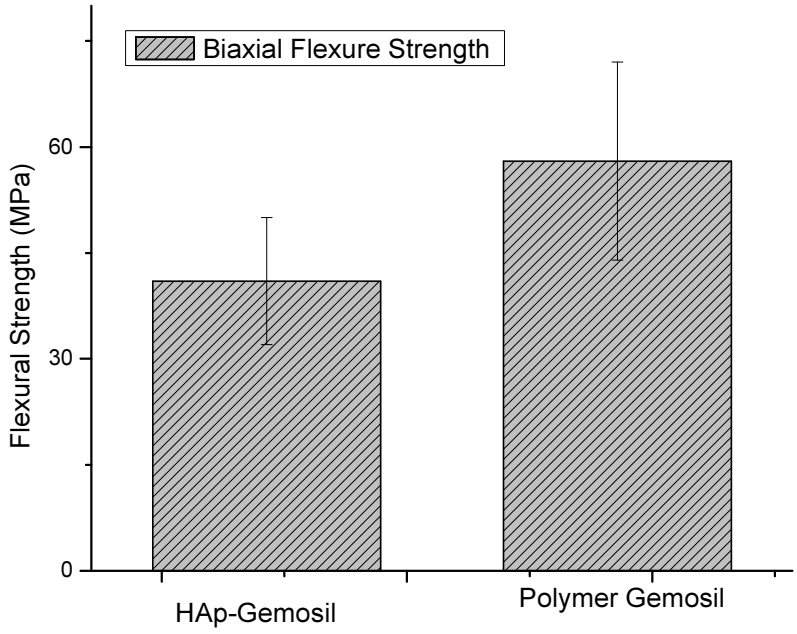

Figure 2.10 *Changes in biaxial flexure strength between HAp-Gemosil and HAp-Gemosil doped with P(LLA-co-PC)AS13.5% co polymers.*

The stiffness of the force-displacement curve recorded from the biaxial bending test did not differ (P=0.08) between the original (2.06 N/mm) and the new (2.15 N/mm) composites. In our in-house data, the HAp-Gemosil had a compressive modulus around 862±129 MPa and a reduced modulus 18.0±4.9 GPa measured by the nanoindentation tester (Hysitron Inc.) Based on the stiffness data, we expect that the new composite might have similar modulus values although future tests are required.

Though the results from initial biocompatibility and mechanical tests are promising, this polymer system presents several key limitations. Primarily, the sensitivity of the P(LLA-*co*-PC)(AS) lead to premature cross-linking of polymer bound silanes. This in turn made complete blending of composite cements with the polymer more difficult. This presented multiple negative

consequences when dealing with this HAp-Gemosil/P(LLA-*co*-PC)(AS) bioceramic composite. Primarily, this limitation can influence reproducibility and utility of composites like those tested in this study. The use of a second, less polar solvent (acetone) during blending helped improve composite formation, making it possible to study the interaction of this polymer within HAp-Gemosil composites. Unfortunately, the use of organic solvents removes our ability to dope this composite with cells for scaffolding applications, and these processing issues hinder the ability to study composite interactions *in vivo*. Furthermore, this second solvent helped blend phases during processing, but ultimately did not solve all problems associated with blending a hydrophobic inorganic ceramic (HAp-Gel) with a hydrophilic polymer phase (P(LLA-*co*-PC)(AS). This mismatch manifested itself in displaying poor interfacial adhesion between components. Although this was still able to provide considerable fiber bridging and improved flexural strength, it led to a large decrease in compressive strength when compared to HAp-Gemosil, showing in **Figure 2.11.**Though HAp-Gemosil did not possess the compressive strength of natural bone, it was sufficiently close for consideration.

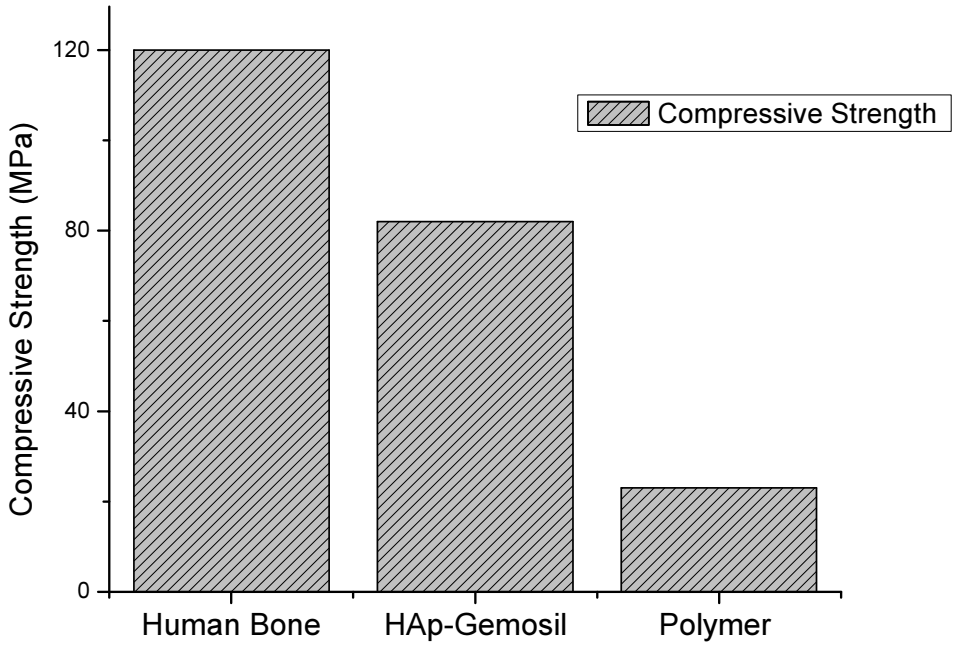

Figure 2.11 *Changes in compressive strength observed between HAp-Gemosil and HAp-Gemosil doped with polymer, compared to natural cortical bone.*

However, the large decrease seen in polymer doped samples makes it insufficient for consideration as a load bearing material for orthopedic applications, further complicating this materials ability to be used for potential scaffolding applications.

Despite the drawbacks, this system still showed merit in improving some properties of HAp-Gemosil composites, while preserving their biocompatibility. Improvements in cross-linking chemistry are required to allow for better processability and material performance. These improvements would allow this system to be more rigorously studied *in vivo* to determine the efficacy of this polymer/ceramic system for future scaffolding applications.

2.5. Conclusions

In summary, we have synthesized a derivatized TMC monomer, PC, which is capable of undergoing ROP with L-Lactide to afford copolymers with tunable MW, mol % PC incorporation and T_g. The ability of these monomers to copolymerize and yield potentially biodegradable and biocompatible polymers of tunable properties makes this an attractive system for biological applications. In the current demonstration, we coupled the copolymer with AS graft agents inspired by enTMOS, converting the copolymer into "cross-linkable" via these pendant silane groups. After being processed into the original HAp-Gemosil cement composite facilitated by the amino-silane enTMOS, these AS functionalized polymers were capable of bridging the new composite and providing enhanced long range adhesion, while still maintaining the biocompatibility of the new composite.

The current grafting approach did have some key limitations, however. Notably, the sensitivity of polymer bound silanes prevented extensive purification after CuAAC coupling. As a result, some residual copper from CuAAC was generally trapped in the composite after

coupling, which could lead to the possibility of increased cell morbidity. Furthermore, the premature cross-linking could contribute to an inability of these polymers to fully cross-link into the enTMOS silsesquioxane matrix, leading to poor adhesion between the hydrophobic polymer and the hydrophilic HAp-Gel moieties in the composite. Therefore, further work remains to be done, especially regarding the graft monomer and cross-linking. Fortunately, the PC monomer introduces a pendant acetylene group on the copolymer, which provides a synthetic handle for post-polymerization modification to give more synthetic freedom. This 'acetylene handle' allows various pendant groups to be attached to the copolymer, thus one can further alter the composite properties to obtain unique, applications specific properties. Future composites will be synthesized using similar P(LLA-*co*-PC) polymers as the chemistry and properties of these copolymers have been elucidated in this study, but emphasis will be placed on utilizing alternate "click" reactions which can preclude the use of potentially toxic catalysis. Alternate graft monomers will also be investigated to determine a method for cross-linking which can be easily degraded. This will eliminate potential problems caused by residual material left after degradation. Additionally, a less sensitive method of cross-linking would be ideal as to allow better control of cross-linking reactions and thereby improve processing of the final composite. If these issues can be sufficiently addressed, this HAp-Gemosil-P(LLA-co-PC)(AS) copolymer system will provide a new springboard to undertake further scaffolding composite work.

2.6 Experimental Details

General Methods

All moisture sensitive reactions were performed in flame-dried glassware under an atmosphere of Ar. Reaction temperatures were recorded as external bath temperatures. The phrase "concentrated under reduced pressure" refers to the removal of volatile materials by

distillation using a Büchi rotary evaporator at water aspirator pressure (< 20 torr) followed by removal of residual volatile materials under high vacuum (< 1 torr). The term "high vacuum" refers to vacuum achieved by a standard belt-drive oil pump (< 1 torr).

^{1}H and ^{13}C NMR spectra were recorded on Bruker AC-400 (400 MHz) spectrometers. Chemical shifts are reported in parts per million (ppm) relative to residual solvent peaks (CHCl3: 1H: d 7.26). Peak multiplicity is reported as: singlet (s), doublet (d), triplet (t), quartet (q), multiplet (m), and broad (br).

Materials

Ethyl chloroformate (99%) and CaH_2 (60% in mineral oil), and 4-*tert* butyl benzyl alcohol (98%) were obtained from Acros Organic and used as received. 1,1,1-Tris(hydroxyl methyl)ethane (THME, 99%), triethylamine (TEA, 99%), 5-bromovaleryl chloride (98%) and CuBr (98%) were obtained from Alfa Aesar and used as received. Benzaldehyde (Aldrich 98%), *p*-toluene sulfonic acid (TsOH, Aldrich, 98.5%), (*N*, *N'*-bis [(3-trimethoxysilyl)propyl]ethylene diamine (enTMOS, 95% in MeOH, Gelest), tin(II) 2-ethyl hexanoate ($SnOct_2$ 98% MP Biomedicals), propargyl bromide (80% in toluene, TCI) and 3-aminopropyl trimethoxy silane (96% TCI) were used as received. L-Lactide was generously donated by Purac and used without further purification. Hexanes, acetone, chloroform, dichloromethane (DCM), anhydrous toluene, anhydrous methanol (MeOH), ethyl acetate and tetrahydrofuran (THF) were obtained from Fisher. THF was freshly distilled over sodium before use.

Synthesis of (Propargyl Carbonate (PC)) Monomer

Synthesis of PC monomer is adapted from previously reported work by Chen et al.[39] A typical synthesis of PC is presented and outlined in **Figure 2.1**. THME (26 g, 0.217 mmol) and TsOH (1.2 g, 6.3 mmol) were dissolved in anhydrous THF (400 mL) and stirred at room

temperature. To this stirring solution, benzaldehyde (23.2 mL, 0.23 mmol) was added dropwise and allowed to react for 16 hours. The reaction was then neutralized with aqueous ammonia and concentrated by rotary evaporation. The product was then dissolved in DCM and washed 3 times with water before again concentrating under rotary evaporation to yield 39 g (94%) of **C1** as a colorless solid. ^{1}H NMR (400 MHz, $CDCl_3$): δ 0.81 (s, 3H), 3.66 (d,2H), 3.91 (s, 2H), 4.06 (d, 2H), 5.44 (s, 1H), 7.35-7.49 (m, 5H).

C1 (35 g, 168 mmol) in THF (50 mL) were added dropwise to a cold stirring solution of NaH (60% in mineral oil, 12 g, 302 mmol) at 0 ºC to yield a milky white solution. After 30 minutes of cold stirring, the solution was heated on oil bath to 60 ºC for 2 hours, yielding a pale yellow solution. Propargyl bromide (25 g, 211 mmol) was then added dropwise and allowed to stir for 16 hours. This solution was then quenched with water to afford a deep red solution with precipitate. This solution was extracted 3 times with brine and concentrated under high vacuum to yield crude **C2** as a red oil.

Crude **C2** (12 g, 48.7 mmol) was stirred in 400 mL 1:1 v/v MeOH:1M HCl for 2 hours. 1M NaOH was then used to raise the pH to 7 before MeOH was removed by rotary evaporation. The product was extracted using ethyl acetate to yield crude **C3**. Purification via flash chromatography using 2:1 ethyl acetate: hexanes yielded 6.1g (54% over 2 steps) **C3** as an orange oil. ^{1}H NMR (400 MHz, CDCl3): δ 0.84 (s, 3H), 1.65 (b, 2H) 2.45 (s, 1H) 3.49 (s, 2H) 3.58(d, 2H), 3.67(d, 2H), 4.15(s, 2H)

C3 was dissolved (5.18 g, 32.7 mmol) with ethyl chloroformate (6.68 g, 65 mmol) in THF (300 mL). Triethyl amine(7.1 g, 65 mmol) was then added to this stirring solution dropwise and allowed to react for 4 hours. Water was then used to quench the reaction slowly and the reaction was washed with brine. The organic layer was then concentrated by rotary

evaporation and then purified via flash chromatography with 2:1 hexanes: ethyl acetate to yield 4.52 g (75%) Propargyl Carbonate (PC). ^{1}H NMR (400 MHz, CDCl3): δ 1.11 (s, 3H) 2.46 (s, 1H), 3.49(s, 2H), 4.07 (d, 2H), 4.17 (s, 2H) 4.33 (d, 2H). ^{13}C NMR (400 MHz, $CDCl_3$) δ 17.26, 32.8, 58.7, 70.66, 73.81, 75.25, 78.83, 148.17

Synthesis of Graft Monomer: 5-azido-*N*-(3-(trimethoxysilyl) propyl) pentanamide (AS)

Synthesis of AS is shown in **Figure 2.2**. To a dry flask, (3-aminopropyl)trimethoxysilane (1.44 g, 8 mmol) were dissolved in THF with TEA (1 g, 10 mmol) and set to stir (clear solution). 5-bromovaleryl chloride (2 g, 10 mmol) was then added dropwise, forming a white precipitate. This solution was allowed to react for 16 hours under argon. The solution was subsequently filtered to remove the salt and concentrated by rotary evaporation to yield 2.73 g (99%) **G1** without further purification. ^{1}H NMR (400 MHz, CDCl3): δ 0.65 (q, 2H), 1.63 (p, 2H), 1.80 (m, 4H), 2.19 (t, 2H), 3.24 (t, 2H) 3.4 (t, 2H), 3.57 (s, 9H), 5.65 (b,1H)

G1 (2.73 g, 8 mmol) was then dissolved in anhydrous DMF and added to NaN_3 under dry conditions. This was allowed to react for 16 hours under argon atmosphere. DMF was then removed under vacuum for 36 hours before dry EtOAc was used to extract AS and the compound was again concentrated to yield pure AS 2.4 g (98%) which was stored under dry conditions in a glovebox. ^{1}H NMR (400 MHz, CDCl3): δ 0.65 (t, 2H), 1.78 (m, 6H), 2.19 (t, 2H), 3.26 (m, 4H), 3.41 (s, 9H), 5.69 (s, 1H). ^{13}C NMR (400MHz, $CDCl_3$) δ 6.46, 22.68, 22.81, 28.34, 35.83, 41.77, 50.45, 51.09, 172.27

Synthesis of Copolymers by $Sn(Oct)_2$ Catalyzed ROP

PC monomer was purified by flash chromatography and its purity was verified by NMR analysis. The monomer was dried over CaH_2 before use. Polymerization was carried out in toluene at 120 ºC for 20 hours using 4-*tert*-butylbenzyl alcohol as the initiator and stannous-2-

ethyl hexanoate ($Sn(Oct)_2$) as the catalyst as shown in **Figure 2.3**. The ratio of monomers to catalyst to initiator was 100:1:1 [M]:[C]:[I] for all polymerizations. The following is a typical synthesis for copolymer with 10 mol% PC loading. In a glovebox under argon atmosphere, LLA (7 g, 48 mmol) and PC (0.884 g, 4.8 mmol) were added to a high pressure flask with 10 mL anhydrous toluene. To this solution, $Sn(Oct)_2$ and 4-*tert*-butylbenzyl alcohol (0.075 M, 7 mL) were added quickly and the vessel was then sealed. The reaction container was quickly transferred to an oil bath outside of the glovebox and allowed to react for 20 hours before quenching with methanol. The resulting polymer P(LLA-*co*-PC) was isolated by precipitation into cold MeOH, and further purified by precipitation from the DCM solution of the polymer into cold methanol 3 times. NMR analysis revealed this polymer to contain 6.4 mol% PC in the backbone and thus was denoted as P(LLA-*co*-PC) 6.4% for clarity.

Characterization of Polymers

The monomer incorporation ratio of all copolymers was determined using a Bruker spectrometer (400 MHz). $CDCl_3$ was used as the solvent and the chemical shifts were calibrated against residual solvent signals. The molecular weight and polydispersity of the copolymers were determined by a Waters 1515 gel permeation chromatograph (GPC) using THF as the eluent at a flow rate of 1.0 mL/min at 30 ºC. A series of narrow polystyrene standards was used for the calibration of the columns. Thermal behavior was investigated using a TA Q100 differential scanning calorimeter (DSC) under nitrogen atmosphere. All samples were scanned from – 10 ºC to 200 ºC at 10 ºC/min before being quenched with liquid nitrogen. The samples were then rescanned from – 10 ºC to 200 ºC and data were collected. Glass transition (T_g) was taken as the midpoint of heat capacity change and crystallization (T_c) and melting (T_m) were shown by exo- and endo-thermal peaks, respectively.

Post Polymerization Modification of Polymers via CuAAC

CuAAC reactions were performed in anhydrous DMF at room temperature under argon atmosphere. A typical synthesis of P(LLA-*co*-PC) 6.4% follows. The azide containing linking monomer (AS), was dissolved with P(LLA-*co*-PC) 6.4% and CuBr in DMF. Load ratios of AS to acetylene groups of the polymer were 1.1:1 (slight excess of AS) and CuBr was loaded at 2 mol%. Elemental copper was added in trace amounts to help stabilize Cu(I) ions in solution. This reaction is allowed to run for 2 hours before precipitation in cold MeOH to yield white powder of AS functionalized polymer P(LLA-*co*-PC)(AS) 6.4%. Polymers were treated with EDTA prior to precipitation in methanol to help remove excess copper catalyst.

Amalgamation of AS Functionalized Polymer

Composite cement materials were prepared for biaxial flexure and biocompatibility testing using P(LLA-*co*-PC)(AS)13.5% loaded at 10wt% into the composite A typical composite formation is presented here with 10 wt% copolymer in the composite. HAp-Gel (250 mg), prepared as previously reported[25], was mixed with P(LLA-*co*-PC)(AS)13.5% (25 mg) and the blend was ground into a fine powder. Next, 100 μL of enTMOS (95% in MeOH) was added to the powder and mixed thoroughly. To this mixture, a 10% acetone in PBS solution (420 μL) was added while gently kneading the composite into a clay. This clay was then formed into a mold and pressed to remove excess solvent. It was left for a minimum of 72 hours at room temperature to dry. This procedure was repeated for all composites. After drying, a solid material was obtained which could be trimmed and used to test the material's flexural strength.

Biaxial flexure strength

The testing procedure for biaxial flexure strength was performed according to Ban and Anusavice.[43] Four sample disks (diameter 10 mm by thickness 1mm) of each group (HAp-Gemosil and HAp-Gemosil/P(LLA-*co*-PC)AS 13.5%) were prepared in Teflon molds. The upper and lower surfaces were polished in order to obtain parallel surfaces with no apparent defects. After measuring the sample diameter (d) and thickness (t), the disk was supported on three stainless steel balls (3mm in diameter), which were equally spaced along a 3.25mm radius (r_s). Prior to testing, a stainless steel piston (radius = r_p=1.5mm) was aligned concentrically with the three balls (**Figure 2.12**). A crosshead speed of 0.5mm/min was used, and the maximum force at failure (P) was determined using an Instron 4411 Machine (model 4411, Instron Co., Norwood, MA). A Poisson's ratio (ν) of 0.3 was used for both materials. The flexure stress at failure (σ in MPa) was calculated using the following expressions:

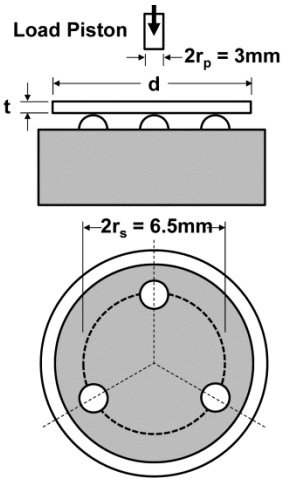

Figure 2.12 *Biaxial flexure test apparatus.*

$$\sigma = AP/t^2$$

and $A = \left(\frac{3}{4}\pi\right)[2(1+\nu)\ln\left(\frac{r_s}{r_o}\right) + (1-\nu)(2r_s^2 - r_o^2)2(\frac{d}{2})^2 + (1+\nu)]$

where $r_o = \left(1.6r_p^2 + t^2\right)^{\frac{1}{2}} - 0.675t$

Viability test: Preosteoblast cell proliferation by MTS Assay

The 6-well transwell plate (Corning Transwell-Clear Permeable Supports) was used for cell proliferation testing. The material disc (diameter 15mm by thickness 1mm) was placed on the permeable membrane support of the transwell, which allowed materials immersed in the

culture medium. The 1×10^{-5} Preosteoblasts MC3T3-E1 were seeded to each well. Every three days, the medium was replenished with 2ml fresh growth medium (α-Minimum Essential Medium with 10% fetal bovine serum and 1% penicillin and streptomycin). At the end of cultivation (1, 7, and 21 days in culture), the disk and the permeable support were removed. 40 µL of 3-(4,5-dimethylthiazol-2-yl)-5-(3-carboxymethoxy-phenyl)-2-(4-sulfophenyl)-2H-tetrazolium salt (MTS) reagent (Promega, Madison, WI USA) was added to each well containing 400 µL of αMEM, and the plate was incubated for 1 hour at 37°C under a humidified atmosphere of 5% CO_2. From each well, 100 µL of the mixed solution was transferred into well of a 96-well plate. Each well was triplicated. The absorbance of each well at 490 nm was measured using a microplate reader (Microplate Reader 550, Bio-Rad laboratories, Philadelphia, USA). Relative cell numbers were quantified on the basis of the concentration of the formazan product of MTS. Three samples will be used at each time point for each material group. Three experimental groups of materials were investigated, including Gemosil, Gemosil/P(LLA-*co*-PC)AS 13.5%, and dishes as received without coating (control).

Acknowledgments

The authors acknowledge funding from NC Biotech Grant #2008-MRG-1108, NIH/NIDCR, K08DE018695 American Association of Orthodontist Foundation, and UNC University Research Council. We thank Wonhee Jeong for many useful discussions regarding our work and John Whitley for his assistance in characterizing and testing polymers and composites. Additionally we thank Purac Biomaterials for their generous donation of L-Lactide for this project.

REFERENCES

(1) Field, R. A.; Riley, M. L.; Mello, F. C.; Corbridge, J. H.; Kotula, A. W. *J. Anim Sci.* **1974**, *39*, 493-499.

(2) Puppi, D.; Chiellini, F.; Piras, A. M.; Chiellini, E. *Progress in Polymer Science* **2010**, *35*, 403-440.

(3) Shoichet, M. S. *Macromolecules* **2009**, *43*, 581-591.

(4) Bongio, M.; van den Beucken, J. J. J. P.; Leeuwenburgh, S. C. G.; Jansen, J. A. *Journal of Materials Chemistry* **2010**, *20*, 8747-8759.

(5) Imam Khasim, H. R.; Henning, S.; Michler, G. H.; Brand, J. *Macromolecular Symposia* **2010**, *294*, 144-152.

(6) Rezwan, K.; Chen, Q. Z.; Blaker, J. J.; Boccaccini, A. R. *Biomaterials* **2006**, *27*, 3413-3431.

(7) Roether, J. A.; Boccaccini, A. R.; Hench, L. L.; Maquet, V.; Gautier, S.; Jérôme, R. *Biomaterials* **2002**, *23*, 3871-3878.

(8) Declercq, H.; Cornelissen, M.; Gorskiy, T.; Schacht, E. *Journal of Materials Science: Materials in Medicine* **2006**, *17*, 113-122.

(9) Oh, J. K. *Soft Matter* **2011**, *7*, 5096-5108.

(10) Jiang, X.; Vogel, E. B.; Smith, M. R.; Baker, G. L. *Macromolecules* **2008**, *41*, 1937-1944.

(11) Shokrollahi, P.; Mirzadeh, H.; Scherman, O. A.; Huck, W. T. S. *Journal of Biomedical Materials Research Part A* **2010**, *95A*, 209-221.

(12) Zhou, Y.; Hutmacher, D. W.; Varawan, S.-L.; Lim, T. M. *Polymer International* **2007**, *56*, 333-342.

(13) Bat, E.; van Kooten, T. G.; Feijen, J.; Grijpma, D. W. *Macromolecular Bioscience* **2011**, *11*, 952-961.

(14) Andronova, N.; Albertsson, A.-C. *Biomacromolecules* **2006**, *7*, 1489-1495.

(15) Dargaville, B. L.; Vaquette, C.; Peng, H.; Rasoul, F.; Chau, Y. Q.; Cooper-White, J. J.; Campbell, J. H.; Whittaker, A. K. *Biomacromolecules* **2011**, *12*, 3856-3869.

(16) Jiang, T.; Nukavarapu, S. P.; Deng, M.; Jabbarzadeh, E.; Kofron, M. D.; Doty, S. B.; Abdel-Fattah, W. I.; Laurencin, C. T. *Acta Biomaterialia* **2010**, *6*, 3457-3470.

(17) Bat, E.; Plantinga, J. e. A.; Harmsen, M. C.; van Luyn, M. J. A.; Zhang, Z.; Grijpma, D. W.; Feijen, J. *Biomacromolecules* **2008**, *9*, 3208-3215.

(18) Middleton, J. C.; Tipton, A. J. *Biomaterials* **2000**, *21*, 2335-2346.

(19) Hench, L. L. *Annual Review of Materials Science* **1975**, *5*, 279-300.

(20) Mukherjee, S.; Gualandi, C.; Focarete, M.; Ravichandran, R.; Venugopal, J.; Raghunath, M.; Ramakrishna, S. *Journal of Materials Science: Materials in Medicine* **2011**, *22*, 1689-1699.

(21) Zheng, L.; Yang, F.; Shen, H.; Hu, X.; Mochizuki, C.; Sato, M.; Wang, S.; Zhang, Y. *Biomaterials* **2011**, *32*, 7053-7059.

(22) Chang, M. C.; Ko, C.-C.; Douglas, W. H. *Biomaterials* **2003**, *24*, 2853-2862.

(23) Ko CC, O. M., Fallgatter AM, Hu W-S. *J. Material Research* **2006**, *21*, 8.

(24) Ko CC, W. Y.-L., Douglas WH, Narayanan R, Edi. Aizenberg J, Landis WJ, Orme C and Wang R, Hu W-S. *Symposium Proceedings Material Research Society Spring Meeting* **2004**, *823*, 5.

(25) Luo, T.-J.; Ko, C.-C.; Chiu, C.-K.; Llyod, J.; Huh, U. *Journal of Sol-Gel Science and Technology* **2010**, *53*, 459-465.

(26) Deng, X.; Hao, J.; Wang, C. *Biomaterials* **2001**, *22*, 2867-2873.

(27) Todo, M.; Kagawa, T. *Journal of Materials Science* **2008**, *43*, 799-801.

(28) Zhang, L.; Goh, S. H.; Lee, S. Y. *Polymer* **1998**, *39*, 4841-4847.

(29) Zhang, C.; Subramanian, H.; Grailer, J. J.; Tiwari, A.; Pilla, S.; Steeber, D. A.; Gong, S. *Polymers for Advanced Technologies* **2009**, *20*, 742-747.

(30) Ruckenstein, E.; Yuan, Y. *Journal of Applied Polymer Science* **1998**, *69*, 1429-1434.

(31) Ji, L.-J.; Lai, K.-L.; He, B.; Wang, G.; Song, L.-Q.; Wu, Y.; Gu, Z.-W. *Biomedical Materials* **2010**, *5*, 045009.

(32) Tyson, T.; Finne-Wistrand, A.; Albertsson, A.-C. *Biomacromolecules* **2008**, *10*, 149-154.

(33) Nederberg, F.; Lohmeijer, B. G. G.; Leibfarth, F.; Pratt, R. C.; Choi, J.; Dove, A. P.; Waymouth, R. M.; Hedrick, J. L. *Biomacromolecules* **2006**, *8*, 153-160.

(34) Vandenberg, E. J.; Tian, D. *Macromolecules* **1999**, *32*, 3613-3619.

(35) Durucan, C.; Brown, P. W. *Advanced Engineering Materials* **2001**, *3*, 227-231.

(36) Hoffmann, F.; Cornelius, M.; Morell, J.; Fröba, M. *Angewandte Chemie International Edition* **2006**, *45*, 3216-3251.

(37) Lutz, J.-F. *Angewandte Chemie International Edition* **2007**, *46*, 1018-1025.

(38) Binder, W. H.; Sachsenhofer, R. *Macromolecular Rapid Communications* **2007**, *28*, 15-54.

(39) Chen, W.; Yang, H.; Wang, R.; Cheng, R.; Meng, F.; Wei, W.; Zhong, Z. *Macromolecules* **2010**, *43*, 201-207.

(40) Valliant, E. M.; Jones, J. R. *Soft Matter* **2011**, *7*, 5083-5095.

(41) Kolb, H. C.; Finn, M. G.; Sharpless, K. B. *Angewandte Chemie International Edition* **2001**, *40*, 2004-2021.

(42) Parrish, B.; Breitenkamp, R. B.; Emrick, T. *Journal of the American Chemical Society* **2005**, *127*, 7404-7410.

(43) Ban, S.; Anusavice, K. J. *Journal of Dental Research* **1990**, *69*, 1791-1799.

CHAPTER 3: THE ROLE OF TEMPERATURE IN FORMING SOL-GEL BIOCOMPOSITES CONTAINING POLYDOPAMINE

In the previous chapter, the utility of adding polymers to bioceramics was discussed. In particular, a novel bioceramic composite known as HAp-Gel was introduced, and its physical properties were improved by the addition of a tri-alkoxy silane cross-linker. However, despite the numerous favorable properties, further improvements were required. The addition of copolymers to these composites was able to improve flexural strength of these materials and increase their potential for future clinical applications.

Copolymers envisioned to mimic the role of collagen in natural bone, and were designed based on the physical properties of their homopolymers. L-Lactide was chosen for its established biocompatibility, good mechanical properties, and established use in bioceramic materials. To compliment this monomer, a trimethylene carbonate derivative was also synthesized to provide a synthetic handle through which the copolymer can be incorporated into the composite to help improve long range order, mimicking the role of collagen in natural bone. Furthermore, this monomer also served to help tune properties in the copolymer to improve composite performance.

While substantial improvements were made in regards to ultimate tensile strength, without compromising biocompatibility and processability of these polymer containing composites, difficulties were also encountered. Specifically, the utilization of a hydrophobic polymer in conjunction with a hydrophilic bioceramic HAp-Gel led to a loss of compressive strength caused by poor interfacial adhesion between the HAp and polymer phases. Though the polymer was able to mimic some aspects of collagen in natural osseous tissue, the poor adhesion to the rest of the composite necessitated improvements in the polymeric component of these materials.

In the following chapter, a logical extension of the chemistry described in **Chapter 2** will be discussed. Since the addition of polymers was able to help performance of these composites, and problems were encountered through poor adhesion, this chapter aims to utilize polymers with better adhesive properties in HAp-Gel composites. In this way, it is believed that the favorable aspects of polymeric blending would be maintained, without the loss of strength due to poor adhesion between inorganic and organic constituents of the composite.

3.1. Motivations and Background on HAp-Gel and Polydopamine Containing Materials

Our previous study has demonstrated the ability of HAp-Gel to provide a suitable substrate for osteoblast attachment, growth, and subsequent osteogenesis.[1] These composites, however, were shown to require cross-linking from bis[3-(trimethoxysilyl)-propyl]ethylenediamine (enTMOS) to increase strength.[2] These composites, termed as HAp-Gemosil (i.e., hydroxyapatite–gelatin modified with siloxane), successfully showed improved compressive strength and processability without sacrificing biocompatibility or osteoconductivity. Unfortunately, the inclusion of the enTMOS network resulted in composites which were still too brittle for *in vivo* use. Prior work with bioceramics has shown that the incorporation of polymer chains into the ceramic matrix can help improve mechanical properties and strength of these composites, as well as *in vivo* and *in vitro* biocompatibility.[3] This trend was also observed in a modified HAp-Gemosil composite utilizing a biodegradable polymer based on L-lactide to improve the flexural strength.[4] Though the flexural strength was indeed increased, the polymer toughened HAp-Gemosil composites were plagued by poor adhesion between the hydrophilic HAp-Gel and the hydrophobic polymer, leading to a loss in the compressive strength. Good adhesion between components of a blend is necessary in order to maintain good mechanical properties and avoid creating internal loci which are prone to mechanical failure.[5] The results obtained by investigating HAp-Gemosil and similar composites with polymers included highlight

the need for alternative polymers and cross-linking routes, in order to further improve important application related properties of these composites.

Recently, investigations into the adhesive properties of several sessile marine organisms have identified a series of proteins from *mytilus edilus* which demonstrate remarkable adhesion to a wide range of substrates.[6] Inspired by fact that these proteins are rich in 3,4-dihydroxy-L-phenylalanine (DOPA) and lysine amino acids (amine), Messersmith and co-workers hypothesized that dopamine, a small molecular that contains both functionalities (DOPA and amine), could structurally mimic these complex proteins and offer similar adhesion behavior. Indeed, the same authors experimentally confirmed that dopamine undergoes self-polymerization under basic conditions to form polydopamines (PD),[7] which can form thin polymer coatings adhering to a variety of organic and inorganic materials. Similar polymerization behavior of dopamine and the excellent adhesion of PD to numerous materials have been further demonstrated by others,[5] though the structure of PD is not well understood.[8,9] Since composites utilizing PD are formed from a homogenous dispersion containing dopamine, this polymerization can potentially introduce a new interconnected polymer network. This newly formed polymer network can serve to connect distal portions of the composite, which can serve to increase long range interactions within a material. The combination of forming a polymer and increasing adhesion can potentially increase both long and short range interactions within a composite. For these reasons, the complex behavior of PD, and its numerous potential applications have become an attractive topic of study when investigating new materials for bioceramics.[10,11]

Inspired by the exciting discoveries and features of polydopamine (PD), we attempted to introduce dopamine into our HAp-Gemosil formulation, and re-named these new composites as HAp-Gemosilamine (i.e., hydroxyapatite-gelatin modified with silane and dopamine). This type

of composite was designed to impart the excellent adhesive properties of PD, the biocompatibility and osteoconductivity of hydroxyapatite, and the mechanical strength of the enTMOS silsesquioxane network into a single phased composite. It was believed the combination of these properties would yield strong, functional materials with possible future biological applications. A number of such HAp-Gemosilamine composites were then formulated and tested (**Figure 1**). Various processing conditions were utilized in order to thoroughly study the setting behavior of these materials. Interestingly, composites which were allowed to begin setting at depressed temperatures, – 20 °C, before finishing setting at 20 °C, showed markedly improved properties when compared with HAp-Gemosil. However, when these composites were processed entirely at 20 °C, their mechanical properties were surprisingly poor. The interesting discrepancies within HAp-Gemosilamine composites prompted us to conduct a careful investigation, which is detailed in this report.

3.2 Forming HAp-Gemosilamine Composites: Observation and Hypothesis

When dealing with these new HAp-Gemosilamine materials, it quickly became apparent that processing temperature played a critical role in forming a robust composite capable of mimicking the mechanical strength found in natural bone. We denote the "warm" samples as the composite allowed to set at room temperature (20 °C) after mixing. The "cold" samples, on the other hand, were allowed to set for approximately 5 minutes at – 20 °C, before subsequent warming to room temperature to finish setting. While this difference in processing condition seems minor, the large difference observed in mechanical properties of the "warm processing" sample and the "cold" sample clearly demonstrates the opposite (**Figure 3.1**). For example, the HAp-Gemosilamine processed under the "cold processing" condition shows a compressive

strength close to 100 MPa, noticeably higher than that of the HAp-Gemosil (~ 80 MPa), and more than doubling that of the HAp-Gemosilamine processed under the "warm" condition.

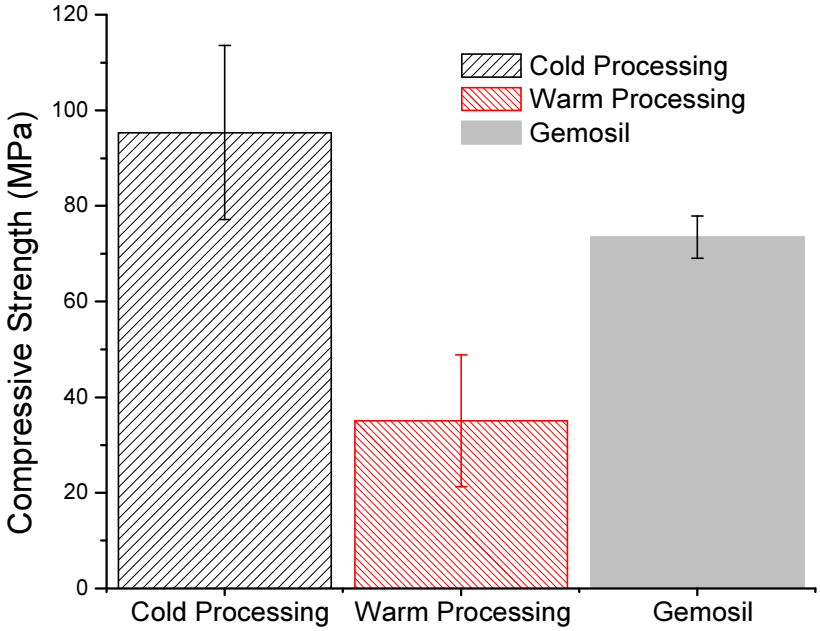

Figure 3.1 *Compressive data for HAp-Gemosil and HAp-Gemosilamine processed at 'warm' (20°C) and 'cold' (-20°C)*

So what causes this interesting temperature dependence behavior? Since HAp-Gemosil composites did not show any processing temperature dependence on their material properties in our previous investigation, we believe that the newly added component, dopamine, must be playing a critical role in the observed temperature dependence of the mechanical properties of HAp-Gemosilamine. We hypothesize that while dopamine is able to polymerize uninterruptedly at both low temperatures and room temperature, the sol-gel reaction of silanes is significantly hindered at low temperatures. Therefore, when the mixture is allowed to react at – 20 °C, only polydopamine (PD) formation proceeds appreciably to form the PD network, whereas the sol-gel reaction of silanes only occurs to a negligible extent. However, the small molecule and liquid

nature of the enTMOS molecules can permeate the entire composite even after the "soft" PD network is formed. When such a composite is allowed to warm up to room temperature, enTMOS starts to polymerize rapidly to form the silsesquioxane matrix that can effectively envelope the newly formed PD network, creating a series of inter-penetrating networks based on both PD and silsesquioxane. Such intricate networks formed by both PD and silsesquioxane help to strengthen the new composite, HAp-Gemosilamine, when compared with the original HAp-Gemosil composite. This "cold" processing, together with its effect on the formation and structure of the composite, is illustrated in **Figure 3.2a**. In contrast, when the entire composite is processed at 20 °C, the rate of polymerization for enTMOS is overwhelmingly faster than that of the dopamine polymerization. Before dopamine can form an effective network via its own polymerization, the polymerization of enTMOS already yields a glassy, highly cross-linked silsesquioxane network. Such a "hard" network will trap dopamine molecules (and oligomers of PD) into isolated regions. This will eventually lead to *segregated* PD domains within the cross-linked silsesquioxane network, which is ultimately detrimental to mechanical properties of these composites.

This scenario, i.e., the "warm" processing, is correspondingly illustrated in **Figure 3.2b**. In summary, we believe the difference in kinetics for these two reactions (i.e., polymerization of dopamine, and sol-gel cross-linking of silanes) and the mechanical nature of these two networks (i.e., soft gel of PD and hard glass of silsesquioxane network)would directly result in the significant difference in the micro/nano structures of these composites processed at different tempera tures.Such structural difference in these composites leads to the observed dramatic difference in the mechanical properties, as were shown in **Figure 3.1**. Specifically, the inclusion of PD in "cold" samples improves mechanical properties when compared with HAp-Gemosil

materials, while the inclusion of PD in "warm" samples causes a dramatic reduction in mechanical strength.

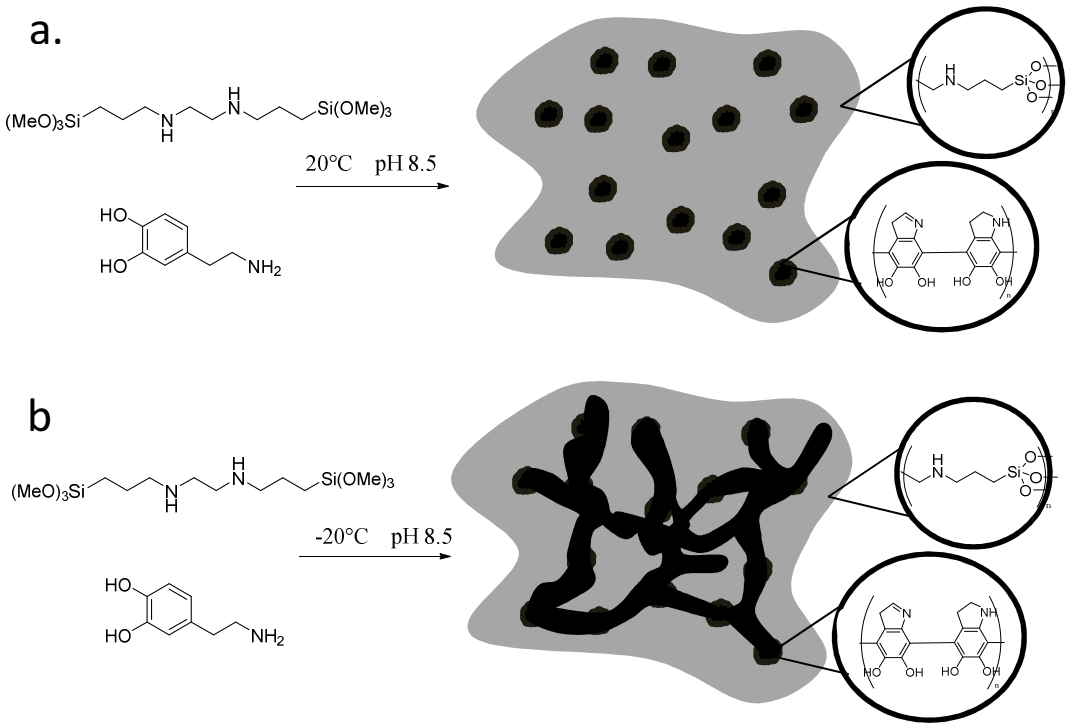

Figure 3.2 *(a) Illustration of polymerizations involved while HAp-Gemosilamine composites are allowed to set under – 20°C. While the composite is held at a cold temperature, PD is able to effectively polymerize, while enTMOS polymerization is suppressed. This allows an extensive, interconnected PD network to form before being encapsulated by the rapid gelation of enTMOS as the composite warms to room temperature to complete setting. (b) The situation would change when HAp-Gemosilamine composites are processed at 20°C. These composites polymerize enTMOS very rapidly, leading to a highly rigid network forming rapidly. This rigid network prevents PD from forming an extensive network, and ultimately creates weak spots in the material by localizing dopamine monomers and macromolecules into small isolated pockets.*

3.3 Experimental Design: Practical Considerations

According to the hypothesis detailed above, investigating the reaction kinetics of each component individually should be the crucial step to experimentally elucidate their effect on final composite performance. This practice helps develop an understanding of how each component is able to work with the others to afford materials whose properties are greater than

the sum of their parts. Such a further understanding would be important for optimizing and utilizing future PD containing bioceramic composites.

Ideally, one should investigate the polymerization behavior of one component (e.g., enTMOS) in the presence of the other component (e.g., dopamine) and other parts of the composites (e.g., HAp-Gel) to obtain the most relevant data. Unfortunately, within the newly developed HAp-Gemosilamine composite, several reactions are occurring between the various components of the material. This complication makes it very difficult to quantify the way a single component is behaving within the actual blend. Therefore it became necessary to simplify these reactions in order to more adequately characterize the behavior of a single component. For example, to further study how temperature can influence the progress of enTMOS sol-gel reactions, a series of experiments with enTMOS as the only component were carried out.

Similarly, to study the behavior of PD in the composite, it became necessary to alter the conditions under which PD was made to polymerize. When preparing HAp-Gemosilamine as stated above, PBS buffer, $Ca(OH)_2$, and Ammonium Persulfate (AP) were added to initiate cross-linking of enTMOS and subsequently PD. However, the actual concentration for dopamine used in HAp-Gemosilamine was too high to be observed via UV-Vis spectroscopy to monitor the reaction progress (*vide infra*). Therefore, we lowered the concentration of dopamine in solution (rather than in an almost solid state as in actual composite) such that the absorbance of the solution would be at the right level to track the progress of the reaction spectroscopically. Finally, because the concentration was lower, the freezing point would not be depressed in a manner similar to what we observed during processing of HAp-Gemosilamine. For this reason, it also became necessary to change solvents from water to methanol, otherwise the entire water based solution of such a low concentration would have been frozen at – 20 °C. This allowed our

"cold" experiments to also be modelled in a manner similar to the way the "warm" samples were. Additionally, for solubility reasons, $Ca(OH)_2$ was replaced with NaOH and AP was not used. AP was omitted to try to keep the reaction from happening too rapidly[10], thereby giving us more time to monitor the reaction progress and to draw meaningful conclusions from our data.

Although these experiments do not exactly mimic the behavior and environment of enTMOS and dopamine within a composite, these data can help illuminate the observed inconsistencies between 20 °C and – 20 °C HAp-Gemosilamine samples.

3.4 Temperature Dependence of The Sol-Gel Reaction of enTMOS

Typically, enTMOS sol-gel polymerizations begin to cross-link and solidify within minutes after initiation at room temperature. Therefore, for a HAp-Gemosilamine composite at 20 °C, the sol-gel reaction of enTMOS occurs rapidly as methanol is removed and an insoluble, glassy composite remains. As a result, this brittle silsesquioxane matrix sets the composite within minutes, effectively blocking further appreciable molecular diffusion. The final weight of this glass is roughly 70% of the initial enTMOS loading, due to the loss of methanol through hydrolysis condensation reactions.

However, this sol-gel reaction of silanes has shown little spectroscopic difference as the reaction proceeds, making it difficult to spectroscopically track the reaction progress in the studied range of 20 °C and – 20 °C. Fortunately, the insolubility of this newly formed silsesquioxane gel allowed us to design a mass loss-based method to monitor the progress of this reaction. Specifically, by washing out the soluble portions of enTMOS (e.g., monomers and oligomers) at various time intervals, it would be possible to track how this reaction proceeds over time and determine what role temperature plays in this cross-linking polymerization. For example, if the reaction had not proceeded appreciably, nearly all of the initial enTMOS

monomers and non-cross-linked oligomers would be washed away, showing a very high mass loss. Conversely, if the reaction had been already in an advanced stage and highly cross-linked, almost no monomers and oligomers would be removed by washing, showing a very low mass loss. By determining the time point at which the cross-linking reaction begins and ends at suppressed and elevated temperatures, we can gain a better understanding on how the reaction is likely proceed within the much more complex composite (e.g., HAp-Gemosilamine).

Figure 3.3 presents the results from these mass loss experiments. These data clearly demonstrate that at – 20 °C, the sol-gel reaction enTMOS is retarded for tens of minutes, and these "cold" composites do not begin setting appreciably until after several hours.

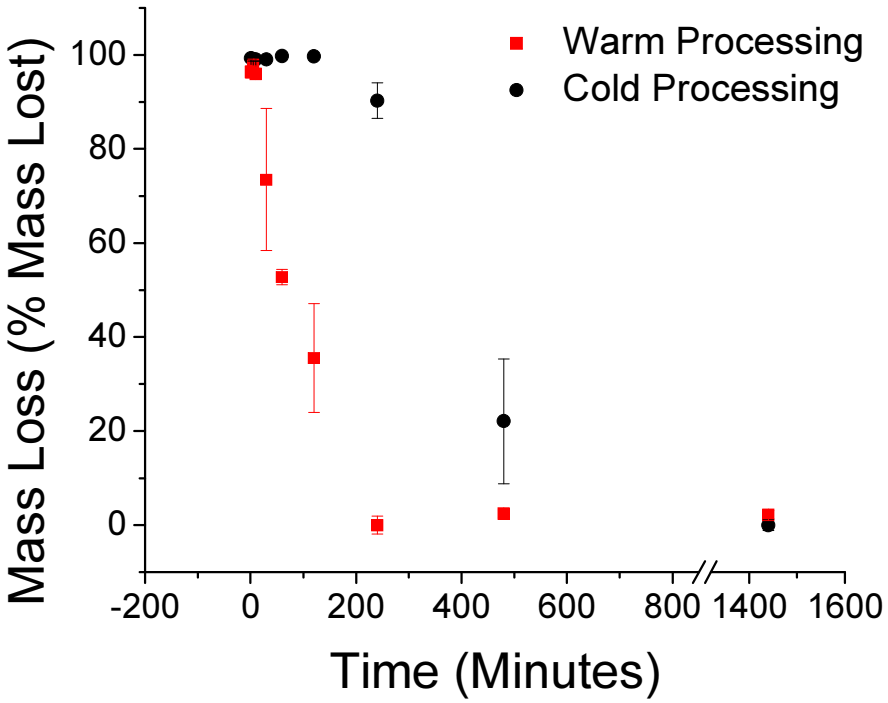

Figure 3.3 *Mass loss data for enTMOS polymerizations. Samples which have reacted extensively will show very high mass loss, since these samples are highly cross-linked and their polymers are insoluble. This phenomenon is observed for the enTMOS samples processed at 20 °C. It can be clearly seen that the opposite trend exists for enTMOS processed at – 20°C, where very little material has reacted even after 3 hours.*

In contrast, this retardation is not observed for the same sol-gel reaction at 20 °C. Over the same time interval, the "warm" enTMOS composites proceed almost to completion. The significant

dependence on temperature of this sol-gel reaction implies that when processing these composites with multiple components (e.g., HAp-Gemosilamine) at room temperature, the rapid polymerization of enTMOS would cause the composite to begin setting quickly at early stage. Afterwards, all reactions within the composite would become heavily diffusion controlled. This diffusion control can hinder the ability of other reactions to take place during the final setting of the composites. The interruption of these other reactions, such as dopamine polymerization, can lead to incomplete setting and poor mechanical strength. Apparently, lowering the temperature to slow down the sol-gel reaction of enTMOS would allow ample time for all desirable reactions to occur synergistically, resulting in a proper setting of the composite with improved mechanical strength.

3.5 Temperature Dependence of Dopamine Polymerization

Fortunately, unlike the enTMOS gelation, it is possible to use spectroscopy to monitor the progress of dopamine polymerization because the oxidation of dopamine to form the PD is accompanied by a characteristic color change. As more monomers become oxidized and subsequently polymerize, the solution turns darker. This is likely caused by increased pi-pi interactions within the newly forming macromolecules. According to the work of Wei *et al*.,[10] the PD formation can be monitored using UV-Vis spectroscopy at 350 nm. This offers us a simple method for monitoring the formation of PD and is indicative of the extent of PD polymerization by comparing the intensity of the UV-Vis absorption at different time intervals. Though this does not give us a quantitative measure of dopamine's degree of polymerization, it gives us useful information about how this polymerization is progressing under a certain set of conditions.

In practice, we simplified the system to contain only dopamine, methanol, and NaOH. This simple system still retains the essence of the polymerization of dopamine to PD; more importantly, such a diluted system allows for visualizing and comparing the reactions progress in solution by the UV-Vis absorption. We then conducted these experiments for samples at both – 20 °C and 20 °C and the results are highlighted in **Figure 3.4.**

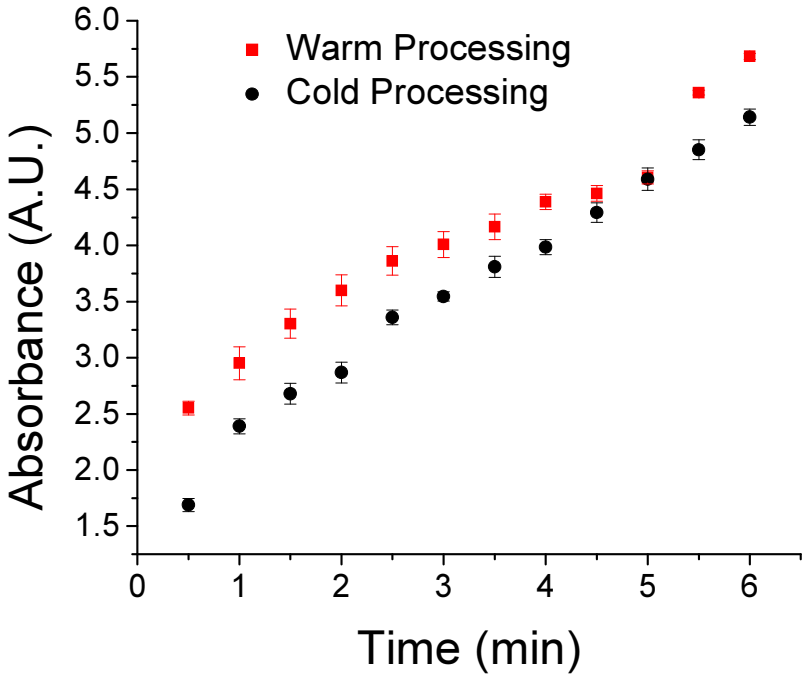

Figure 3.4 *Progress of dopamine polymerization under oxidative conditions over time. Dopamine was polymerized at both 20°C and -20°C. Over this temperature range, it can clearly be seen that the polymerization of dopamine is relatively unaffected.*

It can be seen clearly that, while temperature does influence PD formation, this difference on reaction progress at each time interval is small between – 20 °C and 20 °C. Overall, these results support our hypothesis that the formation of PD is much less influenced by the temperature, showing significantly different reaction kinetics than that of enTMOS reactions (**Figure 3.3**).

In the new multi-component based composite – HAp-Gemosilamine, delaying the onset of the enTMOS gelation at low temperatures affords the composite has more time for the other

components to react more fully before being encapsulated within the new enTMOS silsesquioxane network and completely set. Specifically, the slowed gelation of enTMOS at low temperatures gives a brief time window where dopamine can polymerize relatively unhindered. Though the true mechanism of the formation of PD is still under debate, the work of Hong *et al*.[8] suggests that the polymerization of dopamine could yield regions of trimers and tetramers which are able to stack through pi-pi interactions.[8] These small aggregates of trimers and tetramers can act effectively as weak cross-links between different PD chains, increasing the overall strength of the composite. After this initial cold setting phase, the composite is warmed up and enTMOS is able to then fully polymerize around the connected PD network, encapsulating it within a glassy silsesquioxane network. Therefore the adhesive ability of PD, and the subsequent formation of these interpenetrated polymer networks is key to the observed enhanced mechanical properties of the composite (**Figure 3.1**).

3.6 Biocompatibility: MTS Assay

Though dopamine is found naturally in the human body, its properties as a bulk material outside the brain are not well understood. Because the new composite HAp-Gemosilamine showed improved mechanical properties than those of the original HAp-Gemosil under appropriate processing condition, it was important to verify that using PD as a component in HAp-Gemosilamine would not negatively impact the biological compatibility. MTS assays were then carried out to determine cell viability over a 21 day period. The growth of preosteoblasts (MC3T3-E1) on three variant surfaces was shown in **Figure 3.5**. Interestingly, during the first 5 days, the cells were sporadic and did not spread in HAp-Gemosil. In contrast, adding PD appeared to increase initial cell growth in the same period of time. After day 7, there were no

statistical differences in cell numbers among three groups, indicating excellent biocompatibility of the new composite HAp-Gemosilamine and warranting further investigation.

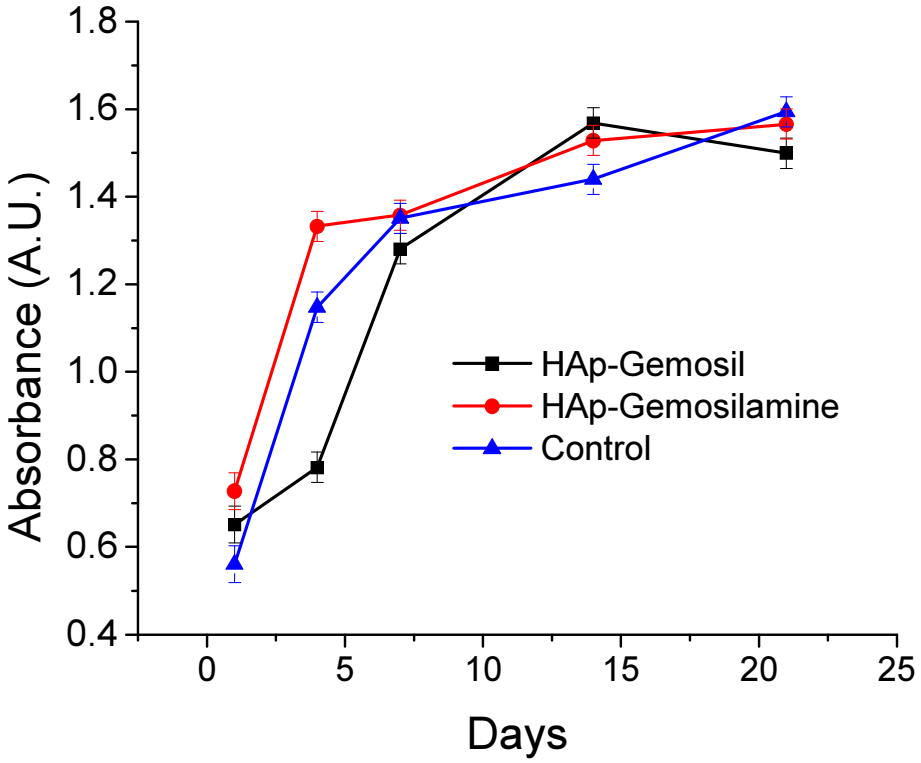

Figure 3.5 *Results of MTS assays of MC3T3-E1 Preosteoblasts plated on HAp-Gemosil, HAp-Gemosilamine, and control samples. Viability was similar for all three substrates tested.*

3.7 Conclusions

In summary, we have designed a new composite, HAp-Gemosilamine, to combine the favorable aspects of HAp-Gel, enTMOS, and PD into a single useful composite with possible tissue scaffolding applications. While working with this material, interesting results relating to the processing temperature dependence of mechanical properties were observed. When being processed under low temperature (e.g., – 20 °C) before being allowed to warm up (e.g., 20 °C) for final setting, HAp-Gemosilamine showed improved mechanical properties than those of HAp-Gemosil. In contrast, processing HAp-Gemosilamine in a manner similar to the original HAp-Gemosil (e.g., entirely at 20 °C) only resulted in poor mechanical properties. Such a strong

temperature dependence behavior can be ascribed to the different temperature related polymerization kinetics for the PD formation and the enTMOS sol-gel reaction, as demonstrated by control experiments with one component individually. For example, samples which were processed at – 20 °C showed little to no appreciable enTMOS reaction over several hours. During this time, however, PD reactions are able to proceed relatively unhindered. Since both polymerizations are initiated by adding the aqueous phase to the composite powder blend, it is important to have control over which reactions proceed first. This allows a more extensive PD network to form before the practical multi-component based composite is warmed up for the final setting, caused by hydrolysis condensation of alkoxysilanes present on enTMOS. This interesting feature allows a brief time window during which the injected materials can fill arbitrary shapes, which can be very useful in tissue scaffolding applications. As a proof-of-concept, a simple scaffold was prepared by indirect 3D printing this material, as shown in **Figure 3.6**.

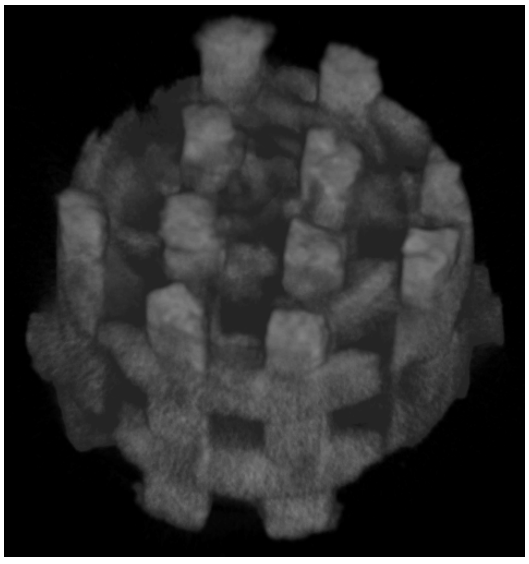

Figure 3.6 *Computed Tomography (CT) image of the 3D scaffold is made of 3D printing and an indirect scaffolding technique. Briefly, a 3D printing wax mold was used to cast the HAp-Gemosilamine, from which the wax was leached and the 3D HAp-Gemosilamine scaffold was designed.*

Furthermore, it was shown that these composites also maintain the biocompatibility of HAp-Gemosil materials. This is a crucial consideration for materials designed with potential tissue engineering applications in mind. Because HAp-Gel and enTMOS were shown to be biocompatible in previous studies, it was vital that the inclusion of PD did not negatively affect this aspect of the composite. However, the results obtained from MTS assays with plated preosteoblast cells show that this substrate shows nearly no difference when compared to control and HAp-Gemosil samples. This demonstrates dopamine's ability to polymerize into a useful material for biological implants without causing a negative biological response. The results of the 21 day assay also demonstrate that these cells are able to proliferate unhindered over time on this material, suggesting also that unreacted monomer and fast degradation times are not a problem for this composite. Though more testing is necessary to determine the full potential of the new HAp-Gemosilamine as a scaffolding material, the initial results are very promising and demonstrate clear advantages to using PD as an additive in bioceramic materials and using temperature as a means for controlling subsequent polymerizations within such materials.

3.8 Experimental Details

Materials and Methods

HAp-Gel slurry was prepared according to the previous co-precipitation method developed by Chang *et al*.[12] The HAp-Gel slurries were freeze-dried at – 80 °C overnight followed by lyophilization until dry to form HAp-Gel powder. The $Ca(OH)_2$ was derived by hydration of CaO which was previously calcinated at 1250 °C for 3 hours.[13] enTMOS and dopamine·HCl were purchased from Gelest, Inc. (Morrisville, PA, USA) and Alfa Aesar, respectively.

Designing and Formulating HAp-Gemosilamine Composites

100 mg of HAp-Gel/HAp, 200 mg of $Ca(OH)_2$ powder, and 10 mg of dopamine·HCl powder were transferred into a mortar and grinded into fine powder. For "cold" samples, the powder mixture was spread on a cold stage to maintain a depressed temperature of – 20 °C. In the cold stage, 383 μL of 62% enTMOS was added to the mixture while the powders and enTMOS were continuously spatulated for 30 seconds. For "warm" samples, spatulating was done at 20 °C without utilizing the cold stage. After spatulating, 40 μL ammonium persulfate solution (1 M in PBS 1×) was added to the mixture to initiate the polydopamine reaction. At this state, the mixture became dark fluid, which can then be injected into a mold to create arbitrary-shaped samples. Once leaving the cold stage, the fluid solidified and stopped shape change within 3 minutes. The samples without dopamine were also made for comparison (denoted as HAp-Gemosil).

Compressive and Biaxial Flexural Testing

Cylindrical model with a 1:2 ratio of diameter (3.5 mm) to length (7.0 mm) was used to prepare compressive samples at two conditions: with and without cold stage mixing. All samples were dehydrated at the room temperature for 7 days. Compressive testing was performed on an Instron machine (model 4204, Canton, MA, USA) with a cross-head speed of 0.5 mm/min. The compressive strength was determined from the maximum strength value on the stress-strain curve. The testing procedure for the biaxial flexure strength was also performed according to methods established in our previous publication.[4] Briefly, disk samples (11 mm diameter by 2.7 mm thickness) of each group were prepared in Teflon molds. The upper and lower surfaces were polished in order to obtain parallel surfaces. A crosshead speed of 0.5 mm/min was used, and the maximum force at failure (P) was determined using an Instron 4411 Machine (model 4411, Instron Co., Norwood, MA, USA). A Poisson's ratio of 0.3 was used and the flexure stress at

failure was calculated. Five samples for each group were used in the above testing. The testing results were analyzed by one-way ANOVA.

Mass-Loss Experiments

Mass-loss experiments were conducted as follows. 200 μL of enTMOS was diluted and mixed thoroughly with 250 μL of a 95% v/v MeOH/H_2O solution in a pre-weighed 2 mL flask. This mixture was then allowed to set for a predetermined period of time. After this time, resulting material was rinsed 3 times with chloroform and 3 times with acetone. The residual solid remaining in the flask was then heated for 24 hours at 100 °C to remove any residual solvent. After 24 hours, the glassy material was again weighed to determine the % mass lost during the rinsing phase. For samples at – 20 °C, an identical approach was taken, however all reagents were kept at – 20 °C for 24 hours before mixing. After mixing the pre-cooled reagents, the material was then stored at – 20 °C for the duration of the time interval until it was finally rinsed and heated as above.

UV-vis Experiments

Progress of dopamine oxidative polymerizations was monitored via UV-vis spectroscopy as follows. Dopamine (2 mL, 0.05 M in MeOH) was added to 1 mL of a saturated NaOH solution in MeOH. This mixture was probed every 30 sec for 6 min at 350 nm. In order to investigate the reactions at – 20 °C, cold dopamine and NaOH solutions were mixed and stored in a controlled environment at – 20 °C. Again, measurements were taken every 30 sec for 6 min at 350 nm, and samples were kept cold until immediately prior to measurement.

Osteoblast Proliferation Assay

Preosteoblasts MC3T3-E1 was used to test viability of the materials in 35mm culture dishes. Cells were seeded at a density of 1×10^4 per milliliter using αMEM medium supplemented with

10% of FBS and 1% penicillin/streptomycin under 37 °C, 5% CO_2 atmosphere. Three groups were investigated, including HAp-Gemosil, HAp-Gemosilamine, and dishes as received without coating (control). The spin coating method was described in the previous reports[13,14] and the coated dishes were UV sterilized and dried for 7 days, which were soaked in 2 ml PBS overnight prior to cell seeding. After 1, 4, 7, 14, and 21 days in culture, 40 μL of 3-(4,5-dimethylthiazol-2-yl)-5-(3-carboxymethoxy-phenyl)-2-(4-sulfophenyl)-2H-tetrazolium salt (MTS) reagent (Promega, Madison, WI, USA) was added to each dish containing 400 μL of Alpha Minimal Essential Media (*α*-MEM, Sigma-Aldrich, St. Louis, MO, USA), and the dish was incubated for 1 hour at 37 °C under a humidified atmosphere of 5% CO_2. Each sample was triplicated by culturing three dishes and each dish was measured three times by transferring 100 μL of MTS solution into each well of the 96-well plate. The absorbance of each well at 490 nm was measured using a microplate reader (Microplate Reader 550, Bio-Rad laboratories, Philadelphia, PA, USA). Relative cell numbers were quantified on the basis of the concentration of the formazan product of MTS. Coated dishes with HAp-Gemosil and HAp-Gemosilamine without cells were used as a blank (background substrate).

3D Printing of HAp-Gemosilamine

A computer generated 3D cylindrical porous template (10 mm diameter by 6 mm height) was design using SolidWork software (Dassault Systemes SolidWorks Co., Waltham, MA, USA). The computer template (stl format) was used to print a 3D polysulfonate mode with 1mm square trusses and 1mm square pore size (continuous space), which was used to cast the HAp-Gemosilamine. The Solidscape 3D printer (Solidscape Inc., Merrimack, NH) was used to fabricate polysulfonate mode. The HAp-Gemosilamine mixture was prepared on the cold plate as described above and injected to fill up the pore spaces of the polysulfonate mode while the

material was in liquid form. The HAp-Gemosilamine was set within 3-5 minutes in room temperature. The polysulfonate and HAp-Gemosilamine complex was then immersed in acetone for 30 minutes to remove the polysulfonate template. The 3D porous HAp-Gemosilamine scaffold is shown in **Figure 3.6**.

Acknowledgements

This study was supported, in part, by NIH/NIDCR K08DE018695 and R01DE022816.

REFERENCES

(1) Ko, C.-C.; Oyen, M.; Fallgatter, A. M.; Kim, J.-H.; Fricton, J.; Hu, W.-S. *Journal of materials research* **2006**, *21*, 3090.

(2) Luo, T.-J. M.; Ko, C.-C.; Chiu, C.-K.; Llyod, J.; Huh, U. *Journal of sol-gel science and technology* **2010**, *53*, 459-465.

(3) Mohamad Yunos, D.; Bretcanu, O.; Boccaccini, A. *J Mater Sci* **2008**, *43*, 4433-4442.

(4) Dyke, J. C.; Knight, K. J.; Zhou, H.; Chiu, C.-K.; Ko, C.-C.; You, W. *Journal of Materials Chemistry* **2012**, *22*, 22888-22898.

(5) Ryu, J.; Ku, S. H.; Lee, H.; Park, C. B. *Advanced Functional Materials* **2010**, *20*, 2132-2139.

(6) Waite, J. H.; Qin, X. *Biochemistry* **2001**, *40*, 2887-2893.

(7) Lee, H.; Dellatore, S. M.; Miller, W. M.; Messersmith, P. B. *Science* **2007**, *318*, 426-430.

(8) Hong, S.; Na, Y. S.; Choi, S.; Song, I. T.; Kim, W. Y.; Lee, H. *Advanced Functional Materials* **2012**, *22*, 4711-4717.

(9) Dreyer, D. R.; Miller, D. J.; Freeman, B. D.; Paul, D. R.; Bielawski, C. W. *Langmuir* **2012**, *28*, 6428-6435.

(10) Wei, Q.; Zhang, F.; Li, J.; Li, B.; Zhao, C. *Polymer Chemistry* **2010**, *1*, 1430-1433.

(11) Oh, K.-H.; Choo, M.-J.; Lee, H.; Park, K. H.; Park, J.-K.; Choi, J. W. *Journal of Materials Chemistry A* **2013**, *1*, 14484-14490.

(12) Chang, M. C.; Ko, C.-C.; Douglas, W. H. *Biomaterials* **2003**, *24*, 2853-2862.

(13) Kikuchi, M.; Cho, S.-B.; Tanaka, J.; Koyama, Y.; Kobayashi, T.; Takakuda, K.; Akao, M. *Journal of the Japan Society of Powder and Powder Metallurgy* **1998**, *45*, 36-40.

CHAPTER 4: INVESTIGATING NOVEL CATECHOLAMINES FOR ADHESIVE APPLICATIONS

In the previous chapter, the catecholamine polydopamine (PD), was incorporated into HAp-Gemosil materials and helped to improve adhesion between the various components of these bioceramic composites. This route was chosen because dopamine's ability to polymerize under oxidative conditions, yielding polymers with excellent adhesive qualities. This had a double benefit within these composite; first it allows for the formation of a polymer chain, which can help mimic the role of collagen and improve strength through fiber bridging. Second, this newly formed polymer adheres well to nearly all substrates, helping to improve short range interaction as well. Though examples of polydopamine's utility are numerous, an understanding of its adhesive properties and the underlying chemistry is lacking. In this chapter, dopamine and other catecholamines are studied more extensively to try to gain more understanding of the structure property relationships that lead to versatile, adhesive polymers.

4.1. Introduction to Catecholamine inspired adhesives

Adhesive materials have become ubiquitous in modern society due to their ability to bond different materials together, allowing better stress distribution through bonded joints. This makes adhesives vital for fulfilling roles in nearly every aspect of life, from clothing, to construction materials, and even to medical applications. Utilizing adhesives also increases freedom in designing new materials, and accordingly improves their cost effectiveness.[1] Despite

demonstrating value in all walks of life, fundamental problems exist for many applications, many having to do with maintaining their function in the presence of water.[2] Studies by Comyn *et. al* have identified at least 4 ways in which water can degrade adhesives illustrated in **Figure 4.1**.[3]

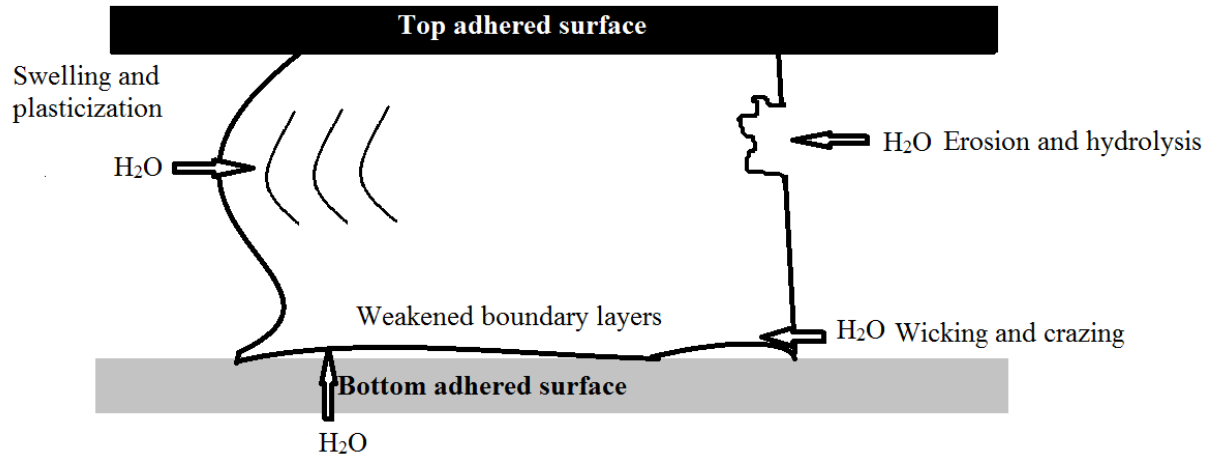

Figure 4.1 *shows how water can damage adhesive bonds in 4 primary ways; the presence of water can create a weak boundary layer at the interface. Water can also wick into the interface, causing loosening. Water can also hydrolyze and erode adhesives, or it can swell and cause increased plasticiziation, harming material adhesive interfaces.*

Despite the inherent drawbacks that water can pose to adhesives, necessity dictates that many adhesives must perform their tasks in aqueous environments. This presents substantial difficulty in designing and perfecting these materials. As mentioned in Chapter 3, the ocean presents a plethora of useful targets to investigate for potential biomimetic inspirations for solutions to this problem. In the sea there are many plants and animals which are capable of sticking to numerous substrates. All of these adhesive interactions seen in aquatic life are set, and persist in aqueous environments. One which has caused a great deal of frustration to ships is known as *mytilus edulis,* the blue mussel. These sessile invertebrates depend on their ability to adhere to wet surfaces to survive. By anchoring themselves to docks and ships, they are able to benefit from the high rate of gas exchange and abundant flow of nutrients hugely found around rough waters. This makes their seemingly hostile environment an ideal location for collecting

nutrients.[4] Despite the seeming disadvantages of their chosen substrates (i.e. rough water, wet substrates,) once attached, these mussels are incredibly difficult to remove. In fact, fouling from these types of marine organisms caused reported losses over $100 Million per year through excessive fuel consumption and required cleaning.[5]

Because of the incredible resilience shown by mussels in the face of traditionally harsh conditions, further studies of the chemistry allowing these exceptional properties was warranted. These studies revealed that 5 "foot proteins" were responsible for the remarkable adhesion observed in *mytilus edulis.* These were designated simply as *mytilus edulis* foot proteins (*mefps*) 1-5. In particular, *mefp*-5 is found most commonly at the interface of the mussel "foot pad" and, by mass it is nearly 40% dihydroxy-phenylalanine. This residue, also known as levadopa (L-Dopa), comprises more than 25% of the total residues of this protein.[6] L-Dopa is a derivative of tyrosine, and is modified through the enzyme *tyrosine hydroxylase.* This modification is outlined in **Figure 4.2.** [4,6] Since the amino acid, levadopa is synthesized from tyrosine, and the fact that no tyrosine is observed in the final structure of many *mefps* demonstrates a significant expenditure of energy by the organism to convert these residues to L-Dopa.

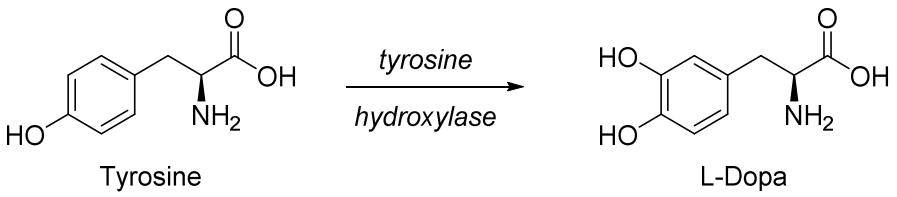

Figure 4.2 *Conversion of tyrosine to L-DOPA*

The discovery that *mytilus edulis* produces so much L-Dopa prompted significant research into the utility of polycatechols as adhesives. It was shown that these materials were capable of performing well as binders of inorganic materials.[7] Catechols, and their derivatives were also used for surface modification applications with good effect, especially on inorganic

surfaces.[8] When processed on the appropriate surfaces and with the appropriate cross-linking agents, these materials were shown to also be quite versatile adhesives.[9] In fact, these catechol based materials could be effectively cured by the addition of coordinating, oxidatively active ions such as dichromate $(Cr_2O_7)^{2-}$ or periodate $(IO_4)^{1-}$ to yield highly cross-linked materials with potential adhesive applications.[10] Furthermore, by adding charged side-chains, these adhesives were shown to also perform well as adhesives underwater, warranting further investigation into this phenomena.[11]

Though this gives a good clue as to the necessity of this catechol functional group, and poly-catechols were observed to adhere well to various inorganic substrates,[12] it was not as successful at binding plastics and other low energy materials.[7] This demonstrated that, while the catechol group is necessary for binding, it is not the only molecule involved. Furthermore, the discovery by White *et al.* that the coexistence of charged amine groups in the vicinity of the polycatechols had profound implications on the performance of these adhesives.[11] Further investigation of *mefp*-5 was able to show that more than 75% of these catecholic L-Dopa residues were flanked by a basic residue (i.e. lysine, arginine, and histidine.) In fact, L-Dopa and its surrounding basic residues were shown to comprise approximately 65 weight% and over 50 mol% of all residues present in these binding proteins, strongly implying that the coexistence of both the catechol and a nearby amine was the key to good adhesion. The structures and mol% of relevant amino-acid residues present in *mefp*-5 is given in **Figure 4.3.**

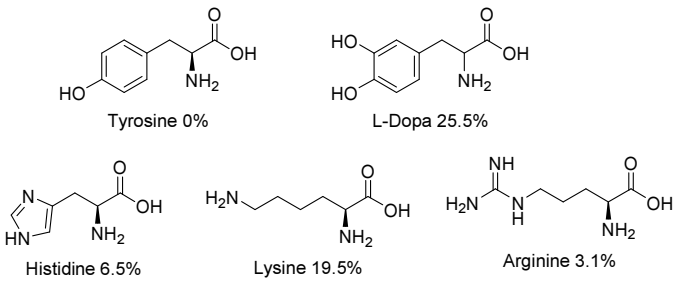

Figure 4.3 *Structures of major Amino Acids in Mytilus Edulis Foot Proteins*

This discovery led to a groundbreaking study in 2007 by Lee *et al.,* which demonstrated the utility of oxidatively polymerizing dopamine to form polydopamine (PD).[13] This common neurotransmitter presents a greatly simplified structure when compared to the complex proteins found in *mytilus edulis.* Despite this simplified structure, dopamine still possessing the two main functional groups shown to give good adhesive properties; a catechol and an amine. By exposing dopamine to basic conditions (pH >8.5), it is able to polymerize, yielding a macromolecule which demonstrates adhesive properties very similar to those observed through various *mefps*. These original works by Messersmith *et al* and numerous subsequent publications have demonstrated the ability of PD to adhere to numerous substrates, beyond those of poly-catechols.[7] The behavior of PD is unique in that it gives the opportunity to change a surface's chemistry in a single step, unlike other methods.[14] Because this route yielded polymers which were able to adhere to virtually all substrates under numerous conditions, substantial effort has been put forth in order to understand the mechanism by which this macromolecule forms, and what functionalities give it such amazing adhesive properties. Despite this work, no clear consensus has been reached as to the mechanism or the final structure of the PD macromolecule that leads to favorable adhesive properties.[15] Early studies hypothesized that the likely the structure of polydopamine was formed through covalent attachment through the aromatic protons. The structure originally proposed by Messersmith *et al*[13] and others[16] is given in **Figure 4.4**.

This structure was hypothesized due to the structural similarity between dopamine and the biopolymer eumelanin.[17] The Eumelanin polymer plays a major role in hair pigments, and is formed through the polymerization of 5, 6-dihydroxyindole (DHI) and 5, 6-dihydroxyindole-2-carboxylic acid (DHICA). In fact, dopamine, DHI, and DHICA are all formed originally from

tyrosine and levodopa as different branches along the same biosynthetic pathway, which shown in **Figure 4.5**. This scheme also shows the eumelanin polymer which was the inspiration for the dopamine polymerization proposed in **Figure 4.4**.

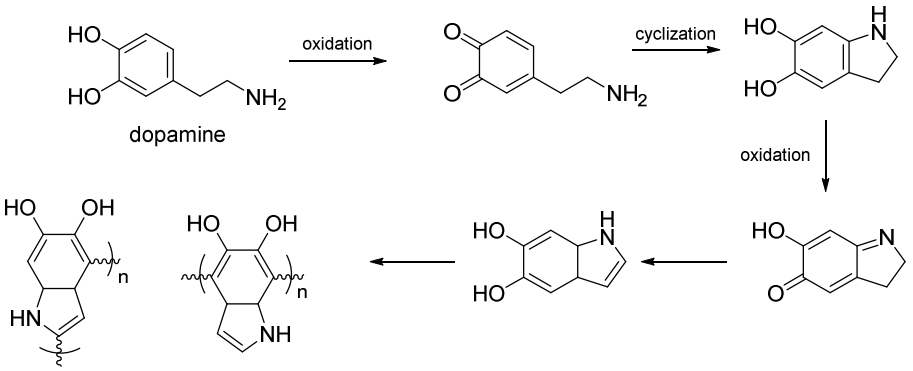

Figure 4.4 *Early proposed mechanism for the polymerization of dopamine*

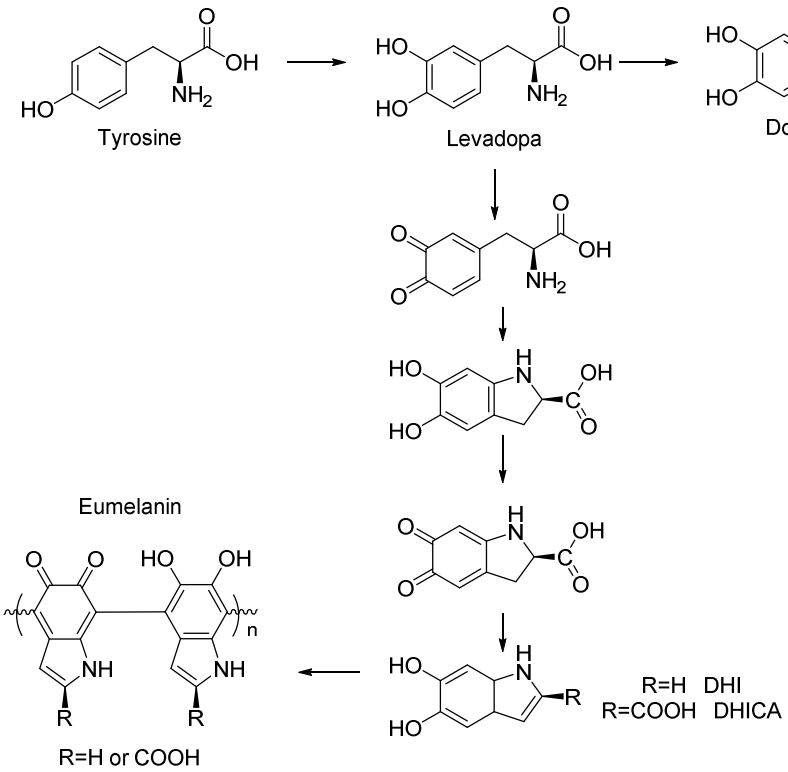

Figure 4.5 *Dopamine and Eumelanin synthetic pathways, showing structural similarities*

Other work has suggested that PD does not contain covalent bonds, but instead is a supramolecular aggregate of dopamine monomers and their derivatives (e.g. 5, 6-

dihydroxyindoline, and its dione derivative.) It has been claimed by Bielawski *et al.* that these monomers are held together through a combination of non-covalent interactions[14] (similar to those observed with benzoquinone and a diol.)[18] This scheme follows three major steps to get to macromolecules based on dopamine (or other tyrosine derivatives.) First, oxidation of the catechol hydroxyls to carbonyls allows cyclization of a pendant amine to follow shortly thereafter. Then, polymerization is achieved via charge transfer, hydrogen bonding and or π-stacking interactions, creating the non-covalent polymer. These key steps and another hypothetical structure of PD are given below in **Figure 4.6**.

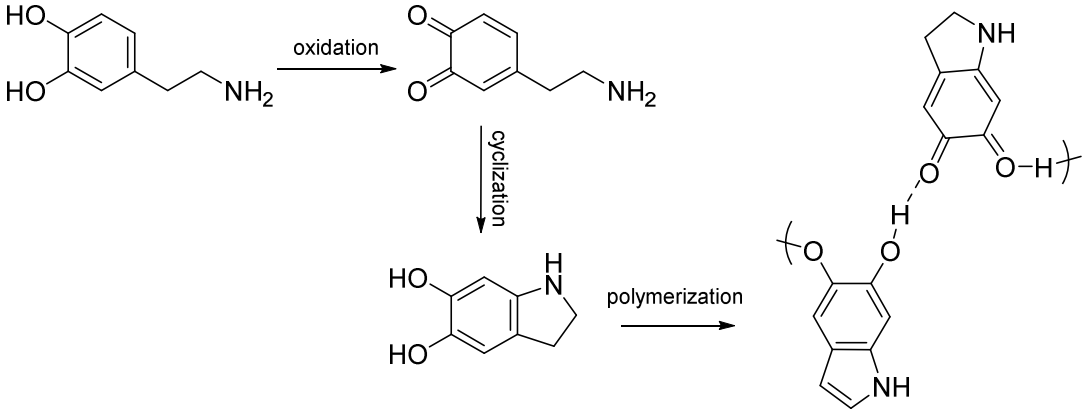

Figure 4.6 *Shows the proposed non-covalent assembly of dopamine leading to polydopamine proposed by Bielawksi*

Other work has suggested a combination of these previous structures; a small number of dimers and trimers are able to form, which are then able to pi-stack and hydrogen bond to form a macromolecule held together by a combination of covalent and non-covalent interactions. Lee *et al.* were able to show evidence for both covalent attachment, and π-stacking interactions.[19] They have recently proposed a mechanism involving the formation of dopamine-DHI dimers and trimers which are then able to stack 3-dimensionally through π-stacking, yielding a

macromolecule which forms as a combination of oxidative polymerization (similar to eumelanin)[17] and physical self-assembly (similar to benzoquinone and diols.)[18]

A few attempts at simplifying the structure of catecholamines have been published, though these mostly focused on using polymeric mimics of *mefps*. For example, Wilker *et al.* was able to use catecholamines which mimic a simplified *mefp* structure in order to obtain excellent adhesive properties on numerous surfaces. These studies demonstrated that these materials were indeed capable of modifying a surface and making adhesive films, helping to demonstrate the unique properties of catecholamines other than dopamine.[7, 16, 20] While little is known with certainty about the final macromolecular structure of PD, much is known about its ability to modify surfaces and alter properties of numerous substrates.[21] [22]However, since mechanistic and structural information is lacking, less work has been devoted to expanding the scope of catecholamines involved in surface modification.

When studying *mefps* in the context of dopamine, it becomes apparent that the structure of dopamine may not be as important as originally thought. In fact, nothing in the structure of *mefps* demonstrates that these functional groups need to be covalently bound, but rather that they simply need to be found close to one another. This is apparent when considering the numerous bonds separating the catechol and amine moieties. With this organization, the amine and catechol don't "know" they are attached, as they do not feel the effects of one another directly. Rather, they simply feel the effects due to their localization in the protein's tertiary structure. This rationale suggests that a solution containing unbound catecholamines (i.e. no covalent attachment of catechol and amine moieties) of sufficient concentration could also polymerize into an adhesive composite.

While these early studies were important in showing that *mefp* mimics can be more versatile than dopamine, they did not investigate unbound catecholamines. This study attempts to simplify catecholamine adhesive formulations even farther, in order to gain a better fundamental understanding of catecholamine systems. Furthermore, by using unbound catecholamine pairs, it should be possible to help understand why these unique physical properties exist for this class of materials. It is also hoped that by studying derivatized catecholamines, it will become clearer what structural features lead to the remarkable properties of dopamine and other catecholamine analogs.

4.2 Using untethered catechol-amine pairs to mimic polydopamine

When investigating alternative catecholamines for polymerization, one of the simplest mimics allowing investigation into the importance of the covalent attachment seen in dopamine would be propyl amine (PA) and catechol. The structures of these molecules are given along with dopamine in **Figure 4.7.** This was an attractive alternative to dopamine as these two molecules are substantially cheaper than while still preserving the relevant functional groups hypothesized to be important for the remarkable adhesion of catecholamines. Furthermore, if an unbound catecholamine pair like Cat-PA is able to behave similarly to PD, it will have profound implications on the design in novel adhesive systems in the future.

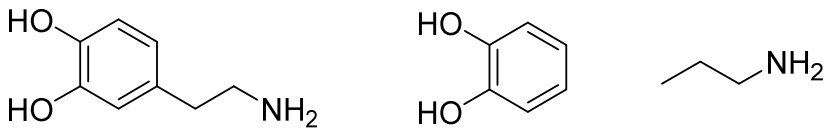

Figure 4.7 *Structures of initial test catecholamines; the "bound" pair dopamine, and the "unbound" pair, catechol and propylamine .*

According to the work of Wei *et al,* a simple method for monitoring the progress of dopamine polymerization is through the UV absorption at 350nm, which is related to the

formation of the quinone. This oxidation is widely agreed upon to be an important first step in the polymerization of dopamine.[14,19,23] This is followed by a broad peak developing around 480nm, indicative of further polymerization caused by 1,4-Michael addition of the amine. [23] These reactions are accompanied by a characteristic color change in solution. Initially, it was noticed that Cat-PA pairs also exhibited this unique color change upon mixing, and monitoring its UV-Vis profile can help give information about catecholamine polymerizations. Normally for these oxidative polymerizations, dopamine requires the addition of a basic component and or an oxidant to initiate the polymerization. However, when utilizing propyl amine this becomes unnecessary, as PA is sufficiently basic to oxidize catechol on its own. The PD and Cat-PA pairs were allowed to polymerize for 5 minutes, with data being collected every minute to observe the similarities and differences between the two systems, and this experiment is shown in **Figure 4.8.**

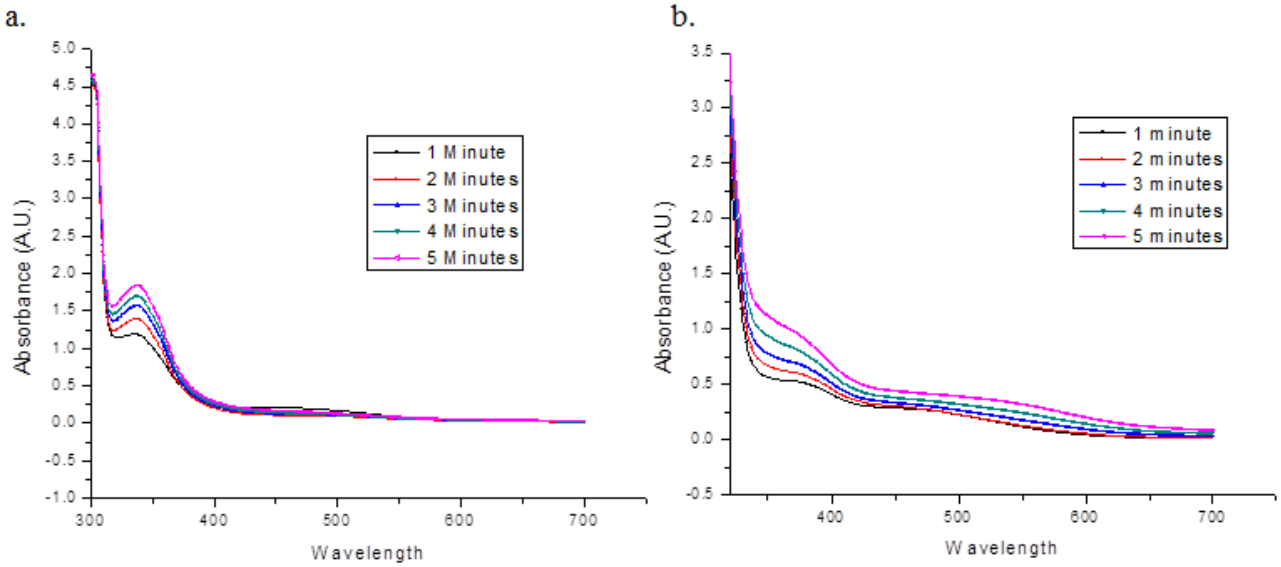

Figure 4.8 *UV-Vis spectra from 700-300nm for a.) Cat-PA and b.) Polydopamine over 5 minutes*

By mixing Cat-PA in a 1:1 stoichiometric loading at the same concentration as dopamine, the same concentration of each functional group is present in both solutions. This helps to identify if it is the covalent linkage, or simply the concentration, that is the important factor in catecholamine polymerizations. It can clearly be seen in **Figure 4.8** that the combination of Cat-PA shows distinct similarities to PD, through the growth of the characteristic quinone peak at 350nm. Both pairs also show a peak appearing in the 480nm range, which is absent from catechol only samples. This indicates the unbound amine is still playing an important role in solution. However, the shape of the PD and Cat-PA curves are slightly different, suggesting a different macromolecular structure forming in Cat-PA than observed in PD. Though on its own, this evidence is insufficient to claim the similarity between these systems, this result presents an excellent starting point for investigating the similarities between the 'bound' catecholamine, dopamine, and its 'unbound' analog, Cat-PA. By comparing these 2 systems side by side, it becomes easier to understand the similarities and differences found between catecholamines and to help understand better the applicability of this system.

4.3 Film Deposition studies

The ability to form films is crucial to PD's ability to modify the surface of numerous substrates and also lies at the heart of its amazing adhesive abilities. After confirming that unique reactions do take place between simplified unbound catecholamines, it was important to study their ability to deposit films as well. X-Ray photoelectron spectroscopy is a technique which utilizes X-rays to probe the surface chemistry of a material. This allows the composition of a material surface to be elucidated, and provides a way to investigate the ability of materials to deposit films on a surface. This technique also allows an estimation of the thickness of a deposited material. Preliminary studies were done comparing PD to Cat-PA by soaking both gold

in these solutions and using XPS to determine the ratio of C and N signals (from catecholamines) to that of Au surface signals. A sample of these results is given in **Figure 4.9.**

This XPS data illustrates another striking similarity between the behavior of PD and Cat-PA. Both were capable of coating the surface, shown by the increasing ratio of C and N signals compared to gold. The appearance of the Na and Cl peaks present in PD films is a result of the added NaOH in order to alter the pH to initiate polymerization. These data clearly indicates that films have been deposited, and surprisingly, the Cat-PA combination was shown to have actually deposited a thicker film (15.5nm) than PD (5nm) over the course of 24 hours.

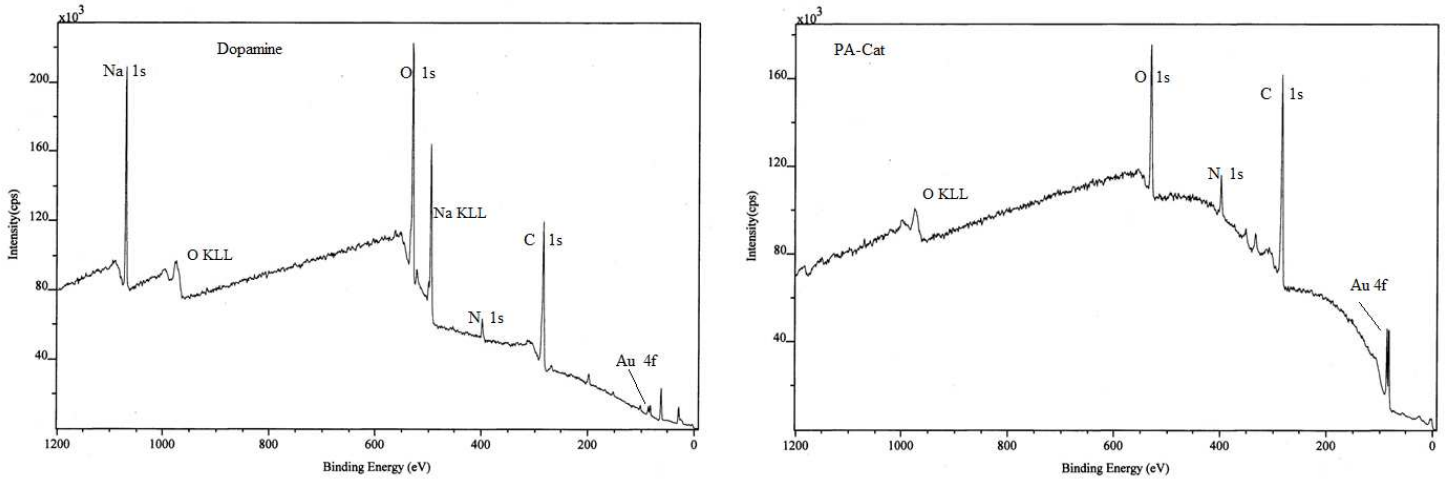

Figure 4.9 *XPS Data for PD (left) and Cat-PA (right) on Au substrates*

These solutions were also compared against the control sample of catechol treated in identical conditions to PD which produced a thinner film, with a thickness of just 2.8nm. This indicates that the reaction of Cat-PA is beyond that of simply oxidizing catechol in the presence of another base.

The utility of catecholamines stems not only from their ability to deposit films, but their ability to deposit films on numerous substrates. For this reason, a less favorable substrate was also investigated. Glass was chosen for its transparency, making spectroscopic tracking of film deposition easier. Glass slides were allowed to soak in a solution of PD and Cat-PA over the course of 5 hours, with a sample being removed every hour for spectroscopic investigation. These results are shown in **Figure 4.10.**

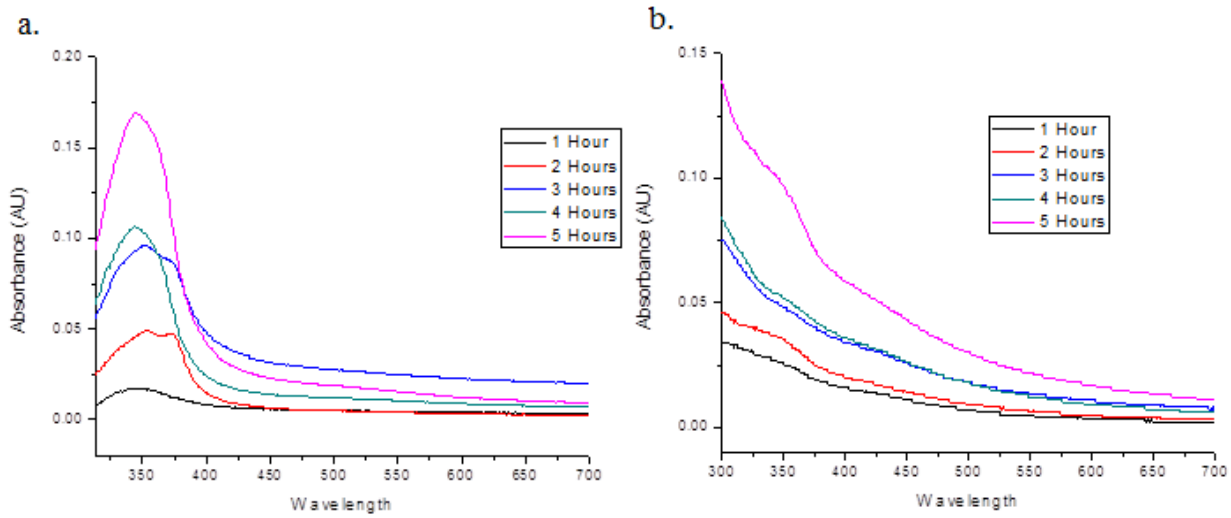

Figure 4.10 *Film Deposition for a.) Cat-PA and b.) PD on glass over 5 hours*

Though the spectra look less similar than those observed for solution polymerizations, indicating a potentially different macromolecular structure on the surface, it can clearly be seen that both materials were capable of depositing films of increasing thickness over time. These glass slides were visibly altered to a very similar brown color, characteristic of dopamine oxidation and polymerization.[13] Furthermore, the observation that these films grew over time is a good indication that they are capable of adhering to the materials surface and polymerizing from there. The UV-Vis signal from 350nm was plotted against time to give an idea of film deposition rate for both PD and Cat-PA and is given in **Figure 4.11.** These data clearly show the increasing

film thickness over time. This is an important consideration for adhesion, as the molecule must form a good interface with the surface in order to create a good adhesive bond.

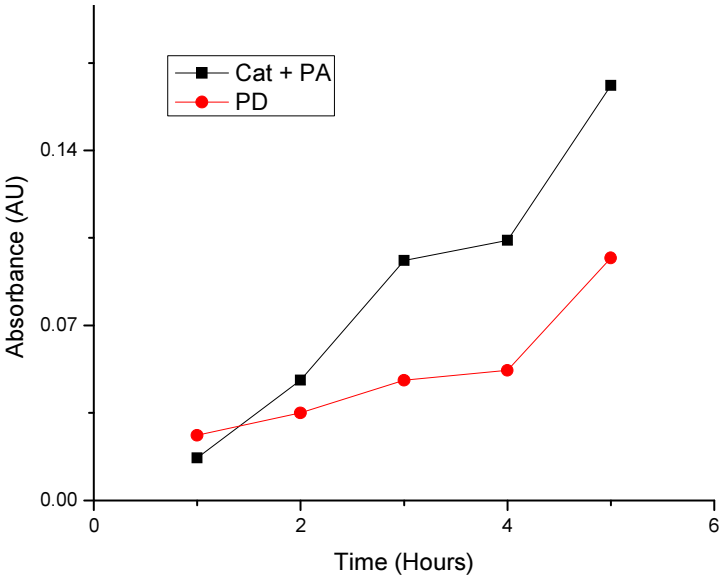

Figure 4.11 *Demonstration of film growth on glass slides via absorbance at 350nm over 5 hours for Cat-PA and PD. The increase in absorbance indicates thicker films over time.*

4.4 Film Adhesion Studies

As mentioned previously, substantial work has been devoted to understanding and replicating the unique adhesive properties of PD. Therefore, the ultimate test for the similarity between Cat-PA comes by testing its adhesive strength. To accomplish this, solutions of various catecholamine pairs, including dopamine, were pressed between glass slides in order to measure their maximum load at failure. By adhering two glass substrates together, it is possible to measure the adhesive force by utilizing lap-shear testing methods. This involves pulling laterally across the adhered surface, trying to separate the adherents by rupturing the adhesive material. This helps give a clear indication as to the adhesive ability of these materials, as better adhesives will show a greater load at failure. Additional catecholamines were chosen in order to investigate how vital the structure of dopamine was to the adhesive properties. In its place were two catecholamine pairs; dopamine with stoichiometric propylamine, and catechol with

poly(ethylenimine). Additionally, catechol was tested under the same conditions as the previous catecholamine pairs in order to ensure that the effect being observed was more than simple oxidation of catechol leading to adhesion. After determining the stress at break, it was easy to calculate the adhesive force for each sample. This was done by dividing the maximum load at failure, in Newtons, by the measured area of adhesive overlap in square meters. Representative stress-strain curves from these experiments are given in **Figure 4.12,** and a summary of the performance of these catecholamines is given in **Table 4.1**

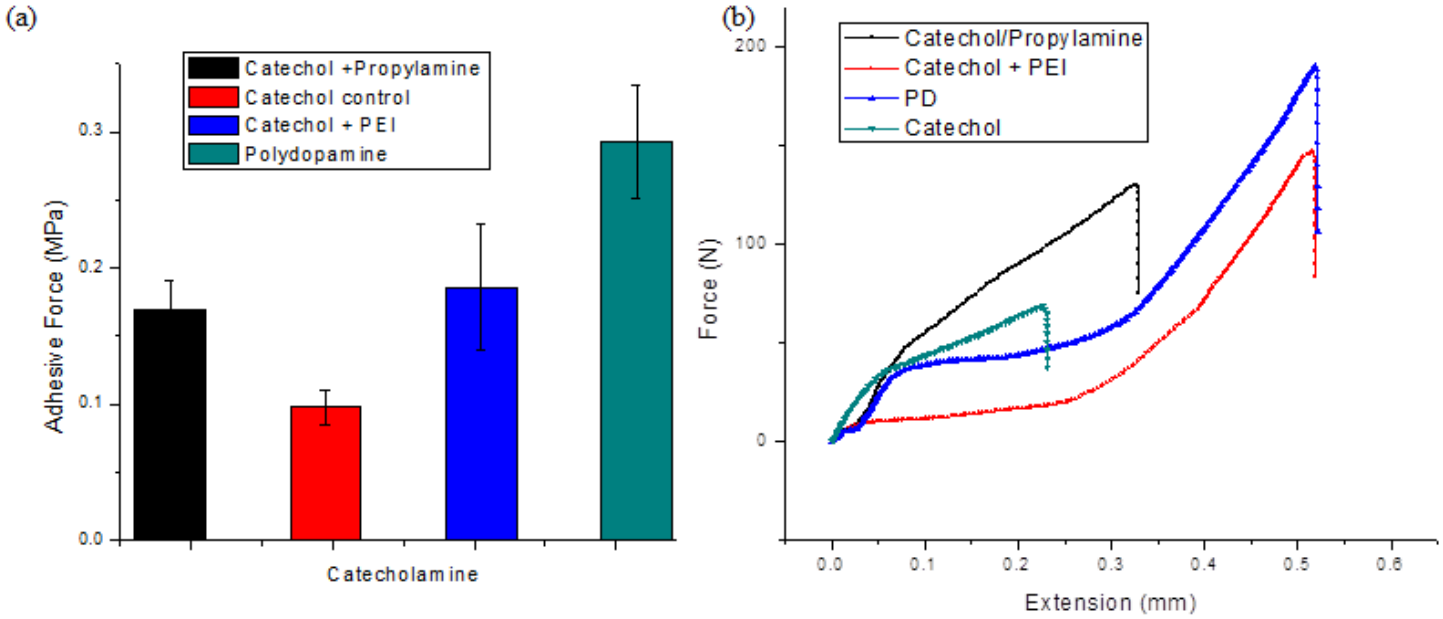

Figure 4.12 (a) Adhesive force for various catecholamines, calculated from **(b)** *Stress-strain curves demonstrating the maximum load at failure for each catecholamine adhesive formulation*

For these tests, pure propylamine and PEI did not provide appreciable adhesion, but rather acted as a viscous layer between the slides, which began sliding at the application of force. With that in mind, these data clearly support the theory that other catecholamines, beyond dopamine, can demonstrate favorable surface interactions and adhesive properties. This is

Table 4.1 Results from Adhesive testing of Catecholamines

Sample	Force at Break (N)	Std. Deviation (%)	Adhesive strength (MPa)
Catechol + Propylamine	103.6667	13.2	0.169252
Catechol Control	59.8	12.7	0.097
Catechol +PEI	113.7	24.9	0.186
Dopamine	179.3	14.3	0.293

confirmed by the fact that both of the catecholamine pairs tested (i.e. Cat-PA and Cat-PEI) had improved adhesive properties when compared to catechol without an amine source. The graphs in **Figure 4.12** demonstrate a long period of time during which the adhesive is resisting the increasing load from the Instron. This resistance to the input stress increases until there is a sharp drop, indicating bond breaking and adhesive failure.

Interestingly, neither of the novel catecholamine adhesives tested was able to surpass the performance of PD. This implies that, while binding of catechol and amine moieties is not required, it may be important to improved adhesive properties. This would make sense, as the covalent attachment of catechol and amine, as seen in dopamine, could provide two distinct advantages. First, the tethering of the catechol and amine moieties helps to keep their local concentration, presenting the possibility for faster reaction times (i.e. the amine is close to the oxidized catechol at all times, helping facilitate 1,4 Michael addition/cyclization prior to polymerization, as seen in **Figure 4.4**) Second, the covalent attachment could help improve the strength of this material by providing another bond which must be broken in order to rupture the adhesive. This is also suggested by the performance of the Cat-PEI pairs compared to the Cat-PA pairs, since the polymeric amine present on PEI provided better adhesion than the small molecule amine from propylamine.

4.5 Conclusions

In summary, we have demonstrated that the adhesive behavior observed with dopamine and other *mefp* analogs is a broader phenomenon than originally believed. Close examination of the *mefps* which inspired this research suggested that the local concentration of an amine and catechol in solution was the key to their remarkable properties. Early attempts to mimic the function of *mefps* focused on using either synthetic polymer analogs(e.g. polymeric catechol/amines)[9,10] or bound small molecule catecholamine pairs (e.g. dopamine)[13] but none capitalized on simpler, unbound small molecule catecholamines. The results obtained regarding both film deposition and adhesive studies suggest that it is indeed the local concentration leading to catecholamine adhesion. The unbound catecholamine adhesives outperformed oxidized catechol alone in adhesive strength and film deposition, and performed similarly to PD.

While this adhesive interaction is not governed by covalent attachment of the catechol and amine, there were some indications that this covalent attachment did lead to improved adhesive properties. Adhesive strength of PD did outperform all of the unbound catecholamine pairs tested. Though using a polymeric amine component did seem to improve the overall adhesion demonstrated by unbound catechol/amine pairs. These results highlight that the covalent attachment of catechol and amine is not vital to observe the unique adhesive properties of these materials, but it may impart improved adhesive performance for these composites.

The fact that this catechol/amine adhesive interaction is more universal than originally thought opens the door for new studies into the applications of these materials. This discovery has profound implications for new routes towards surface modification, tunable polymers, and adhesives. By showing that catecholamine adhesives are more universally applicable, it becomes possible to use small molecules and polymers with special properties introduced through their

design. This allows more high performance materials to take advantage of the unique properties afforded by catecholamine adhesives, without the need to focus on dopamine analogs specifically.

4.6 Experimental

Materials and Methods

Dopamine-HCl and glass slides were purchased from Fisher and used as received. Catechol, Propylamine, PEI, and NaOH were purchased from Sigma-Aldrich and used as received.

XPS Study

Films for XPS studies were prepared by soaking Au coated gold in a solution of catecholamine for 24 hours. For PD samples, of 0.1M Dopamine in water, adjusted to pH 9 using 1M NaOH, was used. For catechol /propylamine, a 0.2M solution of catechol was mixed 1:1 with a 0.2M solution of propylamine, to yield a 0.1M solution of catechol/propylamine in water. After 24 hours, the samples were removed and excess solvent was removed using compressed air before the sample was allowed to sit for additional 24 hours before testing. The results of these experiments are given in **Figure 4.9.**

UV-Vis Study

The progress of catecholamine polymerizations was monitored as follows. 0.1M solutions of PD and Catechol/propylamine were prepared as stated above. For UV-Vis experiments, these solutions were then used to soak glass slides over the course of 5 hours, with a slide being removed every hour. After soaking, these samples were dried using compressed air and allowed to sit for an additional 24 hours before testing. These slides were scanned from 300-700nm utilizing a blank slide as a reference (**Figure 4.8**.) According to Wei *et al,* special attention was

paid to the signal at 350nm, which has been attributed to the polymerization of dopamine, and the absorbance at this point was used to show increasing film thickness over time for these samples (**Figure 4.10 and 4.11)**

Adhesive Testing

Adhesive tests were done using polished glass slides as a substrate for adhesion. To make adhesive samples, a solution of catecholamine 1% by weight was prepared. From this solution, 30uL was pipetted onto a 24.5x25mm square on one of the slides. The other slide was then placed on top and pressed to remove excess solvent. This slide was then clamped together to give the slides adequate time to adhere. After 48 hours, the samples are sufficiently dry to allow testing. These samples were then loaded onto an Instron 5566 mechanical testing apparatus for lap shear testing. These tests involved subjecting the sample to a 2mm/min elongation until break. After breaking, the final load at break was then used to calculate the total adhesive force indirectly. Results from these experiments are given in **Figure 4.12** and **Table 4.1**.

REFERENCES

(1) Kinloch, A. J. *Journal of Material Science* **1980**, *15*, 2141-2166.

(2) Allen, K. W. *The City University of London, UK September 1982* **1982**.

(3) Comyn, J. In *Developments in Adhesives vol 2*; Kinloch, A., Ed.; Applied Science Publishers: Barking UK, 1981; pp 279-313.

(4) Waite, J. H. *Biological Reviews of the Cambridge Philosophical Society* **1983**, *58*, 209-231.

(5) Schultz, M. P. H., W.M *Biofouling* **2011**, *27*, 87-98.

(6) Waite, J. H.; Qin, X. *Biochemistry* **2001**, *40*, 2887-2893.

(7) Sedó, J.; Saiz-Poseu, J.; Busqué, F.; Ruiz-Molina, D. *Advanced Materials* **2013**, *25*, 653-701.

(8) Faure, E.; Falentin-Daudré, C.; Jérôme, C.; Lyskawa, J.; Fournier, D.; Woisel, P.; Detrembleur, C. *Progress in Polymer Science* **2013**, *38*, 236-270.

(9) Matos-Pérez, C. R.; White, J. D.; Wilker, J. J. *Journal of the American Chemical Society* **2012**, *134*, 9498-9505.

(10) Westwood, G.; Horton, T. N.; Wilker, J. J. *Macromolecules* **2007**, *40*, 3960-3964.

(11) White, J. D.; Wilker, J. J. *Macromolecules* **2011**, *44*, 5085-5088.

(12) Fan, X.; Lin, L.; Dalsin, J. L.; Messersmith, P. B. *Journal of the American Chemical Society* **2005**, *127*, 15843-15847.

(13) Lee, H.; Dellatore, S. M.; Miller, W. M.; Messersmith, P. B. *Science* **2007**, *318*, 426-430.

(14) Dreyer, D. R.; Miller, D. J.; Freeman, B. D.; Paul, D. R.; Bielawski, C. W. *Langmuir* **2012**, *28*, 6428-6435.

(15) Liebscher, J.; Mrówczyński, R.; Scheidt, H. A.; Filip, C.; Hădade, N. D.; Turcu, R.; Bende, A.; Beck, S. *Langmuir* **2013**, *29*, 10539-10548.

(16) Yu, F. C., S.: Yin.; Y *Journal of Molecular Structure* **2010**, *982*, 152-161.

(17) Kaxiras, E.; Tsolakidis, A.; Zonios, G.; Meng, S. *Physical Review Letters* **2006**, *97*, 218102.

(18) Patil, A. O.; Pennington, W. T.; Desiraju, G. R.; Curtin, D. Y.; Paul, I. C. *Molecular Crystals and Liquid Crystals* **1986**, *134*, 279-304.

(19) Hong, S.; Na, Y. S.; Choi, S.; Song, I. T.; Kim, W. Y.; Lee, H. *Advanced Functional Materials* **2012**, *22*, 4711-4717.

(20) Deming, T. *Macromolecules* **1998**, *31*, 4739-4754.

(21) Zhang, Y.; Thingholm, B.; Goldie, K. N.; Ogaki, R.; Städler, B. *Langmuir* **2012**, *28*, 17585-17592.

(22) Wood, J. B.; Szyndler, M. W.; Halpern, A. R.; Cho, K.; Corn, R. M. *Langmuir* **2013**, *29*, 10868-10873.

(23) Wei, Q. Z., F.; Li, J.; Li, B.; Zhao, C *Polymer Chemistry* **2010**, *1*, 1430-1433.

CHAPTER 5:CONCLUSIONS AND FUTURE DIRECTIONS

The primary aim of this dissertation was to study and improve synthetic bone replacement materials in order to provide better treatment options. In **Chapter 2**, biomimetic approaches to improving bioceramic composites were explored, demonstrating that the addition of a polymeric component helped to improve fiber bridging in the composite. In **Chapter 3**, the adhesive catecholamine polymer polydopamine (PD) was utilized in order to improve the compressive modulus of bioceramic materials. The processing of these materials was shown to have profound implications on the mechanical performance of these composites, as proper temperature control could yield interpenetrating polymer networks, maximizing strength. In **Chapter 4**, we examined the adhesive ability of other, previously untested, catecholamine formulations. Unlike previous work, we attempted to use catecholamine combinations which were not covalently bound in order to gain a better understanding of the structure-property relationship which give these materials their remarkable properties. These materials ultimately demonstrated properties similar to PD, indicating a more generally applicable structure is capable of yielding these unique adhesive properties. The discoveries of **Chapter 3** and **Chapter 4** presented two new avenues for investigation while continuing work on this project; studying new catecholamines as a route to improve bioceramics, and studying new catecholamines designed to help improve our understanding of these unique polymers.

5.1 Plans for Improving Biomimetic Composites

Our initial results indicated that the inclusion of an adhesive polymer yielded improved mechanical properties in bioceramic materials. We were also able to broader applicability of catecholamine adhesives. Future works will focus on designing and preparing biomimetic polymers which can utilize dopamine cross-linking to try to design stronger composites compared to previously established HAp-Gemosil and HAp-Gemosilamine materials. Also, by grafting these monomers onto a degradable polymer backbone, it is possible to have these polymeric components be temporary, alleviating problems with the permanence of silanes used in our previously studying enTMOS containing composites.

Further tests can be conducted on modified small-molecule catecholamines in these composites. By utilizing peptides or other biomolecules, we can improve and proliferation of cells as well, helping to increase osteoconductivity of our bioceramics. Additives can also be added to these small molecule catecholamine blends to attempt to cross-link,[1] to improve strength without the need for polymeric components.

5.2 Further Studies on Catecholamine Adhesives

Since PD was the initial inspiration into our investigations of catecholamines, but no clear mechanistic understanding of its macromolecular structure, it is important to continue to investigate this aspect of the material. As previously reported, no clear final structure exists for PD, though several sources claim that cyclization of the amine is an important step in the polymerization of this catecholamine.[2-4] While our tests showed that unbound catecholamines do also polymerize, demonstrating the fact that cyclization is not important, they also demonstrated that the bound catecholamines do show slightly improved mechanical properties when compared to the unbound pairs we investigated. To further probe these results, simple dopamine analogs

can be created, utilizing longer linker chains between the amine and catechol like those shown in **Figure 5.1.**

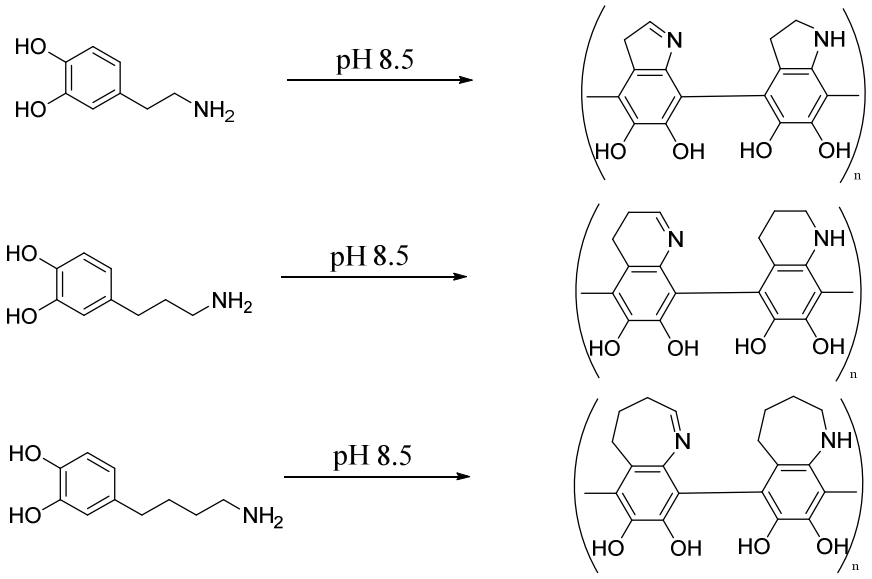

Figure 5.1 *Structure of dopamine analogs with longer side chains and a generic representation of their prospective polymers*

Dopamine's 2 carbon linker allows it to form a 5 membered ring fused to the catechol ring. If this monomer structure is expanded to include 3 or 4 carbon atoms, it is possible to form 6 and 7 membered fused rings, which should both also be energetically favorable to form. This will help gain an understanding if this 5 membered ring is important to the function and properties of dopamine, or if this is unimportant. Further tests could involve dopamine analogs with very long chains (i.e. >10 carbon units,) in order to determine if these are more similar to bound (e.g. dopamine) or unbound (e.g. Cat-PA) catecholamines. By mechanically testing these materials, and comparing them to both PD and other unbound catecholamine pairs, we can also gain a better understanding of the molecular structure which leads to the excellent adhesive properties previously reported for PD.

Further studies are also planned to block the 5 position on the catechol ring (which is where the covalent bonding to fuse the rings together takes place.) These studies should prevent cyclization of dopamine derivatives, and should give further clues and understanding of the mechanistic picture regarding the polymerization of not only dopamine, and also improves our understanding of these materials as adhesives. Furthermore, if the 4 and 5 positions on catechol are blocked and this molecule is treated with propylamine, we will be able to determine if there is covalent attachment between PA and catechol that also helps improve adhesion compared to catechol alone.

5.3 Improving Adhesive properties

Although we have shown that it is not necessary to have the catechol and amine bound together to gain the favorable properties of catecholamines like dopamine, we also discovered that these molecules being bound is important for improving properties. It was seen that dopamine exhibited superior adhesion than Cat-PA solutions. Furthermore, we discovered that mixing catechol with a polymeric amine yielded better properties than propyl amine, suggesting polymers can indeed improve properties of these adhesives. In fact, several attempts at utilizing various poly-catechol and poly-amine pairs have already been established.[5,6] By functionalizing a catechol and an amine molecule with a synthetic handle, it becomes possible to "click" these molecules on to polymers possessing the appropriate synthetic handle. It would then be possible to functionalize nearly any polymer, or small molecule in order to convert it to an adhesive through the utilization of polydopamine. We plan to explore how broadly applicable this system is and whether or not favorable adhesive properties can be imparted onto other polymers important for biomedical applications (e.g. MMA, LLA, TMC) or other traditionally non-stick polymers (e.g. PDMS, PTFE.) Furthermore, we would like to investigate the combination

catechol-modified surfaces with amine functionalized polymers to attempt to investigate if these are capable of forming reversible adhesive as cartooned in **Figure 5.2**

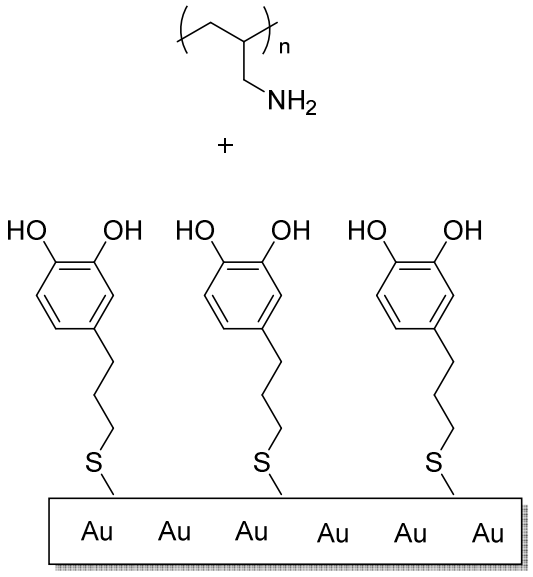

Figure 5.2 *Proposed route towards reversible adhesion on catechol modified substrates.*

.

These experiments will help further our understanding of these materials in order to allow the synthesis of specialized catecholamines functionalized materials.

5.4 Concluding Remarks

Several promising materials have been developed for the replacement of bone tissue, however, none of these have proven an ideal replacement for damaged tissue. To find better materials suitable for these applications, synergistic research efforts from chemists, doctors and engineers is required. This allows a focused approach to designing, synthesizing, and studying novel materials for their therapeutic abilities. Furthermore, novel materials must be explored in order to impart new properties into these tissue replacement materials. This work presents just a small piece of that puzzle, designed to help further our understanding of bioceramic composites and adhesives components used therein. By focusing on our fundamental understanding of the

interactions between polymers and ceramics, as well as better understanding macromolecular catecholamine adhesives, it will be possible to continue to present improved treatment options.

REFERENCES

(1) Matos-Pérez, C. R.; White, J. D.; Wilker, J. J. *Journal of the American Chemical Society* **2012**, *134*, 9498-9505.

(2) Lee, H.; Dellatore, S. M.; Miller, W. M.; Messersmith, P. B. *Science* **2007**, *318*, 426-430.

(3) Dreyer, D. R.; Miller, D. J.; Freeman, B. D.; Paul, D. R.; Bielawski, C. W. *Langmuir* **2012**, *28*, 6428-6435.

(4) Hong, S.; Na, Y. S.; Choi, S.; Song, I. T.; Kim, W. Y.; Lee, H. *Advanced Functional Materials* **2012**, *22*, 4711-4717.

(5) Deming, T. *Macromolecules* **1998**, *31*, 4739-4754.

(6) Sedó, J.; Saiz-Poseu, J.; Busqué, F.; Ruiz-Molina, D. *Advanced Materials* **2013**, *25*, 653-701.